ASM Handbook, Volume 11, *Failure Analysis and Prevention*
B. Miller, R. Shipley, R. Parrington, D. Dennies, editors
DOI 10.31399/asm.hb.v11.a0006783

Forms of Corrosion

Michael Cooney and Richard Hoffman, R.A. Hoffmann Engineering, P.C.

CORROSION is the electrochemical reaction of a material and its environment. This article addresses those forms of corrosion that contribute directly to the failure of metal parts or that render them susceptible to failure by some other mechanism. In particular, mechanisms of corrosive attack for specific forms of corrosion are described. Other articles in this Volume discuss analysis and prevention of several types of failures in which corrosion is a contributing factor. These articles include "Stress-Corrosion Cracking," "Liquid Metal and Solid Metal Induced Embrittlement," "Hydrogen Damage and Embrittlement," "Corrosive Wear Failures," "Biological Corrosion Failures," and "High-Temperature Corrosion-Related Failures." Additional discussion can be found in the articles "Effect of Environment on the Performance of Plastics" and "Corrosion Failures of Industrial Refractories and Technical Ceramics" in *Failure Analysis and Prevention*, Volume 11 of the *ASM Handbook*, 2002.

The rate, extent, and type of corrosive attack that can be tolerated in an object vary widely, depending on the specific application and initial design. Whether the observed corrosion behavior was normal for the material used in the given service conditions helps determine what inspection and maintenance action, if any, should be taken.

All corrosion reactions are electrochemical in nature and depend on the operation of electrochemical cells at the metal surface. This mechanism is discussed in the first section, "Galvanic Corrosion," in this article. Galvanic corrosion applies even to generalized uniform chemical attack—described in the section "Uniform Corrosion"—in which the anodes and cathodes of the cells are numerous, small, and close together. The analysis of corrosion failures and the development of suitable corrective measures require not only a basic understanding of electrochemistry but also the ability to apply fundamental principles of chemistry and metallurgy and materials science.

It is useful to consider these principles in the context of the form that the corrosion takes. Figure 1 is a schematic of several forms of corrosion, including those described in the sections "Pitting and Crevice Corrosion," "Intergranular Corrosion," and "Selective Leaching" in this article. The figure also includes external conditions that produce aggressive corrosion such as velocity-affected corrosion, which is addressed in this article, and stress-corrosion cracking, which is addressed elsewhere in this article. These reviews of corrosion forms and mechanisms are intended to assist the reader in developing an understanding of the underlying principles of corrosion; acquiring such an understanding is the first step in recognizing and analyzing corrosion-related failures and in formulating preventive measures.

More detailed discussions of the fundamentals and mechanisms of corrosion are provided in the References listed at the end of this article and in *Corrosion: Fundamentals, Testing, and Protection*, Volume 13A of the *ASM Handbook*, 2003.

Galvanic Corrosion

Although sometimes considered a form of corrosion, galvanic corrosion is more accurately considered a type of corrosion mechanism, because galvanic action is the basis for, or can accelerate the effects of, other forms of corrosion. Uniform attack, pitting, and crevice corrosion can all be exacerbated by galvanic conditions.

Galvanic corrosion occurs when two dissimilar conducting materials (metallic or nonmetallic) are in electrical contact with an electrolyte or conducting medium. It usually consists of two dissimilar conductors in electrical contact with each other and with a common conducting fluid (an electrolyte), or it may occur when two similar conductors come in contact with each other via dissimilar electrolytes. The former is the more common condition.

When two materials are in electrical contact and connected by an electrolyte, a galvanic current flows between them because of the inherent electrical potential difference between the two. The resulting reaction is referred to as couple action, and the electrically coupled system is known as a galvanic cell. The dissimilar metals/materials couple consists of an anode (which liberates electrons and corrodes typically by metal dissolution and/or metal oxide formation) and a cathode (which gains electrons and typically liberates hydrogen to the electrolyte and/or reduces oxides). Both reactions at the anode and cathode must proceed simultaneously for galvanic corrosion to occur. The overall reaction results in the corrosion of the anode by metal dissolution or oxidation, and an electrical current flows from the more anodic metal through a conducting medium or electrolyte to the other more cathodic metal (liberating hydrogen and/or causing a "reduction" of oxides). This action is seen in Fig. 2 where a couple is made up of steel and mill scale.

The three essential components for galvanic corrosion are:

- Materials possessing different surface potential
- A common electrolyte
- A common electrical path

A mixed-metal system in a common conducting electrolyte, where the components are

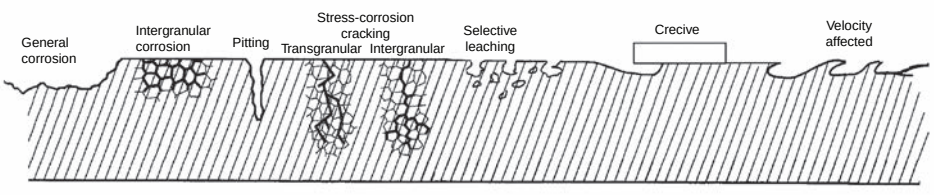

Fig. 1 Forms of corrosion. Adapted from Ref 1

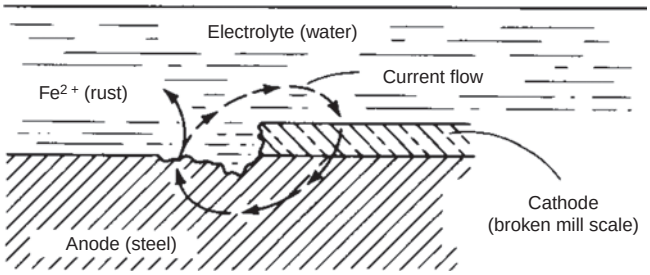

Fig. 2 Breaks in mill scale (Fe_3O_4) leading to galvanic corrosion of steel

electrically isolated, will not experience galvanic corrosion, regardless of the proximity of the metals or their relative potential or size.

Factors Affecting Galvanic Corrosion

The intensity of galvanic corrosion is affected by such factors as:

- The potential difference between the metals or alloys
- The nature of the environment/the electrical conductivity of the solution where the dissimilar metals are in contact
- The polarization behavior of the metals or alloys
- The geometric relationship of the component metals or alloys

The severity of galvanic corrosion depends on the amount of current flow. The relative potentials and polarization behavior of metals and alloys are key considerations discussed later in this article. Current flow also depends on the physical configuration (the relative area, distance, and shape) of the components.

Geometric Factors

Effect of Surface Area

The relative size of the anodic and cathodic surfaces is important. The intensity of galvanic attack is related to the relative size of the metals in electrical contact and the electrolyte. Large cathodic areas coupled to small anodic areas will aggravate galvanic corrosion and cause severe dissolution of the more active metal. The reverse situation—large anodic areas coupled to small cathodic areas—produces very little galvanic current. This is why imperfections or holidays in protective coatings may lead to severe galvanic corrosion in the localized region of the coating imperfection. It is extremely dangerous to coat the anodic member of a couple because this may only reduce its active area, which severely accelerates the attack at these holidays in the otherwise protective coating. If inert barrier coatings are employed, both the anode and cathode must be protected.

Effect of Distance

Dissimilar metals in a galvanic couple that are in close physical proximity usually suffer greater galvanic effects than those that are farther apart. The distance between the cathode and the anode surfaces affects the resistance of the current path in the solution and the external circuit. Thus, if dissimilar pipes are butt welded with the electrolyte flowing through them, the most severe corrosion will occur immediately adjacent to the weld on the anodic member.

Effect of Shape

The geometry of the circuit elements determines the electrical potential gradient, which causes the current to flow.

Galvanic Series

Because galvanic corrosion is directly related to the electrical current caused by the natural potential difference or electromotive force between different metals, it is useful to rank metals according to their relative potentials for a given electrolytic solution. For example, the galvanic series of potentials for metals in a chloride-containing aqueous solution (i.e., seawater) is often used for purposes of general comparison. This series is shown in Fig. 3. When two metals of a galvanic cell are widely separated in the galvanic series, there is a greater flow of current than for metals with small difference in potential. The galvanic series also allows one to determine which metal or alloy in a galvanic couple is more active. Metals that are more anodic in a given galvanic cell are prone to corrode by metal dissolution or electrochemical oxidation. The more cathodic material is more corrosion resistant (i.e., more noble).

Although the measurement of potentials has limitations as previously noted, galvanic series based on seawater or other standard electrolytes are worthwhile for initial materials selection for multiple metal/alloy systems in a given environment. A properly prepared galvanic series is easy to use and can answer simple galvanic-corrosion questions regarding the positions and relative separation of metals and alloys in a galvanic series. However, the comparison of galvanic potentials is only a ranking of general susceptibility; it does not address all the conditions and factors that influence galvanic corrosion. Limitations on the use of galvanic series include:

- No information is available on the rate of corrosion.
- Active-passive metals may display two, widely differing potentials.
- Small changes in electrolyte can change the potentials significantly.
- Potentials may be time dependent.

Creating a galvanic series is a matter of measuring the corrosion potential of various materials of interest in the electrolyte of interest against a reference electrode half-cell, such as saturated calomel, as described by the procedure in ASTM G 82 (Ref 3). To prepare a valid galvanic series for a given set of materials and environment of interest, all the factors affecting the potential must be addressed. This includes material composition, heat treatment, surface preparation (mill scale, coatings, surface finish, etc.), environmental composition (trace contaminants, dissolved gases, etc.), temperature, flow rate, solution concentration, and degree of agitation or aeration. In addition, corrosion product films and other changes in surface composition can also occur in some environments, and so exposure time is important, too.

With certain exceptions, the galvanic series in seawater is broadly applicable in other natural waters and in uncontaminated atmospheres. Bodily fluids are similar to saltwater, so as a first approximation the galvanic series is useful for implants.

However, metals behave differently in different environments. The relative positions of metals and alloys in the galvanic series can vary significantly from one environment to another. The position of alloys in the galvanic series for seawater is not necessarily valid in nonsaline solutions. For example, aluminum is anodic to zinc in an aqueous 1 *M* sodium chromate (Na_2CrO_4) solution and cathodic to iron in an aqueous 1 *M* sodium sulfate (Na_2SO_4) solution (Ref 4).

Electromotive Force Series

The electromotive force (emf) series is a table that lists in order the standard electrode potentials of specified electrochemical reactions. The potentials are measured against a standard reference electrode when the metal is immersed in a solution of its own ions at unit activity (Table 1). Similar to the galvanic series, it is a list of metals and alloys arranged according to their relative potentials in a given environment. Generally, the relative positions of metals and alloys in both emf and galvanic series are the same. An exception is the position of cadmium with respect to iron and its alloys. In the emf series, cadmium is cathodic to iron, but in the galvanic series (at least in seawater), cadmium is anodic to iron. Thus, if only the emf series were used to predict the behavior of a ferrous metal system, cadmium would not be chosen as a sacrificial protective coating, yet this is the principal use for cadmium plating on steel.

Polarization

Polarization represents the condition where the open-circuit electrode potential changes

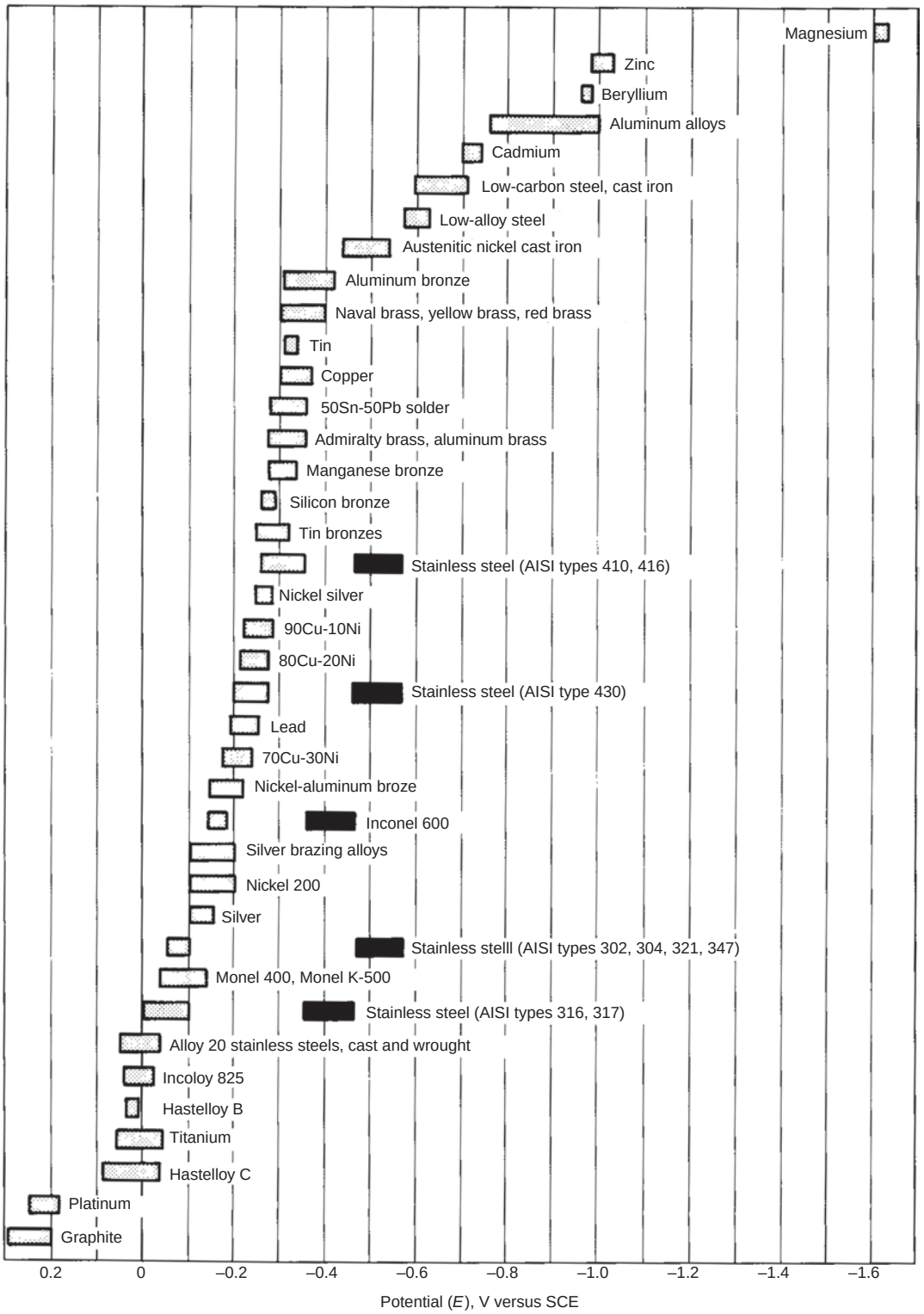

Fig. 3 Galvanic series of metals and alloys in seawater. Alloys are listed in order of the potential they exhibit in flowing seawater; those indicated by a black rectangle were tested in low-velocity or poorly aerated water and at shielded areas may become active and exhibit a potential near −0.5 V. SCE, saturated calomel electrode. Adapted from Ref 2

as a result of the passage of current through the couple and the deposition of anions or cations on the surface of either electrode. This condition is irreversible without external action. This change acts as a retardant to the electrical current flow.

Electron flow occurs between metals or alloys in a galvanic couple. This current flow between the more active and more noble

members causes shifts in potential, because the potentials of the metals or alloys tend to approach each other over time. This shift, where the open-circuit electrode potential changes as a result of the passage of current, is due to polarization of the electrodes. For example, during electrolysis, the potential of an anode becomes more noble, and the potential of the cathode becomes more active than their respective open-circuit (or reversible) potentials. Often, polarization occurs from the formation of a film on the electrode surface.

The magnitude of the shift depends on the environment, as does the initial potential. If the more noble metal or alloy is more easily polarized, its potential is shifted more toward the more active metal or alloy potential. The shift in potential of the more active metal or alloy in the direction of the cathode is therefore minimized so that accelerated galvanic corrosion is not as great as would otherwise be expected. On the other hand, when the more noble metal or alloy is not readily polarized, the potential of the more active metal shifts further toward the cathode (that is, in the direction of anodic polarization) such that appreciable accelerated galvanic corrosion occurs.

Polarization measurements on the members of a galvanic couple can provide precise information concerning their behavior. The polarization curves and the mixed potential for the galvanically coupled metals in a particular environment can be used to determine the magnitude of the galvanic-corrosion effects as well as the type of corrosion.

An important application in the use of polarization measurements in galvanic corrosion is the prediction of localized corrosion. Polarization techniques and critical potentials are used to measure the susceptibility to pitting and crevice corrosion of metals and alloys coupled in chloride solutions. In addition, this technique is valuable in predicting galvanic corrosion among three or more coupled metals or alloys.

Polarization measurements can be made by generating stepped potential or potentiodynamic polarization curves or by obtaining potentiostatic information on polarization behavior. The objective is to obtain a good indication of the amount of current required to hold each material at a given potential. Because all materials in the galvanic system must be at the same potential in systems with low solution resistivity, such as seawater, and because the sum of all currents flowing between the materials must equal 0 by Kirchhoff's law, the coupled potential of all materials and the galvanic currents flowing can be uniquely determined for the system. The corrosion rate can then be related to galvanic current by Faraday's law. Faraday's law establishes the proportionality between current flow and the amount of material dissolved or deposited in electrolysis. Additional information is provided in the article "Kinetics of Aqueous Corrosion" in *Corrosion: Fundamentals, Testing, and Protection*, Volume 13A of the *ASM Handbook*, 2003.

Potentiodynamic Polarization Curves

Potentiodynamic polarization curves are generated by connecting the specimen of interest to a scanning potentiostat. This device applies whatever current is necessary between the specimen and a counterelectrode to maintain that specimen at a given potential versus a reference electrode half-cell placed near the specimen. The current required is plotted as a function of potential over a range that begins at the corrosion potential and proceeds in the direction (anodic or cathodic) required by that material. Such curves would be generated for each material of interest in the system. Additional information on the method for generating these curves is available in ASTM G 5 (Ref 5). The scan rate for potential must be chosen such that sufficient time is allowed for completion of electrical charging at the interface.

Potentiodynamic polarization is particularly effective for materials with time-independent polarization behavior. It is fast, relatively easy, and gives a reasonable, quantitative prediction of corrosion rates in many systems. However, potentiostatic techniques are preferred for time-dependent polarization. To establish polarization characteristics for time-dependent polarization, a series of specimens are used, each held to one of a series of constant potentials with a potentiostat while the current required is monitored as a function of time. After the current has stabilized or after a preselected time period has elapsed, the current at each potential is recorded. Testing of each specimen results in the generation of one potential/current data pair, which gives a point on the polarization curve for that material. The data are then interpolated to trace out the full curve. This technique is very accurate for time-dependent polarization but is expensive and time-consuming. The individual specimens can be weighed before and after testing to determine corrosion rate as a function of potential, thus enabling the errors from using Faraday's law to be easily corrected.

Table 1 Standard electromotive force series of metals

Metal-metal ion equilibrium (unit activity)	Electrode potential versus saturated hydrogen electrode at 25 °C (75 °F), V
Noble or cathodic	
Au-Au^{3+}	1.498
Pt-Pt^{2+}	1.2
Pd-Pd^{2+}	0.987
Ag-Ag^{+}	0.799
Hg-Hg^{2+}	0.788
Cu-Cu^{2+}	0.337
H_2-H^{+}	0.000
Pb-Pb^{2+}	−0.126
Sn-Sn^{2+}	−0.136
Ni-Ni^{2+}	−0.250
Co-Co^{2+}	−0.277
Cd-Cd^{2+}	−0.403
Fe-Fe^{2+}	−0.440
Cr-Cr^{2+}	−0.744
Zn-Zn^{2+}	−0.763
Ti-Ti^{3+}	−1.210
Ti-Ti^{2+}	−1.630
Al-Al^{2+}	−1.662
Mg-Mg^{2+}	−2.363
Na-Na^{+}	−2.714
K-K^{+}	−2.925
Active or anodic	

Process of Predicting Galvanic Corrosion from Polarization Behavior

The process of predicting galvanic corrosion from polarization behavior can be illustrated by the example of a steel-copper system. Steel has the more negative corrosion potential and will therefore suffer increased corrosion upon coupling to copper, but the amount of this corrosion must be predicted from polarization curves. If the polarization of each material is plotted as the absolute value of the log of current density versus potential and if the current density axis of each of these curves is multiplied by the wetted surface area of that material in the service application, then the result will be a plot of the total anodic current for steel and the total cathodic current for copper in this application as a function of potential (Fig. 4).

Furthermore, when the two metals are electrically connected, the anodic current to the steel must be supplied by the copper; that is, the algebraic sum of the anodic and cathodic currents must equal 0. If the polarization curves for the two materials, normalized for surface area as previously mentioned, are plotted together, this current condition is satisfied where the two curves intersect. This point of intersection allows for the prediction of the coupled potential of the materials and the galvanic current flowing between them from the intersection point. This procedure works if there is no significant electrolyte resistance between the two metals; otherwise, this resistance must be taken into account in a complex manner that is beyond the scope of this article.

Combating Circumstances That Promote Galvanic Action

Dissimilar Metals

The combination of dissimilar metals in engineering design is quite common, for

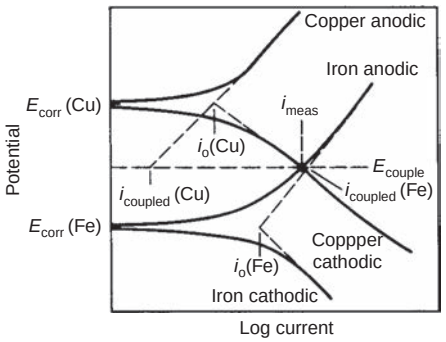

Fig. 4 Prediction of coupled potential and galvanic current from polarization diagrams. *i*, current; i_o, exchange current; E_{corr}, corrosion potential

example, in heating or cooling coils in vessels, heat exchangers, or machinery. Such combinations often lead to galvanic corrosion. The obvious design considerations to minimize the adverse effects of using dissimilar metals are to:

- Select metals with the least difference in "uncoupled" corrosion potentials
- Minimize the area of the more noble metal with respect to that of the active metal
- Insert an electrically insulating gasket between the two dissimilar metals
- Seal the junction from any available electrolyte

Another possibility is coating the cathodic material for corrosion control. Where metallic coatings are used, there may be a risk of galvanic corrosion, especially along the cut edges. Rounded profiles and effective sealants or coatings are beneficial. Ineffective painting of an anode in an assembly can significantly reduce the desired service lifetime because local defects (anodes) effectively multiply the risk of localized corrosion.

It is often necessary to use different materials in close proximity. Sometimes, components that were designed in isolation can end up in direct contact in the plant (Fig. 5). In such instances, the ideals of a total design concept become especially apparent but usually in hindsight.

Where dissimilar materials are to be joined, it is advisable to use a more noble metal in a joint (Fig. 5a, b). Unfavorable area ratios should be avoided. Metal combinations should be used in which the more active metal or alloy surface is relatively large. Rivets, bolts, and other fasteners should be of a more noble metal than the material to be fastened.

Dissimilar-metal crevices, such as at threaded connections, are to be avoided if possible. Crevices should be sealed, preferably by welding or brazing, although putties or nonmetallic sealants are sometimes used effectively. Replaceable sections of the more active member should be used at joints, or the corrosion allowance of this section should be increased, or both. Effective insulation can be useful if it does not lead to crevice corrosion. Some difficulties arise in the use of adhesives, which may not be sealants.

Preventive Measures

In particular cases, it is possible to reduce or eliminate galvanic-corrosion effects between widely dissimilar metals or alloys in a particular environment by altering one or more of the three key factors necessary for galvanic corrosion. Passive and active electrochemical techniques to mitigate galvanic corrosion include electrical isolation, use of transition materials, and cathodic protection.

Electrical Isolation

The joint between dissimilar metals can be isolated to break the electrical continuity. Use of nonmetallic inserts, washers, fittings, and coatings at the joint between the materials will provide sufficient electrical resistance to eliminate galvanic corrosion. The design of the

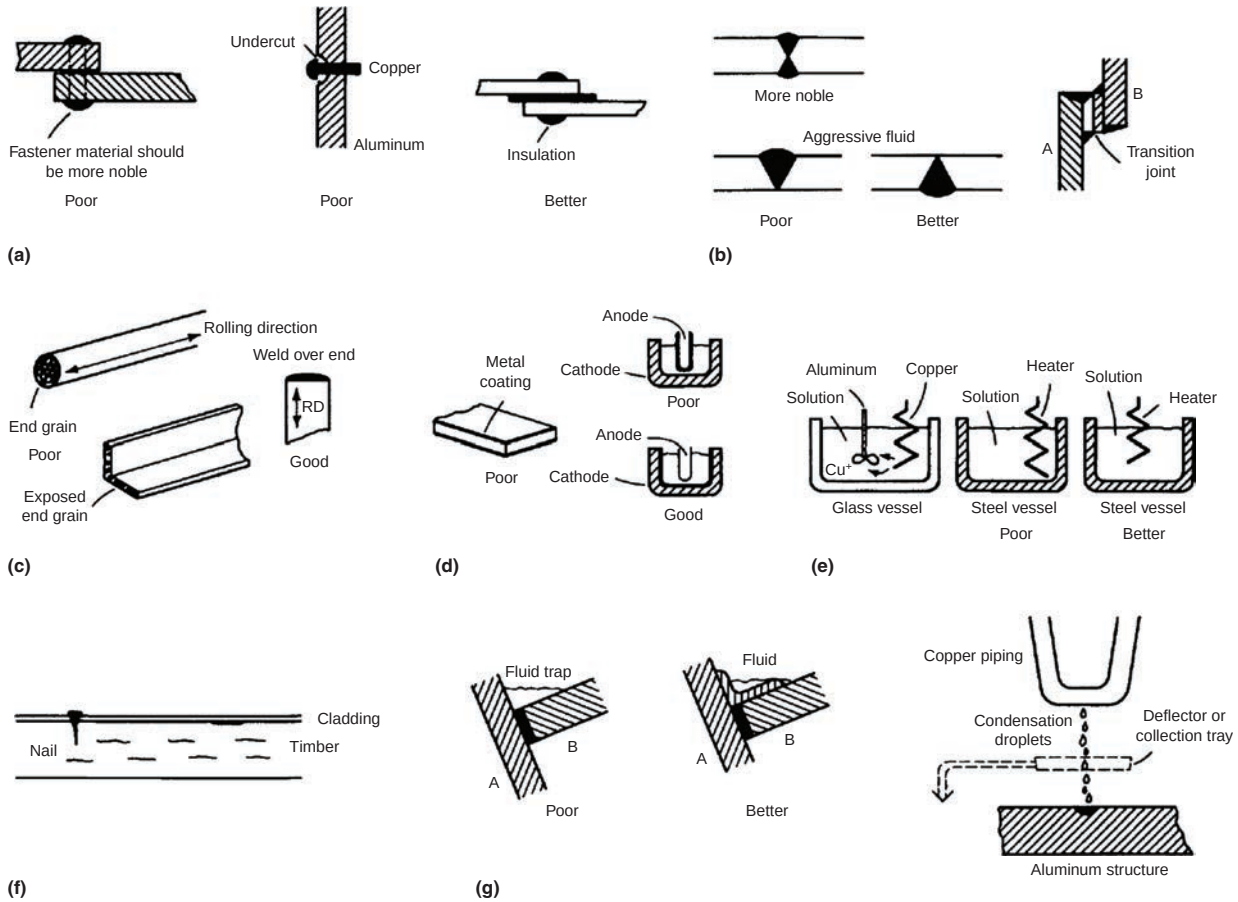

Fig. 5 Design details that can affect galvanic corrosion. (a) Fasteners should be more noble than the components being fastened; undercuts should be avoided, and insulating washers and spaces should be used to completely isolate the fastener. (b) Weld filler metals should be more noble than base metals. Transition joints can be used when a galvanic couple is anticipated at the design stage, and weld beads should be properly oriented to minimize galvanic effects. (c) Local damage can result from cuts across heavily worked areas. End grains should not be left exposed. RD, rolling direction. (d) Galvanic corrosion is possible if a coated component is cut. When necessary, the cathodic component of a couple should be coated. (e) Ion transfer through a fluid can result in galvanic attack of less noble metals. In the example shown at left, copper ions from the copper heater coil could deposit on the aluminum stirrer. A nonmetallic stirrer would be better. At right, the distance from a metal container to a heater coil should be increased to minimize ion transfer. (f) Wood treated with copper preservatives can be corrosive to certain nails. Aluminum cladding can also be at risk. (g) Contact of two metals through a fluid trap can be avoided by using a drain, collection tray, or a deflector.

insulation or maintenance must ensure that the insulator is not bridged by accumulated debris.

Transition Materials

To eliminate a dissimilar-metal junction, a transition piece can be introduced. The transition piece consists of the same metals or alloys as in the galvanic couple bonded together in a laminar structure. The transition piece is inserted between the members of the couple such that the similar metals, which are in contact with each other, form a dissimilar-metals joint.

Cathodic Protection

Cathodic protection is defined as the use of a more active metal to preferentially corrode in place of a less active metal, thereby protecting the less active metal from corrosion. It is a common and economical method of corrosion protection.

A second definition is the application of an external "impressed" electrical current into the metal that is to be protected so its electrical "status" is moved to the electrochemically passive region, which prevents the corrosion deterioration of the more active metal.

This cathodic protection practice can be accomplished through the use of sacrificial metals, such as magnesium or zinc, which act as the more active member and will corrode preferentially while providing cathodic protection to the other members in the galvanic assembly (for example, zinc anodes in cast iron waterboxes of copper alloy water-cooled heat exchangers).

Cathodic protection is often used for the protection of underground or underwater steel structures. The use of cathodic protection for long-term corrosion prevention for structural steels, underground pipelines, oil and gasoline tanks, offshore drilling rigs, well-head structures, steel piling, piers, bulkheads, offshore pipelines, gathering systems, drilling barges, and other underground and underwater structures is a fairly standard procedure. Magnesium, zinc, and aluminum galvanic (sacrificial) anodes are used in a wide range of cathodic protection applications.

The electric potential of an object can be changed to protect it. A direct-current potential can be applied on it through the use of a rectifier, battery, or solar cell. Conversely, stray currents can be a source of increased galvanic degradation.

Altering the Electrolyte

The use of corrosion inhibitors is effective in some cases. Elimination of cathodic depolarizers (deaeration of water by thermomechanical means plus oxygen scavengers such as sodium sulfite or hydrazine) is very effective in some aqueous systems.

Metallic Coatings

Two types of metallic coatings are used in engineering design: noble metal coatings and sacrificial metal coatings. Noble metal coatings are used as barrier coatings over a more reactive metal. Galvanic corrosion of the substrate can occur at pores, damage sites, and edges in the noble metal coating. Sacrificial metal coatings provide cathodic protection of the more-noble base metal, as in the case of galvanized steel or alclad aluminum, which is widely used in the aircraft industry. Thermally sprayed aluminum coatings apply excellent, tough corrosion-protection programs for steels where very long-term atmospheric protection of steel is needed.

Evaluation of Galvanic Corrosion

In terms of general evaluation, the most common method of predicting galvanic corrosion is by immersion testing of the galvanic couple in the environment of interest. Although time-consuming, this is the most desirable method of investigating galvanic corrosion.

In design and materials selection, screening tests are conducted to eliminate as many candidate materials as possible. These screening tests consist of one or more electrochemical techniques:

- Potential measurements
- Polarization measurements
- Current measurements

Potential Measurements

Potential measurements are made to construct a galvanic series of metals and alloys, as described in the next section. As a first approximation, the galvanic series is a useful tool. However, it has several limitations. Metals and alloys that form passive films will exhibit varying potentials with time and are therefore difficult to position in the series with certainty. Also, the galvanic series does not provide information on the polarization characteristics of the materials and so is not helpful in predicting the probable magnitude of galvanic effects. Polarization measurements are discussed in the section "Polarization" in this article.

Measurement of Galvanic Currents

Measurement of galvanic currents between coupled metals or alloys is based on the use of a zero-resistance milliammeter. Zero-resistance electrical continuity between the members of the galvanic couple is maintained electronically, while the resulting current is measured with the ammeter. Use of this technique should take into account certain limitations. First, when localized corrosion such as pitting or crevice corrosion is possible in the galvanic couple, long induction periods may be required before these effects are observed. Test periods must be of sufficient duration to take this effect into account. Also, the measured galvanic current is not always a true measure of the actual corrosion current, because it is the algebraic sum of the currents due to anodic and cathodic reactions. When cathodic currents are appreciable at the mixed potential of the galvanic couple, the measured galvanic current will be significantly lower than the true current. Therefore, large differences between the true corrosion rate calculated by weight loss and that obtained by galvanic current measurements have been observed.

Evaluating Galvanic Corrosion as a Synergistic Corrosion Mechanism

Uniform corrosion, pitting, and crevice corrosion can all be exacerbated by galvanic conditions. In addition, any of the tests used for the more conventional forms of corrosion, such as uniform attack, pitting, or stress corrosion, can be used, with modifications, to determine galvanic-corrosion effects. The modifications can be as simple as connecting a second metal to the system or as complex as necessary to evaluate the appropriate parameters. A change in the method of data interpretation is often all that is needed to convert conventional test methods into galvanic-corrosion tests.

Example 1: Galvanic Corrosion Leading to Fatigue Failure of a Helicopter Tail Rotor (Ref 6).

A tail rotor blade spar shank was constructed of 2014-T652 aluminum alloy. The spar was hollow, with the cavity filled with a lead wool ballast material and sealed with a thermoset material. One blade separated in flight, but fortunately a successful emergency landing was made. The outboard section that had separated was recovered.

Examination

There was a large flat fracture with beach mark features typical of fatigue. The fatigue crack had initiated on the inner surface of the spar at the cavity (Fig. 6). Fluid was found within the cavity, and the thermoset seal cap was broken. Microscopic examination revealed pitting corrosion on the inner surface of the spar cavity.

Conclusion

The seal had failed, allowing moisture into the cavity. This served as an electrolyte for galvanic corrosion between the lead and aluminum components. Corrosion pits formed at contact points of the lead wool and the aluminum spar wall. These pits served as the point of origin for the fatigue crack, leading to failure of the assembly.

Corrective Actions

To prevent this failure, the root causes of galvanic corrosion needed to be eliminated. The integrity of the seal needed to be ensured. A barrier coating between the lead and aluminum wall could be added. Alternate means of encapsulating the lead wool were also suggested. The corrective action taken was not reported.

Examples of Factors Contributing to Galvanic Corrosion

Ion Transfer

Ion transfer results in the deposition of active and noncompatible deposits on a metal surface. For example, an aluminum stirrer plate used in water was extensively pitted because the water bath was heated by a copper heater coil (Fig. 5e). The pits resulted from deposition of copper ions from the heater element. The presence of the copper ions introduced galvanic corrosion of the aluminum stirrer plate.

Nonmetallic Conductors

Less frequently recognized is the influence of nonmetallic conductors as cathodes in galvanic couples. Carbon brick in vessels is strongly cathodic to the common structural metals and alloys. Impervious graphite, especially in heat-exchanger applications, is cathodic to the less noble metals and alloys. Carbon-filled polymers or metal-matrix composites can act as noble metals in a galvanic couple.

Metal Ion Deposition

Ions of a more noble metal may be reduced on the surface of a more active metal, for example, copper on aluminum or steel, or silver on copper. This process is also known as cementation, especially with regard to aluminum alloys. The resulting metallic deposit provides cathodic sites for further galvanic corrosion of the more active metal.

Performance of Alloy Groupings

Magnesium

Magnesium occupies an extremely active position in most galvanic series and is therefore highly susceptible to galvanic corrosion. Metals that combine active potentials with higher hydrogen overvoltages, such as aluminum, zinc, cadmium, and tin, are much less damaging, although not fully compatible with magnesium.

Aluminum alloys that contain small percentages of copper (7000 and 2000 series and 380 die-casting alloy) may cause serious galvanic corrosion of magnesium in saline environments. Very pure aluminum is quite compatible, acting as a polarizable cathode; however, when iron content exceeds 200 ppm, cathodic activity becomes significant (apparently because of the depolarizing effect of the intermetallic compound $FeAl_3$), and galvanic attack of magnesium increases rapidly with increasing iron content. The effect of iron is diminished by the presence of magnesium in the alloy (Fig. 7).

Aluminum and Its Alloys

Aluminum and its alloys also occupy active positions in the galvanic series and are subject to failure by galvanic attack. In chloride-bearing solutions, aluminum alloys are susceptible to galvanically induced localized corrosion, especially in dissimilar-metal crevices. In this type of environment, severe galvanic effects are observed when aluminum alloys are coupled with more noble metals and alloys.

Cementation effects are also observed in the presence of dissolved heavy-metal ions such as copper, mercury, or lead. Some aluminum alloys are used for sacrificial anodes in seawater. An active, anodic alloy is used to clad aluminum, protecting it against pitting in some applications.

Contact of aluminum with more cathodic metals should be avoided in any environment in which aluminum by itself is subject to pitting corrosion. Where such contact is necessary, protective measures should be implemented to minimize sacrificial corrosion of the aluminum. In such an environment, aluminum is already polarized to its pitting potential, and the additional potential imposed by contact with the more cathodic metal greatly increases the corrosion current.

In the absence of chlorides or with low concentrations, as in potable water, aluminum and its alloys may be less active because of greater stability of the protective oxide film. Galvanic effects are not as severe under these conditions. Corrosion of aluminum in contact with more cathodic metals is much less severe in solutions of most nonhalide salts, in which aluminum alone normally is not polarized to its pitting potential.

In many environments, aluminum can be used in contact with chromium or stainless steels with only slight acceleration of corrosion; chromium and stainless steels are easily polarized cathodically in mild environments, so that the corrosion current is small despite the large differences in the open-circuit potentials between these metals and aluminum.

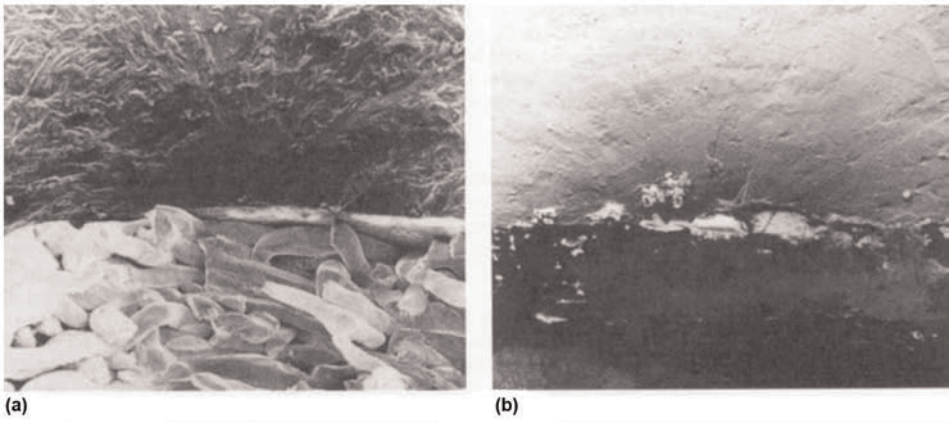

Fig. 6 Fatigue cracking of a helicopter tail rotor blade. (a) Scanning electron micrograph of the blade showing lead wool ballast in contact with the 2014-T652 aluminum spar bore cavity wall at the failure origin. Original magnification: ~13×. (b) Greater magnification (~63×) in this same area shows the multiple pits and associated corrosion products at the failure origin. The beach marks are seen emanating from the pits, typical of fatigue failure mode. Source: Ref 6

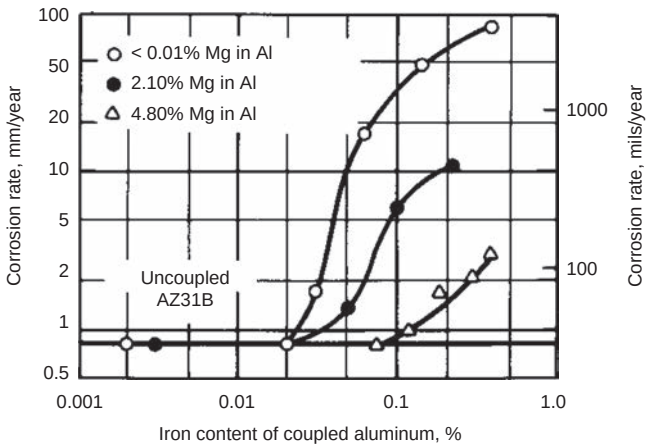

Fig. 7 Corrosion rates in 3% NaCl solution of magnesium alloy AZ31B coupled with aluminum containing varying amounts of iron and magnesium. The corrosion rate of uncoupled AZ31B is shown for comparison.

Galvanic current between aluminum and another metal also can be reduced by removing oxidizing agents from the electrolyte. Thus, the corrosion rate of aluminum coupled to copper in seawater is greatly reduced wherever the seawater is deaerated.

The criterion for cathodic protection of aluminum in soils and waters has been published by NACE International (Ref 7). The suggested practice is to shift the potential at least −0.15 V but not beyond the value of −1.20 V as measured against a saturated copper sulfate ($Cu/CuSO_4$) reference electrode. In some soils, potentials as low as −1.4 V have been encountered without appreciable cathodic corrosion (Ref 8).

Iron and Steel

Iron and steel are fairly active alloys and require protection against galvanic corrosion by the higher alloys. They are, however, more noble than aluminum and its alloys in chloride solutions. However, in low-chloride waters, a reversal of potential can occur that causes iron or steel to become more active than aluminum. A similar reversal can occur between iron and zinc in hot waters of a specific type of chemistry.

Stainless Steels

Galvanic-corrosion behavior of stainless steels is difficult to predict because of the influence of passivity. Passivation of stainless steels is the intentional forming of a complete exterior chromium trioxide (Cr_2O_3) film by completely cleaning the surface and allowing oxygen to contact and react with the surface. In the common galvanic series, a noble position is assumed by stainless steels in the passive state, while a more active position is assumed in the active state (Fig. 3). These are noted by black blocks in the diagram. This dual position in galvanic series in chloride-bearing aqueous environments has been the cause of some serious design errors. More precise information on the galvanic behavior of stainless steels can be obtained by using polarization curves, critical potentials, and the mixed potential of the galvanic couple. In chloride-bearing environments, galvanically induced localized corrosion of many stainless steels occurs in couples with copper or nickel and their alloys and with other more noble materials. However, couples of stainless and copper alloys are often used with impunity in freshwater cooling systems. Iron and steel tend to protect stainless steel in aqueous environments when galvanically coupled. The passive behavior of stainless steels makes them easy to polarize; thus, galvanic effects on other metals or alloys tend to be minimized. However, galvanic corrosion of steel can be induced by stainless steel, particularly in aqueous environments and with adverse area ratios.

Lead, Tin, and Zinc

These three materials occupy similar positions in the galvanic series, although zinc is the most active. The oxide films formed on these materials can shift their potentials to more noble values. Thus, in some environments they may occupy more noble positions than one may otherwise expect. For example, the tin coating in tin cans is anodic to steel under anaerobic conditions in the sealed container but becomes cathodic when the can is opened and exposed to air. Zinc is an active metal. It is susceptible to galvanic corrosion and is widely used for galvanic anodes, in cathodic protection as a sacrificial coating (for example, galvanizing or electroplating), and as a pigment in certain types of coatings.

Copper and Its Alloys

Copper and its alloys occupy an intermediate position in the galvanic series. They are not readily polarized in chloride-bearing aqueous solutions; therefore, they cause severe accelerated corrosion of more active metals, such as aluminum and its alloys and the ferrous metals. Somewhat similar to the nickel alloys, they lie between the active and passive positions for stainless steels (Fig. 3) and therefore induce localized corrosion of the active alloys.

Nickel and Its Alloys

Nickel and its alloys are not readily polarized and will therefore cause accelerated corrosion of more active materials, such as aluminum and ferrous alloys. In chloride-bearing solutions, nickel is somewhat more noble than copper, and the cupronickels lie somewhere in between. Nickel and its alloys are similar to copper alloys in their effects on stainless steels. In some environments, the cast structure of a nickel weld may be anodic to the wrought parent metals.

The combination of their passive surface with their inherent resistance places nickel-chromium alloys such as Inconel alloy 600 and Hastelloy alloy C-276 in more noble positions in the traditional galvanic series. In chloride-bearing solutions, Inconel alloy 600 is reported to occupy two positions because of the existence of active and passive states in a manner similar to the stainless steels (Fig. 3). It is highlighted in black to indicate this. These alloys are readily polarized, and galvanic effects on other less noble metals and alloys therefore tend to be minimized.

Cobalt-Base Alloys

Cobalt-base alloys, most of which are chromium bearing, are resistant to galvanic corrosion because of their noble position in the galvanic series. However, in environments in which their passive film is not stable, they occupy a more active position and can be adversely affected by more noble materials. The fact that they polarize readily tends to reduce their galvanic effects on less noble materials.

Reactive Metals (Titanium, Zirconium, and Tantalum)

Reactive metals (titanium, zirconium, and tantalum) are extremely noble because of their passive films. In general, these alloys are not susceptible to galvanic corrosion, and their ease of polarization tends to minimize adverse galvanic effects on other metals or alloys. Because of the ease with which they pick up hydrogen in the atomic state, they may themselves become embrittled in galvanic couples. Tantalum repair patches in glass-lined vessels have been destroyed by contact with cooling coils or agitators made of less noble alloys. Tantalum is susceptible to attack by alkalis, such as may form in the vicinity of a cathode in neutral solutions.

Noble Metals

The term *noble metal* is applied to silver, gold, and platinum group metals. This designation in itself describes their position in the galvanic series and their corresponding resistance to galvanic corrosion. However, they do not polarize readily and can therefore have a marked effect in galvanic couples with other metals or alloys. This effect is observed with gold and silver coatings on copper, nickel, aluminum, and their alloys.

Uniform Corrosion

Uniform corrosion, or general corrosion, is a corrosion process exhibiting uniform thinning that proceeds without appreciable localized attack. It is the most common form of corrosion and may appear initially as a single penetration, but with thorough examination of the cross section it becomes apparent that the base material has uniformly thinned.

Uniform chemical attack of metals is the simplest form of corrosion, occurring in the atmosphere, in solutions, and in soil, frequently under normal service conditions. Excessive attack can occur when the environment has changed from that initially expected. Weathering steels, magnesium alloys, zinc alloys, and copper alloys are examples of materials that typically exhibit general corrosion. Passive materials, such as stainless steels, aluminum alloys, or nickel-chromium alloys, are generally subject to localized corrosion. Under specific conditions, however, each material may vary from its normal mode of corrosion.

Uniform corrosion commonly occurs on metal surfaces having homogeneous chemical composition and microstructure. Access to the metal by the attacking environment is generally unrestricted and uniform. Any gradient or changes in the attacking environment due to the corrosion reaction or stagnancy can change the degradation mode away from uniform corrosion. At the microlevel, uniform corrosion is found to be an electrochemical reaction between adjacent closely spaced microanodic and microcathodic areas. Consequently, uniform corrosion may be considered to be localized electrolytic attack occurring consistently and evenly over the surface of the metal.

This is well illustrated in binary alloys that contain phases of differing corrosion potentials. The grain in one phase becomes anodic to the grain in the second phase in the microstructure, thus producing an electrolytic cell when the proper electrolyte is present.

Another illustration is ductile cast iron, where there are three compositionally different phases within the material: ferrite, pearlite, and graphite. The corrosion process will initiate as uniform corrosion with the formation of an electrolytic microcell between the graphite cathode and ferrite or pearlite anode (Ref 9, 10). The process can turn into a pitting mechanism if the microcells develop enough to produce acidic gradients within the micropits where the graphite nodules lie or are dislodged. Uniform corrosion occurring by the microelectrolytic or galvanic cell in the ductile cast iron is shown in Fig. 8. Observe the initial stages of micropits being formed by these microcells.

Surface Conditions

All metals are affected by uniform corrosion in some environments; the rusting of steel and the tarnishing of silver are typical examples of uniform corrosion. In some metals, such as steel, uniform corrosion produces a somewhat rough surface by the oxidation/reduction reaction, in which the end product (oxide) either dissolves in the environment and is carried away or produces a loosely adherent, porous coating now greater in thickness. Because of the porosity in the oxidation (rust), this metal is still considered active or able to continue degrading. Coating specialists have been able to formulate a phosphoric-acid-based compound that reacts with the rust to produce an oxide that makes the surface passive and seals the surface from water and other solutions.

In contrast to the active surfaces formed typically on steels, some metals form dense, insulated, tightly adherent passive films from uniform-corrosion processes, with the metal surface remaining somewhat smooth. Examples of these include the tarnishing of silver in air, lead in sulfate-containing environments, and stainless steel in humid air creating passive films.

Classification of Uniform Corrosion

In general terms, uniform corrosion can be classified further according to the specific conditions of environmental or electrochemical attack. For example, uniform thinning can be attributed to various conditions, such as:

- Atmospheric corrosion
- Aqueous corrosion
- Galvanic corrosion
- Stray-current corrosion (which is similar to galvanic corrosion but does not rely on electrochemically induced driving forces to cause rapid attack)
- Biological corrosion (which is a microbial-assisted form of attack that can manifest itself as uniform corrosion by forming weak or cathodic oxides, or it can also produce a localized form of attack)
- Molten salt corrosion and liquid metal corrosion (which have become more of a concern as the demand for higher-temperature heat-transfer fluids increases)
- High-temperature (gaseous) corrosion

Corrosive attack for these conditions is not necessarily restricted to just uniform thinning. Other forms of corrosive attack (such as stress-corrosion cracking, dealloying, or pitting) may also be operative.

Following are some examples of uniform-corrosion-related failures and their prevention and evaluation. Appropriate methods of controlling uniform corrosion in some situations are noted. Selection of a metal that has a suitable resistance to the environment in which the specific part is used and the application of paints and other types of protective coatings are two common methods used to control uniform corrosion. Modification of the environment by changing its composition, concentration, pH, and temperature or by adding an inhibitor is also effective.

Example 2: Uniform Corrosion of Carbon Steel Boiler Feedwater Tubes.

The carbon steel tubes shown in Fig. 9 have been severely reduced, revealing a lacelike pattern of total metal loss. These steel tubes are from a boiler feedwater heater feeding a deaerator. As part of the boiler-water treatment program, it was decided to inject a chelate to control scale formation in the boiler tubes. Unfortunately, the chelate was added ahead of the preheater, where the boiler water still contained oxygen (O_2). As the chelate removed iron oxide, the O_2 formed more iron oxide, and this uniform dissolution of steel reduced the tubing to the totally corroded condition shown. Moving the chelate addition to a point after the deaerator stopped the corrosion and allowed reuse of steel in the preheater.

Fig. 8 Scanning electron micrograph of ductile cast iron graphite nodules and ferritic phase after corrosion tests. Note the loss of material at the interface of the nodule. Original magnification: 2000×. Source: Ref 11, 12

Example 3: Uniform Corrosion of a Copper Pipe Coupling.

The 25 mm (1 in.) copper coupling shown in Fig. 10 has been uniformly degraded around most of the circumference of the bell and partially on the spigot end. One penetration finally occurred through the thinned area on the spigot end of this pipe. The pipe was buried in noncorrosive sandy soil but was found to incur stray currents of 2 V direct current in relation to a $Cu/CuSO_4$ half-cell. Eliminating, moving, or shielding the source of stray current are obvious solutions.

Example 4: Uniform Corrosion of Copper Piping Caused by Microbiological Attack.

Microbiological attack of copper piping has been well documented and was found in a

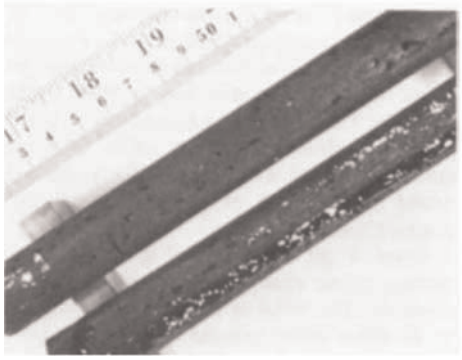

Fig. 9 Uniform corrosion of steel tubes in boiler feedwater containing oxygen (O_2) and a chelating water-treating chemical

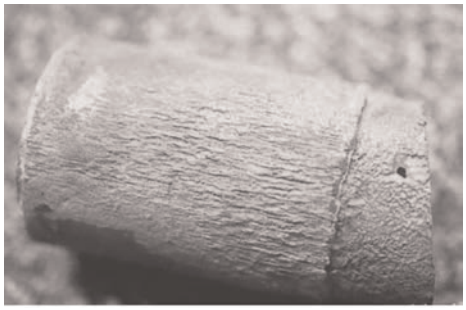

Fig. 10 A 25 mm (1 in.) copper coupling from a potable water system that had degraded uniformly from stray currents. The spigot end has been penetrated near the edge of the bell. Courtesy of MDE Engineers, Inc.

closed-loop water heater system. Figure 11 shows the microbes that were cultured from the corrosion product. They were found to be sulfur-reducing bacteria. Uniform thinning occurred when the resultant copper oxide on the copper pipe surface eroded in low flow rates. The threshold for erosion by turbulent waters is much lower with this type of oxide and found to penetrate this same pipe, as shown in Fig. 12.

Materials Selection

Materials selection is usually straightforward for uniform corrosion, because the corrosion is relatively easy to evaluate and monitor. If a material shows only general attack with a low corrosion rate, or if only negligible contamination is present in a process fluid or on the surface, then cost, availability, and ease of fabrication may be the dominant influence on the material of choice. An acceptable corrosion rate for a relatively low-cost material such as plain carbon steel is approximately 0.25 mm/year (10 mils/year) or less. At this rate and with proper design with adequate corrosion allowance, a carbon steel vessel will provide many years of low-maintenance service.

For more costly materials, such as austenitic stainless steels and copper and nickel alloys, a maximum corrosion rate of 0.1 mm/year (4 mils/year) is generally acceptable. However, a word of caution is in order. One should never assume that the higher-alloyed material or the higher-cost material is more corrosion resistant in a given environment. Proper evaluation is required. For instance, seawater corrodes plain carbon steel fairly uniformly at a rate of 0.1 to 0.2 mm/year (4 to 8 mils/year) but also severely pits certain austenitic stainless steels. The same is true for stagnant solutions; the steel becomes passive or protected, where some austenitic stainless steels will pit due to the formation of autocatalytic corrosion cells.

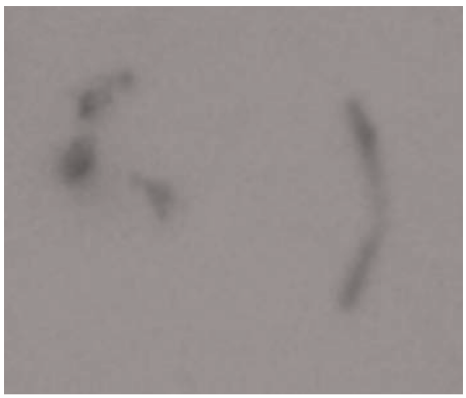

Fig. 11 Micrograph of large bacteria (sulfur-reducing bacteria) that are rod shaped. Note this is a chain of two bacteria cultured from microbiologically induced corrosion product of the pipe failure shown in Fig. 12. Original magnification: 400×. Courtesy of MDE Engineers, Inc.

At times, nonmetallic coatings and linings ranging in thickness from a few tenths to several millimeters are applied to prolong the life of low-cost alloys such as plain carbon steels in environments that cause general corrosion. The thin-film coatings that are widely used include baked phenolics, catalyzed cross-linked epoxy-phenolics, and catalyzed coal tar-epoxy resins (see the section "Protective Coatings and Linings" in the article "Analysis and Prevention of Environmental and Corrosion-Related Failures" in this Volume).

It is not advisable to use thin-film coatings in services where the base metal corrosion rate exceeds 0.5 mm/year (20 mils/year), because corrosion is often accelerated at holidays (pinholes or scratches) in the coating. Thick-film linings—which include glass, fiber- or flake-reinforced furan, polyester and epoxy resins, hot-applied coal tar enamels, and various elastomers such as natural rubber—may be more appropriate.

Effect of Corrosion Products

The by-products of uniform corrosion may be of greater concern in materials selection than the effect on the material itself. For food and chemical processing and biomedical applications, contamination of the process fluid by even trace amounts of corrosion products may be unacceptable. Product purity, rather than corrosion rate, is the prime consideration.

One example is storage of 93% sulfuric acid (H_2SO_4) in plain carbon steel at ambient temperature. The general corrosion rate is 0.25 mm/year (10 mils/year) or less, but traces of iron impart a color that is objectionable in many applications. Therefore, thin-film baked phenolic coatings are used on carbon steel to minimize or eliminate iron contamination. In the same way, thin-film epoxy-coated carbon steel or solid or clad austenitic stainless steels are used to maintain the purity of adipic acid for various food and synthetic fiber applications.

Effect of Concentration

The effect on corrosion rate of a metal part does not follow a uniform pattern with the increase or decrease in the concentration of the corrodent. This is because of ionization effects in aqueous solutions and the effects of even trace amounts of water in nonaqueous environments, and changes that occur in the characteristics of any film of corrosion products that may be present on the surface of the metal. Typical patterns of corrodent-concentration effects on corrosion rates are illustrated in Fig. 13 (Ref 12), which plots the corrosion rate of iron and steel as a function of the concentration of three common inorganic acids in aqueous solutions at room temperature.

The rate of corrosion of a given metal usually increases as the concentration of the corrodent increases, as shown in Fig. 13(a) for the corrosion of iron in hydrochloric acid. However, corrosion rate does not always increase

Fig. 12 Micrograph of 19 mm (0.75 in.) copper piping in a closed-loop water system with microbiologically induced corrosion and erosion of the weak oxide layer. Original magnification: 20×. Courtesy of MDE Engineers, Inc.

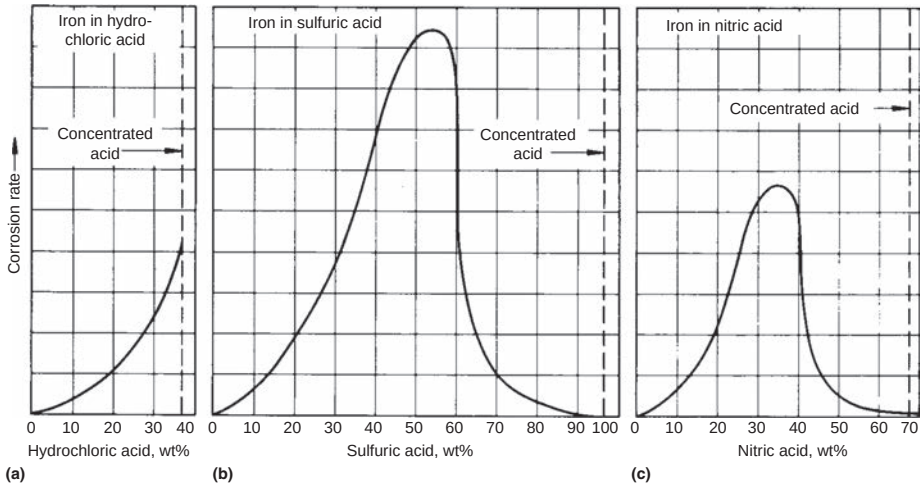

Fig. 13 Effect of acid concentration on the corrosion rate of iron completely immersed in aqueous solutions of three inorganic acids at room temperature. It should be noted that the scales for corrosion rate are not the same for all three charts. As discussed in the text, the corrosion rate of iron (and steel) in nitric acid in concentrations of 70% or higher, although low compared to the maximum rate, is sufficient to make it unsafe to ship or store nitric acid in these metals. Source: Ref 12

with concentration of the corrodent; the maximum rate may occur over a preferred range of corrodent concentration, as shown in Fig. 13(b) and (c) for iron and steel in sulfuric acid and in nitric acid, respectively.

Because corrosion is electrochemical and involves anodic and cathodic reactions, process variables influence corrosion rate if they influence one or both reactions. For example, the main cathodic reaction for iron corroding in dilute inorganic acids is $2H^+ + 2e \rightarrow H_2\uparrow$. The more hydrogen ions available, the faster the rate of the cathodic reaction. In turn, this permits a high rate of anodic dissolution: ($M \rightarrow M^{+n} + ne$), where M stands for metal. This is what happens throughout the concentration range in hydrochloric acid solutions.

In both nitric acid and sulfuric acid solutions, the hydrogen ion concentration increases with acid concentration to a point, but at the higher levels of acid concentration, it decreases again. Iron may be used to handle concentrated sulfuric acid at ambient temperatures. Care must be taken to avoid any contamination with water, because this will dilute the acid and increase the rate of attack. Also, impurities in the acid or the iron can increase the rate of attack.

The corrosion rate of iron and steel at room temperature in nitric acid decreases with increasing concentration above approximately 35% because of the formation of a passive oxide film on the metal surface. However, this passive condition is not completely stable.

The rate of attack for concentrations of 70% or higher, although low compared to the maximum rate shown in Fig. 13, is still greater than 1.3 mm/year (50 mils/year), making iron and steel unsuitable for use in shipping and storing nitric acid at any concentration. Nitric acid in bulk is usually stored and shipped in type 304 stainless steel (up to 95%), aluminum alloy 3003 or 1100, or commercially pure titanium (grade 2).

Metals that have passivity effects, such as Monel 400 in hydrochloric acid solutions and lead in sulfuric acid solutions, corrode at an extremely low rate at low acid concentration at room temperature. They lose their passivity at a certain limiting acid concentration above which the corrosion rate increases rapidly with increasing acid concentration.

Effect of Temperature

When investigating the effect of temperature on the corrosion rate of a metal in a liquid or gaseous environment, the temperature at the metal-corrodent interface must be considered. This temperature may differ substantially from that of the average of the corrodent. Laminar flow would permit temperature gradients to exist. This difference is especially important for heat-transfer surfaces, where the hot-wall effect causes a much higher corrosion rate than may be expected.

A common approximation for chemical activity, called the "10 degree rule," states that an increase of 10 °C (18 °F) in bulk temperature of the solution can increase the corrosion rate by a factor of 2 or more. In atmospheres, the temperature variation is more complex because both temperature and humidity affect corrosion, and they are interdependent.

Hot-wall failures are fairly common in heating coils and heat-exchanger tubes. An example of this hot-wall effect is the corrosion rate of Hastelloy B (nickel-molybdenum, N10001) in 65% H_2SO_4. At 120 °C (250 °F), the corrosion rate would be less than 0.5 mm/year (20 mils/year). However, a Hastelloy B heating coil in the same solution may have a surface-wall temperature of 145 °C (290 °F) and a corrosion rate greater than 5 mm/year (200 mils/year), a factor of 10 greater.

In some metal-corrodent systems, there is a threshold temperature above which the corrosion rate increases dramatically. Caution is advised whenever extrapolating known corrosion rates to higher temperatures.

Temperature changes sometimes affect corrosive attack on metals indirectly. In systems where an adherent protective film on the metal may be stable in a given solution at room temperature, the protective film may be soluble in the solution at higher temperatures, with the result that corrosion can progress rapidly.

When boiling occurs in the solution, other factors also influence the rate of attack on a metal immersed in it. One factor may be simply an increase in velocity of movement of the liquid corrodent against the metal surface, which in turn increases the corrosion rate. More radical changes may occur at the metal surface, such as the substitution of steam and spray in place of liquid as the corrodent or the formation of a solid film on the metal surface—either of which may completely alter the metal-corrodent interface conditions.

There are some exceptions to the general rule that increasing temperature increases the corrosion rate. One is the reduction in rate of attack on steel in water as the temperature is increased, because the increase in temperature decreases the oxygen content of the water, especially as the boiling point of the water is approached. Other exceptions arise where a moderate increase in temperature results in the formation of a thin protective film on the surface of the metal or in passivation of the metal surface.

If thick deposits are formed on a heat-transfer surface, they have a twofold effect by changing the metal surface temperature and making crevice corrosion possible. The existence of the thick deposit may be a failure mode itself, if it limits the heat transfer. Local differences in temperature on a heat-transfer surface exposed to steam can influence corrosion rates by causing differences in the duration of exposure to condensation. For example, the inner surface of a carbon steel tube that carried saturated steam at 234 °C (454 °F) corroded to a greater depth opposite exterior heat-transfer fins than elsewhere on the inner surface (Fig. 14). The heat loss through the fins lowered the temperature of the inner surface of the tube in the area beneath the fins, resulting in the presence of condensate on this area for a greater percentage of the time and in a correspondingly greater loss of metal than elsewhere on the inner surface. All corroded areas were fairly smooth.

Evaluation Factors

Because uniform corrosion is one of the most common forms of corrosion, it must be considered in nearly every design. The damage

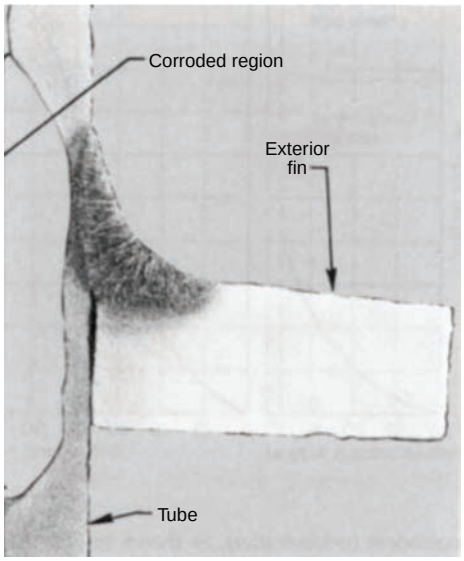

Fig. 14 Carbon steel steam tube that corroded on the inner surface more rapidly opposite the exterior heat-transfer fin than elsewhere along the tube. Etched longitudinal section. Original magnification: 3×

may be just cosmetic at its inception, but as the thickness of the metal decreases uniformly, loss of mechanical function can result. Fortunately, uniform corrosion is usually easy to measure and predict; this facilitates proper design and the ability to take corrective action. Corrosion rate and expected service life can be calculated from periodic measurements of the general thinning produced by uniform corrosion. Because the rate of attack can change over a period of time, periodic inspection at suitable intervals is ordinarily carried out to avoid unexpected failures. Varying conditions can also accelerate some corrosion rates; therefore, generous safety factors regarding thickness allowances should be employed.

Testing Methods

Testing for uniform corrosion can be broadly classified as:

- Laboratory long-term testing
- Laboratory accelerated testing
- In-service or field testing.

Laboratory Long-Term Testing

Laboratory long-term testing usually consists of testing materials in simulated-service conditions on a relatively small scale. The advantage of this type of testing is that the test parameters can be controlled closely; thus, any unintentional disturbances that could occur during plant tests can be avoided.

Accelerated Laboratory Tests

Accelerated laboratory tests, on the other hand, are short term in nature. They are designed to compare materials under severe conditions, and the test environment may not be directly related to the service environment. The environment and the test conditions must be carefully specified. ASTM International has outlined standard methods for testing materials under accelerated conditions. ASTM G 1 (Ref 13) provides details on evaluating corrosion damage.

Service Tests and Plant Tests

Service tests and plant tests involve placing test samples in actual service conditions for evaluation. The advantage of such testing is the relevance of the results to the actual service environment. However, the problems involved in tracking and interrupting normal operations are also associated with this type of corrosion testing.

Testing Goals

The purposes of measuring uniform corrosion by experimental testing are:

- Evaluation and selection of materials for a specific environment or application
- Evaluation of metals and alloys to determine their effectiveness in new environments
- Routine testing to confirm the quality of materials
- Research and development of new materials

In most cases, uniform-corrosion rates are represented as a loss of metal thickness as a function of time. This value can be directly measured from experimental data, or, as is often the case, it can be calculated from mass-loss data. Mass loss is a measure of the difference between the original mass of the specimen and the mass when sampled after exposure. In measuring the mass after exposure, it is important to remove any corrosion product adhering to the sample, as described in the article "Evaluating Uniform Corrosion" in *Corrosion: Fundamentals, Testing, and Protection*, Volume 13A of the *ASM Handbook*, 2003; see also ASTM G 1 (Ref 13).

Evaluations

Evaluations that are often included in testing for uniform corrosion include:

- Visual observations, unaided and using light optical and scanning electron microscopy
- Ion concentration increase
- Hydrogen evolution
- Loss in tensile strength (according to ASTM G 50, Ref 14)
- Electrochemical testing

Initial observations in any corrosion testing should include unaided visual or low-magnification observation of the form of corrosion. Visual evaluation can include reporting of the color and form of corrosion products and can include documentation with photographs.

In addition to the standard measurement of mass loss, the increase of metal ions in solution as the metal corrodes can be measured by analysis of samples of the corrodent removed periodically during the test (Ref 15). It may be possible to relate the increase in concentration to corrosion rate, depending on the structure of the test. In some cases, the amount of hydrogen generated in deaerated tests can be used to measure corrosion rates (Ref 16, 17). These methods are useful during in-service and field testing where the process fluid may be more available for analysis than the corroding object.

Electrochemical tests can also be used to determine corrosion rates and predict uniform-corrosion rates. Electrochemical methods include creating anodic and cathodic polarization curves, extrapolation of Tafel lines, and polarization break testing. Methods for conducting electrochemical tests are addressed in ASTM G 59 (Ref 18), G 3 (Ref 19), and G 5 (Ref 5). Reference 11 also explains some standard practices in this area, and electrochemical test methods are discussed in the article "Electrochemical Methods of Corrosion Testing" in *Corrosion: Fundamentals, Testing, and Protection*, Volume 13A of the *ASM Handbook*, 2003.

Design Considerations

When designing systems where uniform corrosion will likely occur, it is essential to establish regular inspections and preventive maintenance. The criticality of the system, ease of inspection and maintenance, and corrosion rate must be considered when establishing the intervals. It must be understood that applied stresses, changes in loading, and varying environmental conditions could accelerate the rate of attack.

Pitting and Crevice Corrosion

Pitting and crevice corrosion are forms of localized corrosion that are significant causes of failure in metal parts. Both forms attack passivated or otherwise protected materials.

Pitting, characterized by sharply defined holes, is one of the most insidious forms of corrosion. It can cause failure by perforation while producing only a small weight loss on the metal. This perforation can be difficult to detect and its growth rapid, leading to unexpected loss of function of the component.

Crevice corrosion is pitting that occurs in slots and in gaps at metal-to-metal and metal-to-nonmetal interfaces. It is a significant contributor to component failure because such gaps often occur at critical joining surfaces.

Pitting

Causes of pitting corrosion include:

- Local inhomogeneity on the metal surface
- Local loss of passivity
- Mechanical or chemical rupture of a protective oxide coating
- Discontinuity of organic coating (holidays)
- Galvanic corrosion from a relatively distant cathode

- Formation of a metal ion or oxygen-concentration cell under a solid deposit (crevice corrosion)

Every engineering metal or alloy is susceptible to pitting. Pitting occurs when one area of a metal surface becomes anodic with respect to the rest of the surface or when highly localized changes in the corrodent in contact with the metal, as in crevices, cause accelerated localized attack.

Pitting on clean surfaces ordinarily represents the start of breakdown of passivity or local breakdown of inhibitor-produced protection. When pits are few and widely separated and the metal surface has undergone little or no general corrosion, there is a high ratio of cathode-to-anode area. Penetration progresses more rapidly than when pits are numerous and close together.

The most common causes of pitting in steels are surface deposits that set up local concentration cells and dissolved halides that produce local anodes by rupture of the protective oxide film. Anodic corrosion inhibitors, such as chromates, can cause rapid pitting if present in concentrations below a minimum value that depends on the metal-environment combination, temperature, and other factors. Pitting also occurs at mechanical ruptures in protective organic coatings if the external environment is aggressive or if a galvanic cell is active.

Buried pipelines that fail because of corrosion originating on the outside surface usually fail by pitting corrosion. Another form of corrosion affecting pipelines involves a combination of pitting and erosion (erosion-corrosion). This form of corrosive attack is discussed in the section "Velocity-Affected Corrosion" in this article.

Pitting normally occurs in a stagnant environment. With corrosion-resistant alloys, such as stainless steels, the most common cause of pitting corrosion is highly localized destruction of passivity by contact with moisture that contains halide ions, particularly chlorides. Chloride-induced pitting of stainless steels usually results in undercutting, producing enlarged subsurface cavities or caverns.

Example 5: Pitting Corrosion of Stainless Steel by Potable Water in an Organic Chemical Plant Condenser (Ref 20).

Several tubes in a 35 m (115 ft) type 316 stainless steel shell-and-tube condenser leaked unexpectedly in an organic chemical plant that produces vinyl acetate monomer (VAM). Leaks were discovered after five years of operation and relocation of the condenser to another unit in the same plant. Examination of tubes and tube sheets revealed pitting damage on the outside-diameter (OD) surface. Some of the pits had penetrated fully, resulting in holes. Inside-diameter (ID) surfaces were free of corrosion. Macro- and microexaminations indicated that the tubes had been properly manufactured. Pitting was attributed to stagnant water on the shell side. It was recommended that the surfaces not be kept in contact with closed stagnant water for appreciable lengths of time.

Service History

A shell-and-tube condenser is fixed vertically on top of a jacketed reactor that produces VAM (Fig. 15). The VAM vapor enters the tube side at the bottom of the condenser at approximately 80 °C (175 °F), is cooled and condensed by the circulating water on the shell side, and falls back to the reactor under gravity. The cooling water used is municipal supply water. The condenser had been in operation for five years in one of the units when it was shut down for nontechnical reasons. Water had been left stagnant on the shell side in the unit for three months after equipment shutoff until it was shifted to the second unit of the same plant and positioned on top of a similar reactor producing the same VAM vapors. While the shell side was being refilled with water, profuse leakage was noted. Upon opening the shell, it was revealed that almost all the tubes were pitted, with fully penetrating holes.

Pertinent Specifications

The 117 tubes were of type 316 austenitic stainless steel manufactured by the seamless process to specification ASTM A 213. The tubes were 31.75 mm (1.25 in.) OD, had a 1.65 mm (0.065 in.) wall thickness, and were 3.0 m (9.8 ft) long. The tube sheets were also made of type 316 stainless steel, while the shell, tie rod, and baffle materials were of carbon steel. The VAM vapor was free from chlorides, with somewhat acidic condensate. The cooling water was 6.5 to 7 pH, with approximately 20 ppm chlorides.

Visual Examination

Almost all the tubes had pitting damage on the OD surface. Some of the pits had penetrated fully, resulting in holes. Figure 16 shows the pits on the OD surface of two tubes. The nature of the pits indicates that they started on the OD surface and propagated both toward the interior of the tube wall and downward along the outside wall. The ID surfaces of the tubes were free from any form of corrosion. Also free from corrosion was the pipe that connects the reactor and the condenser and is exposed to the VAM vapor and the condensate.

The bottom tube sheet showed deep pit marks on the shell side, while the top tube sheet was free from any form of corrosion. The baffle plates and the tie rods were completely corroded and practically disintegrated. Similarly, the shell, also of carbon steel, showed heavy corrosion on the inside, with a very rough nonuniform surface and thick, brownish rust scale.

Test Results

Chemical analysis of one of the pitted tubes indicated a composition (wt%) of 17.35% Cr, 13.46% Ni, and 2.19% Mo. These values fall within the specification for type 316 stainless steel. Macroexamination of the tested tube indicated that it was seamless. Microexamination of the tubes showed a uniform equiaxed austenitic structure with a grain size of ASTM 8 to 9, free from carbide precipitation. This indicated that the tubes had been properly manufactured.

Conclusions

The test results indicated that there was not a quality problem with the material. The

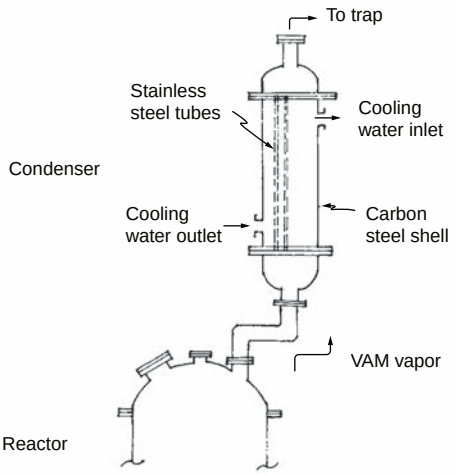

Fig. 15 Layout of a stainless steel reactor condenser that experienced pitting corrosion. VAM, vinyl acetate monomer. Source: Ref 20

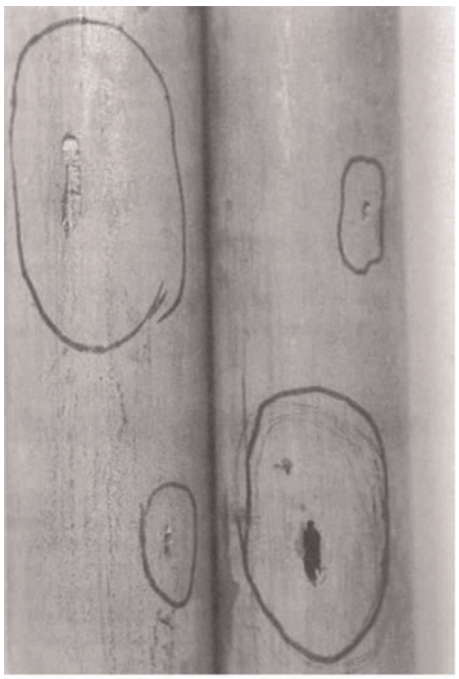

Fig. 16 Pitting on the outside surface of type 316 stainless steel tubes, with downward propagation. Source: Ref 20

discussion with plant personnel indicated that the stagnant water on the shell side (OD side of the tubes) caused the pitting.

Municipal potable water with neutral pH is normally not corrosive to type 316 stainless steel. In this particular case, no corrosion problem had been experienced during operation for five years. However, even such water becomes corrosive to stainless steel if kept stagnant for extended periods. The aggressiveness increases if the stagnant water is kept closed, without access to atmospheric oxygen. Under such conditions, pitting results. Corrosion of the carbon steel contributed to the removal of oxygen in the water.

Once the pits were initiated, the liquid trapped inside the pit became denser and more acidic than the bulk, and corrosion was accelerated, extending partly toward the inner surface of the tube and partly in a downward direction. This explains the propagation and elongation of the pits (Fig. 16).

It was recommended that the stainless steel surface not be kept in contact with closed stagnant water for extended periods, even if the water is of municipal potable quality.

Difficulty of Detection

Pits are generally small and often remain undetected. A small number of isolated pits on a generally uncorroded surface are easily overlooked. A large number of very small pits on a generally uncorroded surface may not be detected by simple visual examination, or their potential for damage may be underestimated. When pits are accompanied by slight or moderate general corrosion, the corrosion products often mask them.

Pitting is sometimes difficult to detect in laboratory tests and in service because there may be a period of months or years, depending on the metal and the corrodent, before the pits initiate and develop to a readily visible size. Delayed pitting sometimes occurs after an unpredictable period of time in service, when some change in the environment causes local destruction of a passive film. When this occurs on stainless steels, for example, there is a substantial increase in solution potential of the active area, and pitting progresses rapidly.

Stages of Pitting

Immediately after a pit has initiated, the local environment and any surface films on the pit-initiation site are unstable. The pit may become inactive after just a few minutes if convection currents sweep away the locally high concentration of hydrogen ions, chloride ions, or other ions that initiated the local attack. Accordingly, the continued development of pits is favored in a stagnant solution. ASTM G 46, "Standard Guide for Examination and Evaluation of Pitting Corrosion," presents the method used by industry to quantify the intensity or severity of the pitting-corrosion mechanism.

When a pit has reached a stable stage, barring drastic changes in the environment, it penetrates the metal at an ever-increasing rate by an autocatalytic process. In the pitting of a metal by an aerated sodium chloride solution, rapid dissolution occurs within the pit, while reduction of oxygen takes place on adjacent surfaces. This process is self-propagating. The rapid dissolution of metal within the pit produces an excess of positive charges in this area, causing migration of chloride ions into the pit.

Thus, in the pit there is a high concentration of MCl_n and, as a result of hydrolysis, a high concentration of hydrogen ions. Both hydrogen and chloride ions stimulate the dissolution of most metals and alloys, and the entire process accelerates with time. Because the solubility of oxygen is virtually zero in concentrated solutions, no reduction of oxygen occurs within a pit. Cathodic reduction of oxygen on the surface areas adjacent to pits tends to suppress corrosion on these surface areas. Thus, isolated pits cathodically protect the surrounding metal surface.

Because the dense, concentrated solution within a pit is necessary for its continuing development, pits are most stable when growing in the direction of gravity. Also, the active anions are more easily retained on the upper surfaces of a piece of metal immersed in or covered by a liquid.

This gravitational effect was seen on the tubes of Fig. 16, as discussed in example 5.

The rate of pitting is related to the aggressiveness of the corrodent at the site of pitting and the electrical conductivity of the solution containing the corrodent. For a given metal, certain specific ions increase the probability of attack from pitting and accelerate that attack once initiated. Pitting is usually associated with metal-environment combinations in which the general corrosion rate is relatively low; for a given combination, the rate of penetration into the metal by pitting can be 10 to 100 times that by general corrosion.

Depth of Penetration

The depth of pitting can be expressed by the pitting factor (Fig. 17) (Ref 21). A value of 1 would represent uniform corrosion. The maximum depth of penetration (p) can be measured by several methods, including metallographic examination, machining, or use of a micrometer or microscope. The average penetration depth (d) is calculated from the weight lost by the sample. The maximum penetration depth is extremely significant if the metal is part of a barrier or tank or a pressurized system. The micrograph in Fig. 18 shows the profile of pits that have degraded an austenitic stainless steel thin-walled bellows.

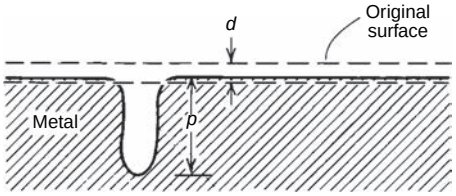

Fig. 17 Measurements used to determine the pitting factor, p/d, where p is the maximum penetration, and d is the average penetration depth

Density and Size of Pitting

For a mechanical component, the density of pits (number per unit surface area) and size may be a more critical characteristic than maximum depth. The loss of effective cross section can decrease the strength of the component, and pits can become sites of stress concentrations. ASTM G 46 points out, conversely, that the loss of mechanical properties can be used to evaluate the severity of pitting corrosion (Ref 22).

Example 6: Corrosion Failure by Oxygen Pitting of a Carbon Steel Boiler Tube.

Four tube sections were removed from two separate fire-tube boilers in a commercial building. The steam generated from the boilers was used for heating. One tube section had leaked during service due to pitting corrosion; the other three tubes exhibited severe pitting on their OD surfaces, but it had not penetrated the full wall thickness of the tubes.

Service History

The pitted tubes were discovered due to excessive make-up water being used for the subject boilers. The specified material grade for the tubes was ASME specification SA178, grade A, "Standard Specification for Electric-Resistance-Welded Carbon Steel and Carbon-Manganese Steel Boiler and Superheater Tubes." The specified dimensions were 63.5 mm (2.5 in.) OD and 11-gage (3.0 mm, or 0.12 in.) minimum wall thickness.

Analysis

The OD surface of the boiler tubes at and away from the pits was not covered with a high level of deposits. The surface of the corrosion pits had a thin layer of corrosion

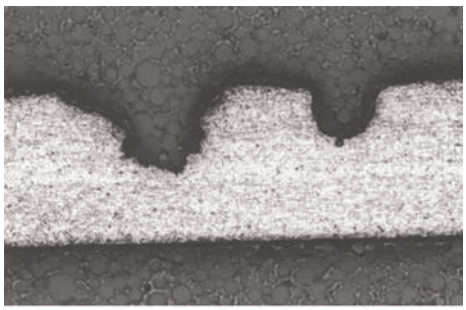

Fig. 18 Light micrograph showing the general microstructure and cross section of corrosion pits in an austenitic stainless steel thin-walled bellows. Total thickness of sheet: ~0.5 mm (0.02 in.). Etchant: 10% oxalic acid. Original magnification: 100×. Courtesy of M.D. Chaudhari, Columbus Metallurgical Service

product, and the corrosion product was primarily composed of an iron oxide. This was confirmed with energy-dispersive x-ray spectroscopy. The depth of the pitting was greater than 80% of the original wall thickness on the tubes where leakage had not occurred. The through-wall pitting location on the failed boiler tube is shown in Fig. 19.

Metallographic Inspection

Metallographic inspection of the through-wall corrosion pit showed a hemispherical pit with a thin layer of corrosion product along the pit surface.

Conclusions

The degradation on the tubes was consistent with severe corrosion pitting along the OD (water side) of the tubes. The physical features of the corrosion pitting were consistent with oxygen pitting. These features consisted of a hemispherical pit geometry with corrosion product consisting predominantly of iron oxide.

Corrective Measures

Oxygen pitting in boiler tubing is the result of excessive levels of oxygen in the boiler feedwater. It was recommended that the water treatment practices for the boiler feedwater and condensate be reviewed to determine if there were deficiencies in the water treatment program resulting in excessive oxygen levels in the feedwater. Also, sources of air leakage into the steam system were to be investigated as another possible source of the excessive oxygen levels.

Example 7: Fatigue Fracture of Stainless Steel Wires in an Electrostatic Precipitator at a Paper Plant (Ref 23).

Several type 316L stainless steel wires in an electrostatic precipitator at a paper plant fractured in an unexpectedly short time. The wires were 2.6 mm (0.10 in.) in diameter. The chemical specification of the steel from which the wires were made was similar to a type 316L stainless steel. The wires were also specified to be ¾ hard (heat treat condition).

Service Conditions

Wires were subjected to stress by weights hung from them and were exposed to a very corrosive gas effluent. They were periodically vibrated to free particles that adhered to them.

Analysis

Failed wires were examined using optical and scanning electron microscopes, and hardness tests were conducted. Fractography clearly established that fracture was caused by fatigue originating at corrosion pits on the surface of the wire (Fig. 20). Similar pits were found on all wires at the fatigue crack origin and along the surface of the wires (Fig. 21).

Corrective Recommendation

The gas effluent was very corrosive, but the general attack on the surface of the wires appears slight. Thus, an austenitic stainless steel appears to be a reasonable choice. Also, specifying a steel similar to type 316L is reasonable because the molybdenum content (2 to 3%) is designed to inhibit pitting corrosion. However, pitting did occur; thus, it was recommended that a higher-molybdenum austenitic stainless steel, type 317L (3 to 4% Mo), be used (although the lower limit of molybdenum content is identical to the upper limit of type 316L). It was also recommended that the wires be used in the annealed condition, unless other aspects (e.g., static loading) required a material of high tensile strength.

Fracture Origins

Origins of corrosion-fatigue fractures are often surrounded by crack-arrest lines, or beach marks (Fig. 22). Often, there are several origins, particularly when fracture has been initiated by pitting (Fig. 23). Occasionally, no well-defined origin can be resolved.

Features at the origin of a corrosion-fatigue fracture are often indistinct because the compression portion of each stress cycle has forced mating fracture surfaces together and has formed an extremely rubbed, discolored origin (arrow, Fig. 22). Also, the area of the origin is exposed to the environment for the longest

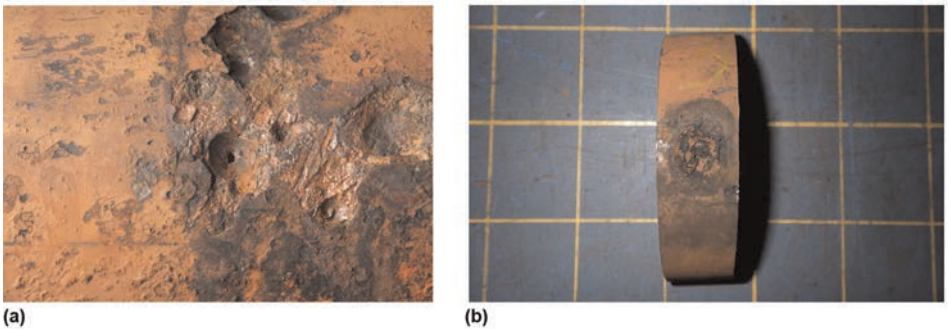

Fig. 19 Oxygen pitting along the outside-diameter surface of boiler tubes from a fire-tube boiler. (a) Through-wall pitting due to oxygen pitting. (b) Oxygen pitting had penetrated approximately 80% of the boiler tube wall thickness on this sample.

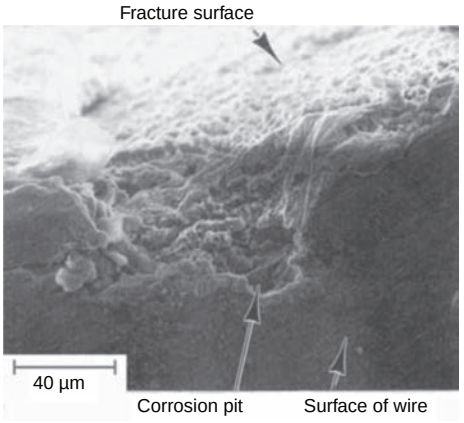

Fig. 20 Scanning electron micrograph showing a corrosion pit at the origin of a fatigue fracture in a stainless steel wire. Source: Ref 23

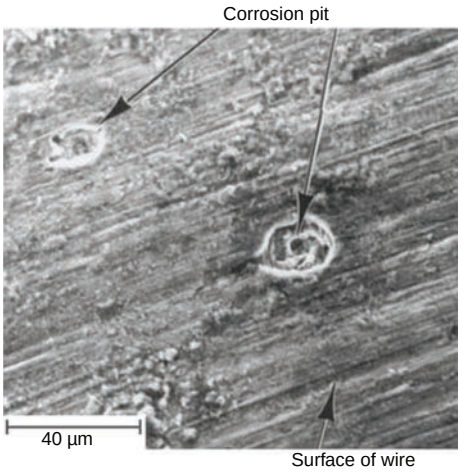

Fig. 21 Scanning electron micrograph of the surface of a stainless steel wire showing corrosion pits. Source: Ref 23

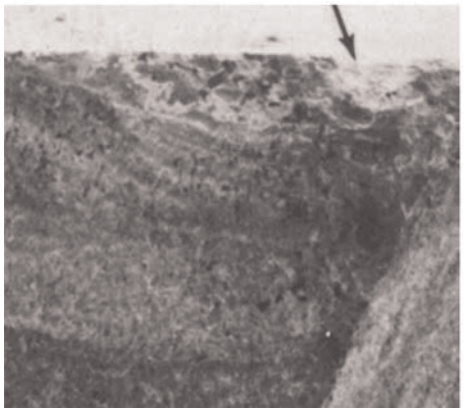

Fig. 22 Single-origin corrosion-fatigue crack in type 403 stainless steel exposed to steam showing rubbed origin (arrow) and beach marks. Scanning electron fractograph (secondary electron image). Original magnification: 60×

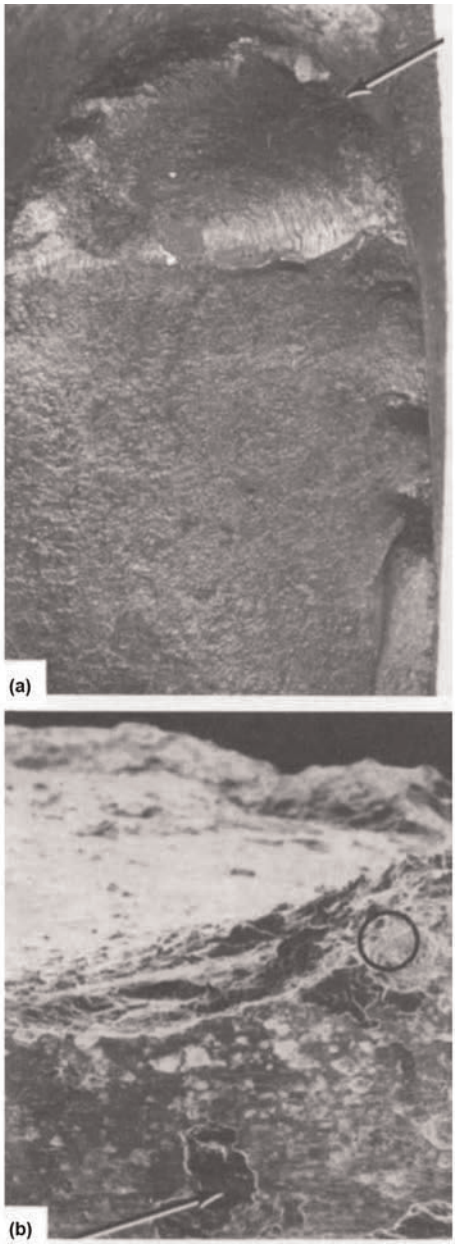

Fig. 23 Two views of the fracture surface of a forged 17-4 PH stainless steel steam-turbine blade that failed by corrosion fatigue originating at severe corrosion pitting. (a) Light fractograph showing primary origin (arrow) and three secondary origins (along right edge below primary origin). Original magnification: 7.5×. (b) Scanning electron fractograph (secondary electron image) of area surrounding primary origin (in circle). Original magnification: 50×. White areas are corrosion pits. Black areas, one of which is indicated by arrow, are remnants of corrosion product left after the fracture surface was electrolytically cleaned.

time and thus may exhibit more extensive residues of a corrosion product than the rest of the fracture surface. A corrosion product at fatigue origins can be misleading when viewed macroscopically. The oxide may be flat and tenacious, globular, or nodular. At magnifications of less than 60, globular or nodular oxide particles are easily mistaken for intergranular facets; therefore, no conclusions should be drawn until other metallographic or fractographic techniques confirm the mechanism of crack initiation. Occasionally, oxidation is so severe that no information other than location of origin can be obtained.

Other features that can be observed macroscopically are secondary cracks, pits, and fissures, all of which are often adjacent to the main origin of a particular fracture. In corrosion-fatigue failures, cracks and fissures adjacent to the primary origin are indicative of a uniform state of stress at that location. Therefore, the primary fracture simply propagated from the flaw that either induced the most severe stress concentration or was exposed to the most aggressive local environment. Sometimes, the primary crack origin is related more to heterogeneous microstructure than to the stress distribution.

Pitting of Various Metals

With carbon and low-alloy steels in relatively mild corrodents, pits are often generally distributed over the surface and change locations as they propagate. If they blend together, the individual pits become virtually indistinguishable, and the final effect is a toughened surface but a generally uniform reduction in cross section. If the initial pits on carbon steel do not combine in this way, the result is rapid penetration of the metal at the sites of the pits and little general corrosion.

Despite their good resistance to general corrosion, stainless steels are more susceptible to pitting than other metals. High-alloy stainless steels containing chromium, nickel, and molybdenum are also more resistant to pitting but are not immune under all service conditions.

The pitting resistance equivalent number (PREN), or pitting index, is devised to quantify and compare the resistance of alloys to pitting:

$$\text{PREN} = \%\text{Cr} + 3.3(\%\text{Mo}) + 16(\%\text{N}) \qquad \text{(Eq 1)}$$

The higher the number, the more resistant the alloy is to pitting and crevice corrosion. A variety of PREN equations have been developed for specific alloy and weld material groups (Ref 24). Equations include effects of nickel, manganese, nitrogen, tungsten, and carbon.

Pitting failures of corrosion-resistant nickel alloys, such as Hastelloy C, Hastelloy G, and Incoloy 825, are relatively uncommon in solutions that do not contain halides, although any mechanism that permits the establishment of an electrolytic cell in which a small anode is in contact with a large cathodic area offers the opportunity for pitting attack.

In active metals, such as aluminum and magnesium and their alloys, pitting also begins with the establishment of a local anode. However, a major effect on the rate of pitting penetration is that the corrosion products of these metals produce a high pH in the pit, thus accelerating the dissolution of the protective oxide film. Although the surrounding metal may be exposed to relatively pure water, the metal at the bottom of a pit corrodes at an appreciable rate, even in the absence of galvanic effects. Maintaining surface cleanness helps avoid pitting of these metals.

Pitting of aluminum and magnesium and their alloys in aqueous solutions is often accelerated by galvanic effects, which occur because these metals are anodic to most other metals, and by the effects of dissolved metallic ions and suspended particles in the solution. Pitting of these metals can be caused by even a few parts per billion of dissolved copper compounds as well as by particles of metallic iron (which produce both crevice and galvanic effects) that are embedded in or adhering to their surfaces.

Example 8: Corrosion by "Green Death" in Reboiler Bypass Duct Damper in Power-Generation Plant (Ref 24).

"Green Death" is a corrosive medium used to test for pitting resistance composed of 11.9% H_2SO_4 + 1.3% HCl + 1% $FeCl_3$ + 1% $CuCl_2$. The solution is heated to boiling, 103 °C (217 °F), for the test. Such a corrosive environment occurs at power plants.

Service Environment

A continuous supply of flue gas comes in contact with a closed bypass duct. The unscrubbed combustion products condense on the cold duct. Then the closed damper conducts heat from the chimney and reheats the condensate. The environment was severe enough to cause the C-276 nickel alloy welds (N10276) on the C-276 duct floor to completely corrode in less than half a year.

Corrective Measures

686CPT weld alloy was used to repair the C-276 plates. The plate continued to corrode at a rate greater than 1 mm/year (40 mils/year). The plate itself was then replaced by alloy 686 plate (N06686) welded with 686CPT.

Conclusions

Although the original materials are recognized for their resistance to corrosion and heat, the 686 alloy composition has superior pitting resistance, as indicated by higher PREN or pitting index values according to several formulas. Tests of welded coupons corroborate this conclusion.

Crevice Corrosion

A crevice at a joint between two metallic surfaces, between a metallic and a nonmetallic surface, or beneath a particle of solid matter on a metallic surface provides conditions that are conducive to the development of the type of concentration-cell corrosion called crevice corrosion. Crevice corrosion can progress very rapidly (tens to hundreds of times faster than the normal rate of general corrosion in the same given solution). The classic example of

this is a demonstration that a sheet of stainless steel can be cut (corroded) into two pieces simply by wrapping a rubber band around it, then immersing the sheet in seawater or dilute ferric chloride solution. The open surfaces will pit slowly, but the metal under the rubber band will be attacked rapidly for as long as the crevice between the rubber band and the steel surface exists.

In a metal-ion-concentration cell, the accelerated corrosion occurs at the edge of or slightly outside of a crevice. In an oxygen-concentration cell, the accelerated corrosion usually occurs within the crevice between the mating surfaces.

Riveted and Bolted Joints

Riveted and bolted joints must be considered prime sites for crevice corrosion; therefore, they require careful attention in design and assembly to minimize crevices, as well as provisions to ensure uniform aeration and moderate but not excessive flow rates at the joints. Not only does the geometry of the joint itself promote crevice corrosion, but corners and cracks can collect debris, which exacerbates the potential for corrosion.

Replacement with welded joints can eliminate crevice corrosion, provided special care is taken in welding and subsequent finishing of the welds to provide smooth, defect-free joints. Adhesive bonding alone or adhesive bonding prior to riveting is used to overcome crevice corrosion in aluminum (Ref 25).

Figure 24 is an example of crevice corrosion where type 316 stainless steel bubble caps contacted a type 316 tray deck. At the contact points, the type 316 stainless steel was selectively corroded by the concentrated acetic acid solution. In this part of the distillation column, the oxidizing capacity of the acid stream is nearly exhausted but is sufficient to prevent corrosion of the open surfaces. A change to a higher-alloy stainless steel was necessary to fully resist these corrosive conditions. Any layer of solid matter on the surface of a metal that offers the opportunity for exclusion of oxygen from the surface or for accumulation of metal ions beneath the deposit because of restricted diffusion is a probable site for crevice corrosion.

Differential aeration beneath solid deposits or at cracks in mill scale is a frequent cause of crevice corrosion in boilers and heat exchangers. Suitable water treatment to provide thin protective films, together with special attention to cleaning, rinsing, and drying when boilers are shut down, minimizes the occurrence of crevice corrosion in such equipment. Breaks (holidays) in protective organic coatings or linings on vessels containing corrosive chemicals are also likely sites for the development of crevice corrosion.

Example 9: Crevice Corrosion on Stainless Steel Tube.

A steel tube meeting type 304 specification (0.008 max C, 18.00 to 20.00 Cr, 2.00 max Mn, 8.00 to 10.50 Ni, with all values in weight percent) was found to be corroded, as shown in Fig. 25. The tube was part of a piping system, not yet placed in service, that was exposed to an outdoor marine environment containing chlorides. As part of the assembly, a fabric bag containing palladium oxide (PdO_2) was taped to the tube. The palladium served as a "getter." The corrosion in this area was discovered during routine inspection. A closeup (Fig. 26) of the tube shows the corrosion products. Pits are the darkest areas. Slightly lighter areas include remnants of the fabric bag.

Analysis

Corrosion debris was analyzed using an electron-dispersive spectrometer. The profiles confirmed the presence of chlorides and palladium. Both contributed to corrosion in the crevice created by the tape on the tube, which was periodically exposed to water.

Corrective Measures

Steps were taken to prevent water from entering and being trapped in this area of the assembly.

Liquid-Level Effects

Crevice corrosion often occurs underneath deposits of solid substances that sometimes collect just above the liquid level on a metal part that is partly immersed in an electrolyte. The deposits usually remain moist or are intermittently moist and dry.

Where the liquid level fluctuates or where the liquid is agitated, the area of the metal that is intermittently wetted is called the splash zone. Splash zones are encountered in all types of tanks and equipment containing liquids; corrosion occurring in these areas is called splash-zone corrosion.

Example 10: Crevice Corrosion of a Carbon Steel Brine Tank.

A failure caused by this type of crevice corrosion occurred in a carbon steel tank that contained a saturated solution of sodium chloride (brine) at room temperature. When a pump that was apparently in good condition failed to deliver brine, inspection showed that a steel suction line, partly immersed in the liquid and used to transfer small amounts of brine to other equipment, had corroded through in the intermittently wetted area. Further inspection showed that the tank had also been attacked in the intermittently wetted area. The corrosion problem was eliminated by replacing the steel suction line with a glass-fiber-reinforced epoxy pipe and by lining the tank with a coal-tar epoxy coating.

Example 11: Corrosion of Steel Pilings.

Rust films that have little opportunity to dry do not develop protective properties. Such unfavorable conditions exist in the splash zone above the high-tide level along the seashore.

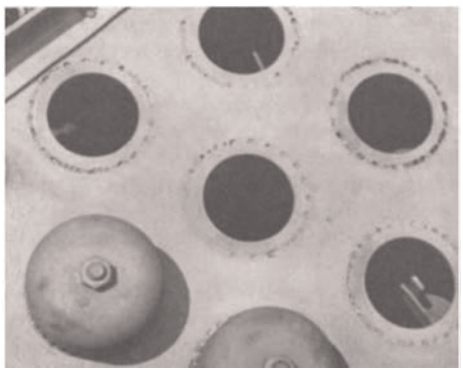

Fig. 24 Crevice corrosion pitting that has taken place where type 316 bubble caps contact a type 316 stainless steel tray deck. The oxygen-concentration cell corrosion occurred in concentrated acetic acid with minimal oxidizing capacity. 1/8 actual size

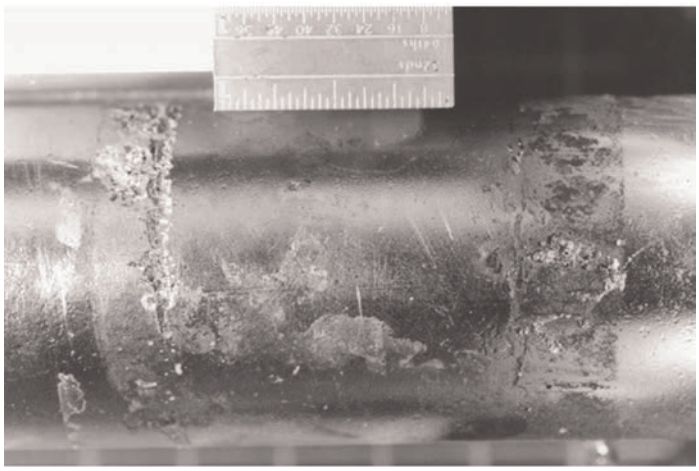

Fig. 25 Austenitic stainless steel tube that was corroded where a fabric bag was taped to it. Courtesy of M.D. Chaudhari, Columbus Metallurgical Service

The corrosivity of the moist rust films is further aggravated by the high oxygen content of the splashing seawater. Observations of old steel piling along the seashore usually reveal holes just above the water line, where the rate of corrosion is several times greater than that for continuous immersion in seawater.

Corrosion Under Insulation

This form of corrosion is the result of the application of an insulating product or blanket that retains moisture from the exterior process conditions or from the condensation of atmospheric moisture on cold surfaces and the retention of that moisture by the insulating system, resulting in long-term corrosion deterioration of the metal surface it is covering. This condition can take place with thermal insulation for hot or cold surface protection.

The application of thermal insulation to carbon steel and stainless steel equipment presents a special case of crevice corrosion. It is special because there are a number of misconceptions about the role of thermal insulation in this corrosion situation, and the phenomenon is not, strictly speaking, crevice corrosion but does not comfortably fit in any other category. Thermal insulation is used to maintain temperature of equipment, either below ambient or above ambient; therefore, the metal normally will operate at temperatures different from the surrounding temperature. Because of this situation, the thermal insulation system—which consists of the metal outer surface, the annular space between the metal and the insulation, the insulation itself, and its weather barrier—is a dynamic, pervious combination of materials. The weather barrier or weather proofing, coating, wrapping, or cladding, while intended to protect the insulation from the ravages of weather and other mechanical damage, does not prevent the entry of humidity and moisture to the annular space between the metal surface and the inner side of the insulation.

Therefore, with moisture present on the metal surface, the insulation acts as a barrier in terms of the evaporation of the moisture and maintains it in a vapor phase in contact with the metal surface. The corrosion process is accelerated by the presence of oxygen as well as contaminants/corrodents (chlorides) that may be in the insulation. This system can then become very aggressive when the metal temperature is operating in the range of 40 to 120 °C (100 to 250 °F). At these elevated temperatures, the humid annular space can corrode steel at rates as high as 0.8 mm/year (0.03 in./year) or, in the case of stainless steel, can initiate chloride stress-corrosion cracking with relatively rapid failure times.

The approach to preventing corrosion under insulation has been examined by many investigators (Ref 26). Attempts are being made to produce insulation materials of high purity and with silicate-type inhibitors added. However, they offer limited protection against aggressive atmospheres that may be introduced beneath the insulation through cracks, crevices, and other openings in the insulation. The most widespread approach at this time is to use a protective coating on the metal to protect it from the water vapor existing in the annular space.

The most severe environments develop when the vessels or piping operate with cycling temperatures, that is, operate below ambient for a period of time and then go through a heating cycle that tends to evaporate the water but go through the hot metal corrosion temperature zone.

The problem of corrosion under thermal insulation has become widely recognized as one of significant concern. Because of the hidden nature of the problem, a well-insulated vessel may operate for many years without any apparent external signs of damage, while significant corrosion is taking place under the insulation.

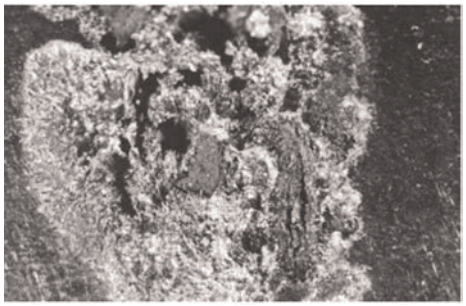

Fig. 26 Micrograph of an area approximately 10 mm (3/8 in.) wide from the tube shown in Fig. 25. Pits are the dark areas in the center. Lighter areas include fragments of the bag among the corrosion products. Courtesy of M.D. Chaudhari, Columbus Metallurgical Service

Effects of Solid Deposits

In power-generation equipment, crevice-corrosion failures have occurred in main-station condenser tubes cooled with seawater as a result of the formation of solid deposits and the attachment of marine organisms to the tube wall. These failures have occurred particularly in condensers with stainless steel tubing.

Failures on the inside of tanks have been attributed to weld splatter that went undetected. The splatter created unnecessary and unwanted crevices. Good practices would have dictated that such weld splatter be ground off.

Weld Crater Crack Corrosion

Many alloys experience the formation of crater cracking at the termination of the weld bead because of poor welding practice. These cracks are identified as crater cracks, which act as a crevice in a corrosive medium.

In type 347 austenitic stainless steel, poor welding practice can form a crater crack at the termination or stop point of a weld bead. Metallurgically, this failure is related to microsegregation of certain constituents in the pool of molten metal that is the last to solidify on a weld. In a manner similar to zone-melting refinement, the moving weld pool continuously sweeps selected constituents ahead of it, and the concentration of these selected constituents in the pool increases continuously until the welding is stopped and the pool solidifies. The center of the stop point is attacked rapidly in oxidizing acids, such as nitric acid, in a form of self-accelerating crevice corrosion. The final solidification pool need not extend through the thickness of the part for full perforation to occur, as described in Example 12.

Example 12: Weld Craters in Stainless Steel Heat-Exchanger Tubes.

Beveled weld-joint V-sections were fabricated to connect inlet and outlet sections of tubes in a type 347 stainless steel heat exchanger for a nitric acid concentrator. Each V-section was permanently marked with the tube numbers by a small electric-arc pencil.

After one to two years of service, multiple leaks were observed in the heat-exchanger tubes. When the tubes were removed and examined, it was found that the general corrosion rate was normal for service of heat-exchanger tubes in a nitric acid concentrator, but that crater corrosion had perforated the tubes.

The weld crater crack crevice corrosion occurred at two general locations. One location was at the stop point of the welds used to connect the inlet and outlet legs of the heat exchanger. The other location was at the stop points on the identifying numerals. The material was changed to type 304L stainless steel, in which the zone-melting concentration does not take place.

Crevice Corrosion of Implant Materials

A large number of stainless steels have been evaluated with a modified PREN equation for resistance to crevice corrosion in body fluids (Ref 27). To avoid allergies due to nickel, high-manganese stainless steel is under consideration, along with duplex stainless steels and other austenitic stainless steels. Titanium is widely used, and cobalt-chromium alloys also exhibit a passive nature in the body.

ASTM F 746 (Ref 28) is a test method for evaluating the crevice and pitting corrosion resistance of a material to rank its suitability for surgical implants. Evaluation is based on the critical electrical potential for pitting or crevice corrosion. The test is severe, so it does not follow that materials that corrode in the test will corrode when implanted. This is but one of the criteria in the materials selection process. Obviously, the effect of corrosion products within the body is of paramount importance.

It has been known for some time that certain stainless steel implants had been subject to crevice corrosion. The reaction of implants to body fluids is quite like the reaction to

seawater. Crevices occur at the interface where screws attach the implant, chlorides are present, and oxygen is depleted in the crevice. Evidence of crevice corrosion was observed in 90% of stainless steels in one study cited in 1985 (Ref 29). In a 1980 study (Ref 30), it was noted that in stainless steel devices where more than one component was present, such as bone plates, interfacial corrosion approached 100%.

Failure analysis is complicated by the fact that it is difficult to determine if the screw-plate interface of surgically recovered damaged implants was damaged prior to implantation, during implantation, or during removal.

Microbiologically Influenced Corrosion (Ref 31)

Microbiologically influenced corrosion (MIC) is a corrosion process that is affected by the presence or actions of microorganisms that may be present in biofilms on the surface of corroding materials. The corrosion degradation resulting from MIC typically propagates either as a corrosion pit or as crevice corrosion. Microbiologically influenced corrosion is covered in greater detail in the article "Biological Corrosion Failures" in this Volume.

Microbiologically influenced corrosion can occur in many environments, including water and petroleum products, and can affect many metals and their alloys. The degradation resulting from MIC can be associated with the metabolic process of the responsible microorganisms or attack from by-products produced by the microorganisms.

Some of the specific characteristics associated with the microorganisms that can cause and/or contribute to MIC include the following:

- They can withstand a wide range of temperatures, pH levels, and oxygen concentrations.
- Many species produce organic acids, such as formic and succinic acids, which can initiate or accelerate pitting corrosion on many metals.
- Some microorganisms produce mineral acids that generate sulfuric acid, which can be highly corrosive to many metals.
- A number of organisms can form ammonia from the metabolism of amino acids. This process forms ammonium ions in solution, which may play a role in the corrosion of certain alloys, such as copper alloys.
- Many organisms produce carbon dioxide and hydrogen gas as a result of their fermentative type of metabolism. Carbon dioxide in solution with water forms carbonic acid, which can be corrosive to some metals. Hydrogen can depolarize metals such as stainless steel or may even cause embrittlement of certain metals.

Many of the by-products or metabolic activity of the microorganisms that cause and/or contribute to MIC result in pitting corrosion. The biofilm associated with these microorganisms can also produce a crevice that results in crevice corrosion.

Reducing Failures due to Pitting and Crevice Corrosion

Steps to minimize pitting and crevice corrosion include:

- Reducing the harshness of the environment
- Selecting appropriate materials
- Avoiding galvanic couples
- Avoiding rupture of any natural or applied protective coatings
- Avoiding contact with stagnant solutions or providing circulation of otherwise stagnant solutions
- Modifying component design to eliminate crevices and ensure proper drainage
- Inspecting and maintaining critical components so that pitting and crevice corrosion do not develop into more catastrophic failures

Testing can point the way to the most effective approach to avoiding failures. Testing for localized corrosion resistance is used to (Ref 32):

- Rank alloys for development and materials selection
- Analyze failures
- Determine effects of changes in process parameters
- Predict penetration rates

Currently available tests aid in making more informed decisions regarding materials selection and system and process design.

Intergranular Corrosion

Intergranular corrosion is the preferential dissolution of the anodic component, the grain-boundary phases, or the zones immediately adjacent to them, usually with slight or negligible attack on the main body of the grains. The galvanic potential of the grain-boundary areas of an alloy is anodic to that of the grain interiors due to differences of composition or structure. These differences may be due to the environmental interactions or metallurgical changes in the grain-boundary regions during manufacturing or service exposure.

Development of Intergranular Corrosion

Intergranular corrosion is usually (but not exclusively) a consequence of composition changes in the grain boundaries from elevated-temperature exposure. In general, grain boundaries can be susceptible to changes in composition, because grain boundaries are generally slightly more active chemically than the grains themselves. This is due to the areas of mismatch in the grain-boundary regions relative to the more orderly and stable crystal lattice structure within the grains. The relative disorder in the grain boundaries provides a rapid diffusion path, which is further enhanced by elevated-temperature exposure. Therefore, a variety of chemical changes may occur preferentially in the grain-boundary areas, such as segregation of specific elements or compounds, enrichment of an alloying element, or the depletion of an element when precipitates nucleate and grow preferentially in this region. Impurities that segregate at grain boundaries may also promote galvanic action in a corrosive environment.

When the compositional changes in the grain boundary result in a more anodic material or galvanic potential difference, the metal becomes "sensitized" and may be susceptible to intergranular attack in a corrosive environment. A well-known example of this is the sensitization of austenitic stainless steels caused by diffusion of chromium and trace amounts of carbon around the grain boundaries during the elevated-temperature "sensitizing" exposure and precipitation of chromium carbides. This process is always associated with the welding of unstabilized austenitic 300-series stainless steels and can be corrected by using the low-carbon-modification (L-grade) alloys or stabilized stainless steels through the addition of titanium or columbium plus tantalum. Some aluminum alloys exhibit similar behavior with the precipitation of $CuAl_2$ or Mg_2Al_3, depending on the alloy.

Example 13: Intergranular Corrosion of an Aluminum Alloy Ship Hull.

The 5*xxx* series of aluminum alloys are often selected for weldability and are generally very resistant to corrosion. However, if the material has prolonged exposure at slightly elevated temperatures of 66 to 180 °C (150 to 350 °F), an alloy such as 5083 can become susceptible to intergranular corrosion.

This sensitizing has occurred in ship hulls with disastrous consequences in the corrosive marine environment. This sensitization occurred in a new ship hull after only three months in service. Figure 27 is typical of many cracks that were discovered. The microstructure revealed the familiar ditch structure of sensitized aluminum alloy (Fig. 28, 29).

A corrosion test was performed according to ASTM G 67 (Ref 33). The test confirmed the susceptibility of this particular material to intergranular corrosion, because the test sample suffered a mass loss of 67 mg/cm^2 (429 mg/in.^{2}). By the standard, susceptible materials have a mass loss ranging from 25 to 75 mg/cm^2 (160 to 480 mg/in.^{2}). This relatively large mass loss occurs because corrosion around grain boundaries causes grains to separate from the sample. A material considered not

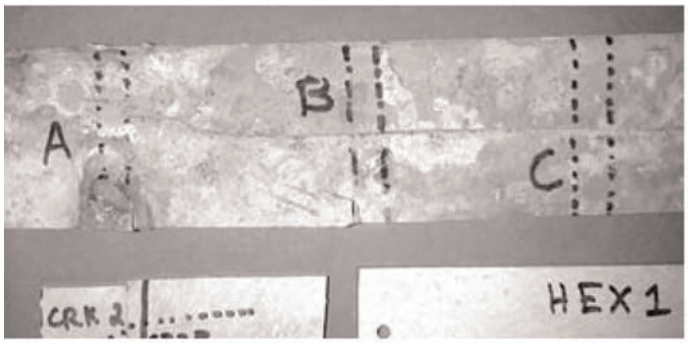

Fig. 27 Cracking in a 5083 aluminum alloy ship hull caused by sensitization. Courtesy of MDE Engineers, Inc.

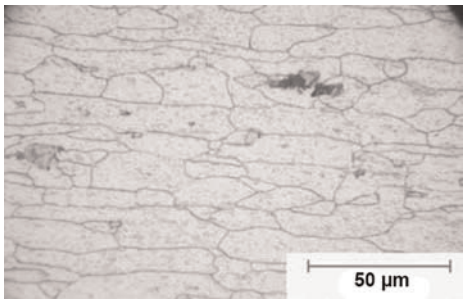

Fig. 28 Microstructure of 5083 aluminum alloy ship hull that has been sensitized. Courtesy of MDE Engineers, Inc.

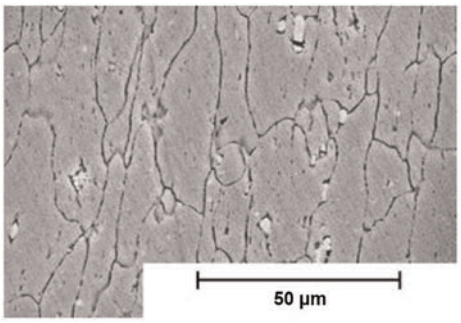

Fig. 29 Scanning electron micrograph of sensitized 5083 aluminum microstructure shown in Fig. 28. Courtesy of MDE Engineers, Inc.

susceptible to intergranular corrosion would suffer a mass loss from 1 to 15 mg/cm^2 (10 to 100 mg/in.^{2}).

During exposures to chloride solutions such as seawater, the galvanic couples formed between these precipitates and the alloy matrix result in severe intergranular attack.

Alloy Susceptibility

Intergranular corrosion can occur in many alloy systems under specific circumstances; susceptibility depends on the corrosive solution and on the metallurgical factors of alloy composition, fabrication, and heat treatment parameters. Comprehensive coverage of alloy system-environment combinations is beyond the scope of this article. However, the general evaluation and some commonly occurring conditions of intergranular corrosion are briefly described in the following sections. Individual alloy families are addressed. Susceptibility of a component to intergranular corrosion can be corrected by proper heat treatment (to distribute alloying elements more uniformly), modification of the alloy, or the use of a completely different alloy.

Although grain-boundary corrosion is sometimes associated with differences in electrochemical potential (as in some aluminum alloys; see example 13 in this article), intergranular corrosion is usually not the result of active grain boundaries and a passive matrix. Usually the corroding surface is at one potential. Differences in composition produce different corrosion rates at the same potential in the passive region. Figure 30 illustrates the electrochemistry of intergranular corrosion by comparing the polarization curves for grain-boundary and matrix areas. The corrosion rates are close or the same in the active and transpassive ranges but vary considerably with potential in the passive range.

Susceptibility to intergranular corrosion cannot be taken as a general indication of increased susceptibility to other forms of corrosion, such as pitting or uniform corrosion. Likewise, testing for susceptibility to intergranular attack should not be considered equivalent to evaluating the resistance of the alloy to general and localized corrosion, even though the tests used for evaluating susceptibility to intergranular attack may be severe. They are not intended to duplicate conditions for the wide range of chemical exposures present in an industrial plant.

When the attack is severe, entire grains may be dislodged because of the complete deterioration of their boundaries. When an alloy is undergoing intergranular corrosion, its rate of weight loss may accelerate with time. As the grain-boundary area dissolves, the unaffected grains are undermined and separate from the material; this increases the rate of weight loss.

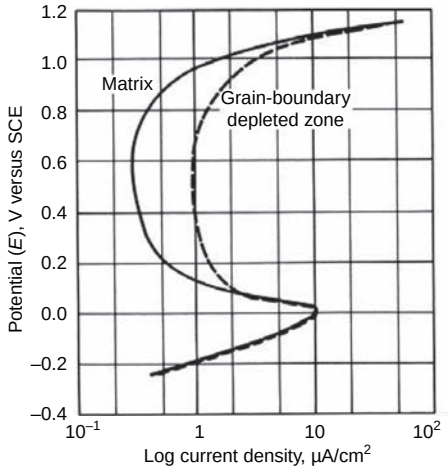

Fig. 30 Anodic polarization behavior of an active-passive alloy with grain-boundary depleted zones. SCE, saturated calomel electrode

Typical weight-loss curves for an alloy undergoing intergranular corrosion are shown in Fig. 31 (Ref 34).

Evaluation of Intergranular Corrosion

The metallurgical changes that lead to intergranular corrosion are not always observable in the microstructure; therefore, corrosion tests may sometimes be the most sensitive indication of metallurgical changes. Corrosion tests for evaluating the susceptibility of an alloy to intergranular attack are typically classified as either simulated-service or accelerated tests. Simulated-service testing is a valuable predictor of corrosion behavior; however, accelerated tests may also be needed to evaluate the long-term susceptibility of alloys.

Over the years, specific tests have been developed and standardized for evaluating the susceptibility of various alloys to intergranular attack. Various aspects of the phenomenon of sensitization, the mechanism of intergranular corrosion, tests for sensitization, and recent advances in such testing are reviewed in Ref 35 for austenitic stainless steels. The standard practice for detecting susceptibility of austenitic stainless steels is ASTM A 262 (Ref 36), which describes five practices that are either destructive to the sample or qualitative in nature. With modification of evaluation criteria, the practices in ASTM A 262 can be used to evaluate susceptibility of ferritic stainless steels, duplex stainless steels, and nickel-base alloys to intergranular corrosion.

Electrochemical Potentiokinetic Reactivation Technique

The electrochemical potentiokinetic reactivation (EPR) technique is described in ASTM G 108 (Ref 37). This test method overcomes the limitations of practices in ASTM A 262 by providing a nondestructive means of

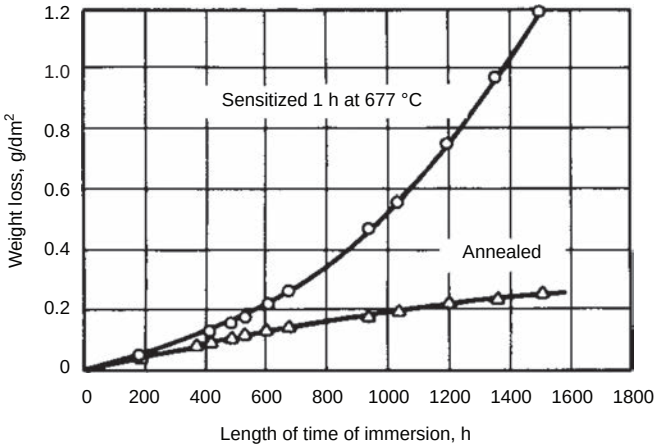

Fig. 31 Corrosion of type 304 steel in inhibited boiling 10% (H_2SO_4). Inhibitor: 0.47 g Fe^{3+}/L of solution added as $Fe_2(SO_4)_3$. Source: Ref 30

quantifying the degree of sensitization in austenitic stainless steels (Ref 38). This test method also has found wide acceptance in quantitative nondestructive evaluation of sensitization on intergranular corrosion and intergranular stress-corrosion cracking (IGSCC) of ferritic stainless steels, duplex stainless steels, and nickel-base alloys.

The EPR technique detects the extent of the chromium-depleted region in stainless steels by passivating the metal and then reactivating it through a decreasing potential sweep (Ref 39). This nondestructive test provides a quantitative indication of the degree of sensitization. The EPR measurements are done by either single-loop (Ref 40) or double-loop (Ref 41, 42) procedures. Post-EPR replica metallography is also an effective means to confirm EPR results (Ref 43). The EPR test is also considered for on-site measurement with portable equipment (Ref 44).

Intergranular Corrosion and Stress-Corrosion Cracking

Intergranular corrosion and stress-corrosion cracking (SCC) may occur under similar conditions for some alloys. An example of this involves the strain-hardened 5*xxx* series of aluminum-magnesium alloys. They are susceptible to intergranular attack caused by continuous grain-boundary precipitation of highly anodic Mg_2Al_3 compounds during certain manufacturing conditions, or after being subjected to elevated temperatures up to approximately 175 °C (350 °F). There is a parallel relationship between the susceptibility to intergranular attack (including exfoliation) and SCC for these alloys.

However, the susceptibility to intergranular corrosion does not necessarily equate with a susceptibility to IGSCC. In the presence of residual or applied stress, failure by SCC can occur before substantial intergranular attack has occurred. Conversely, some nickel-base alloys are actually more resistant to SCC when they are sensitized to intergranular corrosion (Ref 45).

Intergranular Corrosion of Stainless Steels

Although stainless steels provide resistance against general corrosion and pitting, the 300 and 400 series of stainless steels may be susceptible to intergranular corrosion by sensitization. It is caused by the precipitation of chromium carbides and/or nitrides at grain boundaries during exposure to temperatures from 450 to 870 °C (840 to 1600 °F), with the maximum effect occurring near 675 °C (1250 °F). The resulting depletion in chromium adjacent to the chromium-rich carbides/nitrides provides a selective path for intergranular corrosion by specific media, such as hot oxidizing (nitric, chromic) and hot organic (acetic, formic) acids. A partial list of environments known to cause intergranular corrosion in sensitized austenitic stainless steel is given in Table 2 (Ref 46).

The extent of the sensitization effect is a function of time, temperature, and the alloy composition. The latest varieties of intergranular-corrosion-resistant stainless steels are described in Ref 47 along with general remedies for intergranular corrosion in various stainless steels and recently introduced procedures for intergranular corrosion testing procedures, such as the copper-copper sulfate-sulfuric acid test and the EPR test. Economical evaluation of stainless steels for their resistance to intergranular corrosion is reviewed in Ref 48.

The typical appearance of intergranular corrosion of stainless steels is shown in Fig. 32 for an attack on sensitized type 304 stainless steel at 80 °C (180 °F) in water containing a low concentration of fluorides in solution. Intergranular corrosion of the type shown in Fig. 32 is more or less randomly oriented and does not have highly localized propagation, as does intergranular stress corrosion, in which cracking progresses in a direction normal to applied or residual stresses. For austenitic stainless steels, the susceptibility to intergranular corrosion is mitigated by solution heat treating at 1065 to 1120 °C (1950 to 2050 °F) and with water quenching. By this procedure, chromium carbides are dissolved and retained in solid solution. However, solution heat treatment may be difficult on many welded assemblies and is generally impracticable on large equipment or when making repairs.

Susceptible stainless steels are those that have normal carbon contents (generally >0.04%) and do not contain carbide-stabilizing

Table 2 Partial listing of environments known to cause intergranular corrosion in sensitized austenitic stainless steels

Environment	Concentration, %	Temperature, °C (°F)
Nitric acid	1	Boiling
	10	Boiling
	30	Boiling
	65	60 (140) to boiling
	90	Room to boiling
	98	Room to boiling
Lactic acid	50–85	Boiling
Sulfuric acid	30	Room
	95	Room
Acetic acid	99.5	Boiling
Formic acid	90	Boiling
	10 (plus Fe^{3+})	Boiling
Chromic acid	10	Boiling
Oxalic acid	10 (plus Fe^{3+})	Boiling
Phosphoric acid	60–85	Boiling
Hydrofluoric acid	2 (plus Fe^{3+})	77 (170)
Ferric chloride	5	Boiling
	25	Room
Acetic acid anhydride mixture	Unknown	100–110 (212–230)
Maleic anhydride	Unknown	60 (140)
Cornstarch slurry, pH 1.5	Unknown	49 (120)
Seawater	...	Room
Sugar liquor, pH 7	66–67	75 (167)
Phthalic anhydride (crude)	Unknown	232 (450)

Source: Ref 46

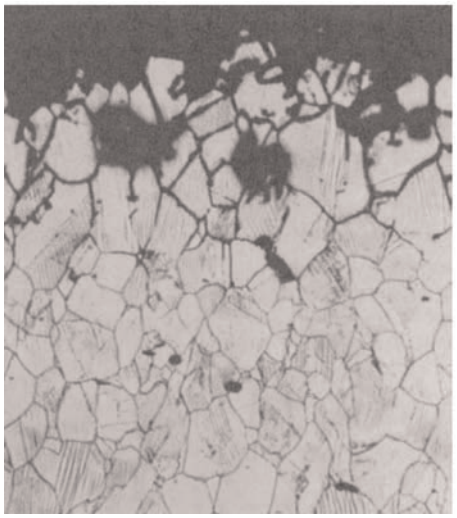

Fig. 32 Sensitized 304 stainless steel exhibiting intergranular attack. Original magnification: 100×

elements (titanium and niobium). Examples are AISI types 302, 304, 309, 310, 316, 317, 430, and 446. Using stainless steels that contain less than 0.03% C reduces susceptibility to intergranular corrosion sufficiently for serviceability in many applications. Somewhat better performance can be obtained from stabilized types, such as types 347 or 321 stainless steel, which contain sufficient titanium and niobium (or niobium plus tantalum), respectively, to combine with all of the carbon in the steel.

Under conditions such as multipass welding or cross welding, stabilized alloys will sensitize. They are also susceptible to a highly localized form of intergranular corrosion known as knifeline attack, which occurs in base metal at the weld fusion line. In some cases, these alloys are given stabilizing heat treatments after solution heat treatment for maximum resistance to intergranular corrosion in the as-welded condition. For example, type 321 stainless steel is stabilize-annealed at 900 °C (1650 °F) for 2 h before fabrication to avoid sensitization and knifeline attack. So treated, type 321 may still be susceptible because titanium has a tendency to form an oxide during welding; therefore, its role as a carbide stabilizer may be diminished. For this reason, type 321 is always welded with a niobium-stabilized weld filler metal, such as type 347 stainless.

In many applications involving exposure to environments that cause intergranular corrosion, low-carbon/nitrogen or stabilized alloy grades are specified. Types 304L, 316L, and 317L, with carbon limited to 0.03% (maximum) and nitrogen contents limited to 0.10% (maximum), are used instead of their higher-carbon counterparts. These low carbon levels are readily and economically achieved with the advent of the argon-oxygen decarburization (AOD) refining process used by most alloy producers. By limiting the interstitial element content, sensitization is limited or avoided entirely during subsequent welding and other reheating operations. However, lowering the carbon/nitrogen content also lowers the maximum allowable design stresses, as noted in appropriate sections of applicable fabrication codes, such as ASME Section 8, Division 1 for unfired pressure vessels and ANSI B31.3 for process piping.

Sensitization and intergranular corrosion also occur in ferritic stainless steels. A wider range of corrosive environments can produce intergranular attack in ferritic grades than is the case for austenitic grades. The thermal processes causing intergranular corrosion in ferritic stainless steels are also different from those for austenitic stainless steels. In the case of welds, the attacked region is usually larger for ferritic grades than for austenitic grades because temperatures above 925 °C (1700 °F) are involved in causing sensitization. Ferritic grades with less than 15% Cr are not susceptible (Ref 49). New grades of ferritic stainless steels are also alternatives to the more common 300- and 400-series stainless steels. Ferritic stainless steel UNS S44800 with 0.025% C (maximum) plus nitrogen is replacing the higher-carbon 446 grade in applications in which resistance to intergranular corrosion is a requirement. Other grades that are potentially lower-cost alternatives to higher alloys include:

- Ferritic alloys 26Cr-1Mo (UNS S44627) and 27Cr-3Mo-2Ni (UNS S44660)
- Duplex ferritic-austenitic alloys 26Cr-1.5Ni-4.5Mo (UNS S32900) and 26Cr-5Ni-2Cu-3.3Mo (UNS S32550)

Duplex stainless steels are resistant to intergranular corrosion when aged in the region of 480 to 700 °C (895 to 1290 °F). It has been recognized for some time that duplex grades with 20 to 40 vol% ferrite exhibit excellent resistance to intergranular corrosion. The aging of duplex stainless steels produces a variety of phases, as discussed further in Ref 49 along with an overall review of intergranular corrosion of stainless steels.

Cast Stainless Steels

Intergranular corrosion is a leading cause of failure of pump and valve castings in the chemical process industry. For cast stainless steels, when solution treatment is impractical or impossible, the low-carbon grades CF-3 and CF-3M are commonly used to preclude sensitization incurred during welding. The low carbon content (0.03% C maximum) of these alloys prevents the formation of an extensive number of chromium carbides. In addition, these alloys normally contain 3 to 30% ferrite in an austenitic matrix. By virtue of rapid carbide-precipitation kinetics at ferrite-austenite interfaces compared to austenite-austenite interfaces, carbide precipitation is confined to ferrite-austenite boundaries in alloys containing a minimum of approximately 3 to 5% ferrite (Ref 50, 51). If the ferrite network is discontinuous in the austenite matrix (depending on the amount, size, and distribution of ferrite pools), extensive intergranular corrosion may not be a problem in most of the environments.

High-alloy austenitic stainless steels of the CN7M type also are frequently used because they are highly resistant to sulfuric acid and other aggressive chemicals. Specifications normally require a solution anneal after weld repair to eliminate carbide precipitation in the heat-affected zone (HAZ). The introduction of the AOD secondary refining process in many stainless foundries has allowed the production of CN7M and similar alloys with very low carbon levels. Test results also have demonstrated that the heat generated by welding is insufficient to induce sensitization in the HAZ of the weld in AOD CN7M (Ref 52).

Sensitization can be induced by exposure in a furnace at 675 °C (1250 °F), but the findings indicate that AOD-refined high-alloy, fully austenitic castings behave similarly to the lower-alloyed CF3M types. A postweld solution anneal is unnecessary for material with a carbon content <0.03% after welding with a low-carbon filler.

Evaluating Intergranular Corrosion of Stainless Steels

The austenitic and ferritic stainless steels, as well as most nickel-base alloys, are generally supplied in a solution-treated condition. However, because these alloys may become sensitized from welding, improper heat treatment, or other thermal exposure, acceptance tests are implemented as a quality-control check to evaluate stainless steels and nickel-base alloys.

As noted previously, the standardized methods of testing austenitic stainless steels for susceptibility to intergranular corrosion include immersion tests described in ASTM A 262 (Ref 36) and EPR methods described in ASTM G 108 (Ref 37). There are five acid immersion tests and one etching test described in ASTM A 262. The oxalic acid etch test is used to screen samples to determine the need for further testing. Samples that have acceptable microstructures are considered to be unsusceptible to intergranular corrosion and require no further testing. Samples with microstructures indicative of carbide precipitation must be subjected to one of the immersion tests. Electrochemical potentiokinetic reactivation methods can provide a nondestructive means of quantifying the degree of sensitization. The methods have wide acceptance in studies of the effects of sensitization on intergranular corrosion and IGSCC of stainless steels and nickel-base alloys.

The theory and application of acceptance tests for detecting the susceptibility of stainless steels and nickel-base alloys to intergranular attack are extensively reviewed in Ref 34 and 53. Some standard tests include acceptance criteria, but others do not (Ref 34). A criterion is needed that can clearly separate material susceptible to intergranular attack from that resistant to attack, as listed in Table 3 (Ref 54). The evaluation tests and acceptance criteria for various stainless steels and nickel-base alloys in Table 3 have been used by the DuPont Company, the U.S. Department of Energy, and others in the chemical-processing industry.

It also should be noted that not all instances of stainless steel intergranular corrosion are associated with sensitization. Intergranular corrosion is rare in nonsensitized ferritic and austenitic stainless steels and nickel-base alloys, but one environment known to be an exception is boiling HNO_3 containing an oxidizing ion such as dichromate (Ref 55), vanadate, and/or cupric. Intergranular corrosion has also occurred in low-carbon, stabilized, and/or properly solution heat treated alloys cast in resin sand molds (Ref 56). Carbon pickup on the surface of the castings from metal-resin reactions has resulted in severe

Table 3 Appropriate evaluation tests and acceptance criteria for wrought alloys

UNS No.	Alloy name	Sensitizing treatment	Applicable tests (ASTM International standards)	Exposure time, h	Criteria for passing, appearance, or maximum allowable corrosion rate, mm/month (mils/month)
S43000	Type 430	None	Ferric sulfate (A 763–X)	24	1.14 (45)
S44600	Type 446	None	Ferric sulfate (A 763–X)	72	0.25 (10)
S44625	26-1	None	Ferric sulfate (A 763–X)	120	0.05 (2) and no significant grain dropping
S44626	26-1S	None	Cupric sulfate (A 763-Y)	120	No significant grain dropping
S44700	29-4	None	Ferric sulfate (A 763–X)	120	No significant grain dropping
S44800	29-4-2	None	Ferric sulfate (A 763–X)	120	No significant grain dropping
S30400	Type 304	None	Oxalic acid (A 262-A)	···	(a)
			Ferric sulfate (A 262-B)	120	0.1 (4)
S30403	Type 304L	1 h at 675 °C (1250 °F)	Oxalic acid (A 262–A)	···	(a)
			Nitric acid (A 262–C)	240	0.05 (2)
S30908	Type 309S	None	Nitric acid (A 262–C)	240	0.025 (1)
S31600	Type 316	None	Oxalic acid (A 262–A)	···	(a)
			Ferric sulfate (A 262–B)	120	0.1 (4)
S31603	Type 316L	1 h at 675 °C (1250 °F)	Oxalic acid (A 262-A)	···	(a)
			Ferric sulfate (A 262-B)	120	0.1 (4)
S31700	Type 317	None	Oxalic acid (A 262-A)	···	(a)
			Ferric sulfate (A 262-B)	120	0.1 (4)
S31703	Type 317L	1 h at 675 °C (1250 °F)	Oxalic acid (A 262-A)	···	(a)
			Ferric sulfate (A 262-B)	120	0.1 (4)
S32100	Type 321	1 h at 675 °C (1250 °F)	Nitric acid (A-262-C)	240	0.05 (2)
S34700	Type 347	1 h at 675 °C (1250 °F)	Nitric acid (A 262-C)	240	0.05 (2)
N08020	20Cb-3	1 h at 675 °C (1250 °F)	Ferric sulfate (G 28-A)	120	0.05 (2)
N08904	904L	None	Ferric sulfate (G 28-A)	120	0.05 (2)
N08825	Incoloy 825	1 h at 675 °C (1250 °F)	Nitric acid (A 262-C)	240	0.075 (3)
N06007	Hastelloy G	None	Ferric sulfate (G 28-A)	120	0.043 (1.7) sheet, plate, and bar; 0.05 (2) pipe and tubing
N06985	Hastelloy G-3	None	Ferric sulfate (G 28-A)	120	0.043 (1.7) sheet, plate, and bar; 0.05 (2) pipe and tubing
N06625	Inconel 625	None	Ferric sulfate (G 28-A)	120	0.075 (3)
N06690	Inconel 690	1 h at 540 °C (1000 °F)	Nitric acid (A 262-C)	240	0.025 (1)
N10276	Hastelloy C-276	None	Ferric sulfate (G 28-A)	24	1 (40)
N06455	Hastelloy C-4	None	Ferric sulfate (G 28-A)	24	0.43 (17)
N06110	Allcorr	None	Ferric sulfate (G 28-B)	24	0.64 (25)
N10001	Hastelloy B	None	20% hydrochloric acid	24	0.075 (3) sheet, plate, and bar; 0.1 (4) pipe and tubing
N10665	Hastelloy B-2	None	20% hydrochloric acid	24	0.05 (2) sheet, plate, and bar; 0.086 (3.4) pipe and tubing
A95005–A95657	Aluminum Association 5*xxx* alloys	None	Concentrated nitric acid (G 67)	24	(b)

(a) See ASTM A 262, practice A (Ref 36). (b) See ASTM G 67, section 4.1 (Ref 33). Source: Ref 54

intergranular corrosion in certain environments. Susceptibility goes undetected in the evaluation tests mentioned previously because test samples obtained from castings generally have the carbon-rich layers removed. This problem is avoided by casting these alloys in ceramic noncarbonaceous molds.

Finally, another unique circumstance of intergranular corrosion is the following example of improper materials selection that led to intergranular corrosion of a type 303 stainless steel valve in a soda-dispensing system. This is a classic case of how materials selection may involve a trade-off between manufacturing characteristics and service performance.

Example 14: Localized Corrosion of Inclusions in a Type 303 Stainless Steel Vending-Machine Valve (Ref 57).

After approximately two years in service, a valve in contact with a carbonated soft drink in a vending machine occasionally dispensed a discolored drink with a sulfide odor, causing complaints from customers. Manufacturing specifications called for the valve body to be made of type 303 stainless steel, a free-machining steel chosen because of the substantial amount of machining necessary to make the parts. Other machine parts in contact with the drink were made from type 304 stainless steel or inert plastics. According to the laboratory at the bottling plant, the soft drink in question was one of the most strongly acidic of the commercial soft drinks, containing citric and phosphoric acids and having a pH of 2.4 to 2.5.

Investigation

The body of the valve, through which the premixed drink was discharged to the machine outlet, had an abnormal appearance on some portions of the end surface that were continuously in contact with the liquid, even during idle periods. These regions showed dark stains and severe localized corrosive attack in the stained areas. The remaining portions of the valve surface and other metal parts that had also been in contact with the liquid appeared bright and unaffected. Examination at low magnification confirmed the presence of severe highly localized attack in the stained areas.

The valve bodies were supplied by two different vendors. Chemical analysis of drillings from a corroded valve body supplied by vendor A and from an unused valve body supplied by vendor B showed that both parts met the composition requirements for type 303 stainless steel. This alloy had been specified for the valve bodies for at least nine years before complaints about its performance had come to the attention of the valve manufacturers.

Several of the valve bodies, one used and five unused, selected at random from parts on hand supplied by the two vendors, were cleaned in acetone and then continuously immersed in the highly acidic soft-drink mixture for several days. The results were:

Valve	Vendor	Initial condition	Effect of test on valve
1	A	Stained and corroded	None
2	B	Unused	Black stain(a)
3, 4	A	Unused	None
5, 6	B	Unused	None

(a) The test also discolored the mixture and gave it a pronounced sulfide odor, making it completely unpalatable.

The valve body that was stained and corroded (from vendor A, valve body 1 in the table), the unused valve body that had stained in the immersion test (from vendor B, valve

body 2 in the table), and an unused valve body from vendor A that had not been subjected to immersion testing were all sectioned through the end that would be continuously exposed to the soft drink in the vending machine and were examined metallographically at magnifications of 50 to 400×. Numerous stringer-type inclusions of manganese sulfide were observed in each of the three metallographic specimens.

Figure 33 shows a micrograph of an unetched specimen from the corroded region on the end of the used valve body (valve body 1 in the immersion test). The corroded surface is an end-grain surface, and the corrosion began at the exposed ends of manganese sulfide stringer-type inclusions, which were anodic to the surrounding metal and readily attacked by the acidic soft drink. The attack extended along the inclusion lines to a maximum depth of approximately 0.64 mm (0.025 in.), with the depth apparently depending on the length of the exposed sulfide stringers. A continuous line of attack that extended at least 0.58 mm (0.023 in.) below the surface of the metal is shown in Fig. 33, which also illustrates the distribution and dimensions of the sulfide stringers generally characteristic of the three specimens that were examined metallographically. No significant attack was found on the metallographic specimen taken from unused valve body 2 from vendor B, which had turned black during laboratory immersion in the soft-drink mixture.

Conclusions

Type 303 stainless steel has only marginal corrosion resistance for this application, because of the size and distribution of sulfide stringers found in some lots of standard grades of this alloy. The sulfide stringers are anodic to the surrounding stainless steel and are preferentially corroded away. The failure of valve body 1 occurred because manganese sulfide stringers were present in significant size and concentration and were exposed at end-grain surfaces in contact with the sufficiently acidic beverage. The exposed sulfide stringers, which were anodic to the surrounding metal, were thus subject to corrosion to produce a hydrogen sulfide concentration in the immediately adjacent liquid, thus making at least the first cup of beverage dispensed discolored and unpalatable, especially after the machine stood unused overnight or over a weekend.

The inconsistent results obtained on immersing unused valve bodies 2 to 6 from the two vendors in the beverage for several days were not surprising in view of this marginal corrosion resistance, the locally varying distribution and dimensions of the sulfide stringers, and the use of only solvent cleaning before the immersion test. The complete resistance of the stained and corroded valve body (valve body 1 in the immersion tests) is not inconsistent with its past history. Any available sulfides on the corroded surface of the valve body could have already been consumed and its passivity restored during exposure to the air after removal from service.

Recommendations

Specification of type 304 stainless steel (which contains a maximum of 0.030% S) for these and similarly exposed metal parts was recommended to avoid possible adverse effects on sales, even if the failures were infrequent. This alloy is generally satisfactory for processing and dispensing soft drinks and has been widely used for these purposes.

Example 15: Leaking Welds in a Ferritic Stainless Steel Wastewater Vaporizer.

A nozzle in a wastewater vaporizer began leaking after approximately three years of service with acetic and formic acid wastewaters at 105 °C (225 °F) and 414 kPa (60 psig).

Investigation

The shell of the vessel was weld fabricated in 1972 from 6.4 mm (0.25 in.) E-Brite stainless steel plate. The shell measured 1.5 m (58 in.) in diameter and 8.5 m (28 ft) in length. Nondestructive examination included 100% radiography, dye-penetrant inspection, and hydrostatic testing of all E-Brite welds.

An internal inspection of the vessel revealed that portions of the circumferential and longitudinal seam welds, in addition to the leaking nozzle weld, displayed intergranular corrosion. At the point of leakage, there was a small intergranular crack. Figure 34 shows a typical example of a corroded weld. A transverse cross section through this weld will characteristically display intergranular corrosion with grains having separated from surrounding microstructure (Fig. 35). It was also noted that the HAZ next to the weld fusion line also experienced intergranular corrosion a couple of grains deep as a result of sensitization (Fig. 36).

The evidence indicated weldment contamination; therefore, effort was directed at finding the levels of carbon, nitrogen, and oxygen in the various components present before and after welding. The averaged results were:

	Component, ppm			
Content	C	N	C + N	O
E-Brite base plate	6	108	114	57
Corroded longitudinal weld	133	328	461	262
Corroded circumferential weld	34	169	203	225
E-Brite weld wire	3	53	56	55
Sound longitudinal weld	10	124	134	188
Sound circumferential weld	20	106	126	85

These results confirmed suspicions that failure was due to excessive amounts of nitrogen, carbon, and oxygen. To characterize the condition of the vessel further, Charpy V-notch impact tests were run on the unaffected base metal, the HAZ, and the uncorroded (sound) weld metal. These tests showed ductile-to-brittle transition temperatures as:

	Ductile-to-brittle transition temperature	
Specimen	°C	°F
Base metal	40 ± 3	105 ± 5
Heat-affected zone	85 ± 3	180 ± 5
Weld	5 ± 3	40 ± 5

Fig. 33 Unetched section through a type 303 stainless steel valve exposed to an acidic soft drink in a vending machine. Micrograph shows localized corrosion along manganese sulfide stringer inclusions at the end-grain surface. Original magnification: 100×

Fig. 34 Top view of a longitudinal weld in 6.4 mm (0.25 in.) E-Brite ferritic stainless steel plate showing intergranular corrosion. The weld was made with matching filler metal. Original magnification: ~4×

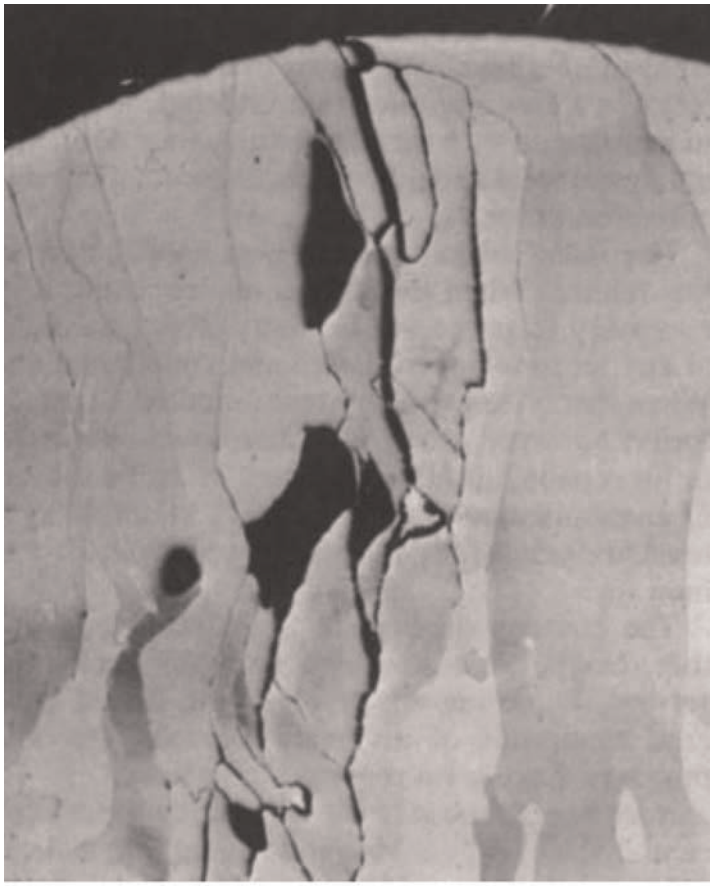

Fig. 35 Intergranular corrosion of a contaminated E-Brite ferritic stainless steel weld. Electrolytically etched with 10% oxalic acid. Original magnification: 200×

Fig. 36 Intergranular corrosion of the inside surface heat-affected zone of E-Brite stainless steel adjacent to the weld fusion line. Electrolytically etched with 10% oxalic acid. Original magnification: 100×

Comparison of the interstitial levels of the corroded welds, sound welds, base metal, and filler wire suggested that insufficient joint preparation (carbon pickup) and faulty gas shielding were probably the main contributing factors that caused this weld corrosion failure. Discussions with the vendor uncovered two discrepancies. First, the welder was using a large, 19 mm (0.75 in.) ID ceramic nozzle with a gas lens but was flowing only 19 L/min (40 ft^3/h) of argon; this was the flow rate previously used with a 13 mm (0.5 in.) ID gas lens nozzle. Second, a manifold system was used to distribute pure argon welding gas from a large liquid argon tank to various satellite welding stations in the welding shop. The exact cause for the carbon pickup was not determined.

Conclusions

Failure of the nozzle weld was the result of intergranular corrosion caused by the pickup of interstitial elements and subsequent precipitation of chromium carbides and nitrides. Carbon pickup was believed to have been caused by inadequate joint cleaning prior to welding. The increase in the weld nitrogen level was a direct result of inadequate argon gas shielding of the molten weld puddle. Two areas of inadequate shielding were identified:

- Improper gas flow rate for a 19 mm (0.75 in.) diameter gas lens nozzle
- Contamination of the manifold gas system

To preserve the structural integrity and corrosion performance of the new generation of ferritic stainless steels, it is important to avoid pickup of the interstitial elements carbon, nitrogen, oxygen, and hydrogen. In this particular case, the vendor used a flow rate intended for a smaller welding torch nozzle. The metal supplier recommended a flow rate of 23 to 28 L/min (50 to 60 ft^3/min) of argon for a 19 mm (0.75 in.) gas lens nozzle. The gas lens collect body is an important and necessary part of the torch used to weld these alloys. Failure to use a gas lens will result in a flow condition that is turbulent enough to aspirate air into the gas stream, thus contaminating the weld and destroying its mechanical and corrosion properties.

The manifold gas system also contributed to this failure. When this system is first used, it is necessary to purge the contents of the manifold of any air to avoid oxidation and contamination. When that is done, the system functions satisfactorily; however, when it is shut down overnight or for repairs, air infiltrates back in, and a source of contamination is reestablished. Manifold systems are never fully purged, and leaks are common.

The contaminated welds were removed, and the vessels were rewelded and put back into service. Some rework involved the use of covered electrodes of dissimilar composition. No problems were reported.

Recommendations

First, to ensure proper joint cleaning, solvent washing and wiping with a clean lint-free cloth should be performed immediately before welding. The filler wire should be wiped with a clean cloth just prior to welding. Also, a word of caution: solvents are generally flammable and can be toxic. Ventilation should be adequate. Cleaning should continue until cloths are free of any residues.

Second, when gas tungsten arc welding, a 19 mm (0.75 in.) diameter ceramic nozzle with gas lens collect body is recommended. An argon gas flow rate of 28 L/min (60 ft^3/min) is optimum. Smaller nozzles are not recommended. Argon back gas shielding is mandatory at a slight positive pressure to avoid disrupting the flow of the welding torch.

Third, the tip of the filler wire should be kept within the torch shielding gas envelope to avoid contamination and pickup of nitrogen and oxygen (they embrittle the weld). If the tip

becomes contaminated, welding should be stopped, the contaminated weld area ground out, and the tip of the filler wire that has been oxidized should be snipped off before proceeding with welding.

Fourth, a manifold gas system should not be used to supply shielding and backing gas. Individual argon gas cylinders have been found to provide optimal performance. A weld button spot test should be performed to confirm the integrity of the argon cylinder and all hose connections. In this test, the weld button sample should be absolutely bright and shiny. Any cloudiness is an indication of contamination. It is necessary to check for leaks or to replace the cylinder.

Fifth, it is important to remember that corrosion resistance is not the only criterion when evaluating these new ferritic stainless steels. Welds must also be tough and ductile.

Lastly, dissimilar weld filler metals can be successfully used. To avoid premature failure, the dissimilar combination should be corrosion tested to ensure suitability for the intended service.

Intergranular Corrosion of Nickel Alloys

The metallurgy of high-nickel alloys is more complicated than that of the austenitic stainless steels, because carbon becomes less soluble in the matrix as the nickel content rises. As in stainless steels, low carbon content is beneficial for resistance to intergranular corrosion. Stabilized grades (with additions of titanium, niobium, or other strong carbide-forming elements) are also beneficial, although they do not produce stabilized alloys in the same sense that stainless steels are stabilized. In other words, no simple ratio of titanium and niobium to carbon can be given that will make a particular alloy immune to intergranular corrosion. For example, titanium as a carbide-stabilizing element is used in Incoloy alloy 825 (UNS N08825) at a minimum concentration of approximately five times the carbon-plus-nitrogen content. The higher-nickel alloys 20Cb-3, Inconel 625, and Hastelloy G contain even higher concentrations of niobium, up to a maximum of approximately 4% in the case of alloy 625.

Nickel alloys susceptible to intergranular corrosion sensitization include:

- Inconel alloys 600 (UNS N06600) and 601 (UNS N06601)
- Incoloy alloy 800 (UNS N08800) despite the presence of titanium
- Incoloy 800H (UNS N08810)
- Nickel 200 (UNS N02200)
- Hastelloy alloys B (UNS N10001) and C (UNS N10002)

Solid-solution nickel-base alloys, such as Inconel 600, are subject to grain-boundary carbide precipitation if held at or slowly cooled through the temperature range of 540 to 760 °C (1000 to 1400 °F). If thus sensitized, they are susceptible to intergranular corrosion in hot caustic solutions, in boiling 75% HNO_3, and in high-temperature water containing low concentrations of chlorides or other salts. The ability of the thermal treatment to eliminate chromium depletion and provide good corrosion resistance is critically dependent on the grain size and carbon content of the alloy (Ref 58). Reference 58 includes a thermal treatment index, which allows calculation of the period at 700 °C (1300 °F) necessary to complete resolution of carbon. Resistance to intergranular attack also has a close dependency on the segregated impurity concentration and the morphology and distribution of intergranular carbides (Ref 59). Evaluation of alloy 600 has also been done in examining the potential impact of grain-boundary design and control as a practical application in the general field of corrosion prevention and control (Ref 60).

Hastelloy B and C are susceptible after being heated at 500 to 705 °C (930 to 1300 °F) but are made immune to intergranular corrosion by heat treatment at 1150 to 1175 °C (2100 to 2150 °F) for Hastelloy B and at 1210 to 1240 °C (2210 to 2260 °F) for Hastelloy C, followed by rapid cooling in air or water.

Precipitation-hardenable nickel alloys corrode intergranularly in some environments. lnconel X-750 is susceptible to intergranular corrosion in hot caustic solutions, in boiling 75% HNO_3, and in high-temperature water containing low concentrations of chlorides or other salts. It can be made resistant to intergranular corrosion in these corrodents, but not necessarily in others, by heat treating the cold-worked alloy at 900 °C (1650 °F).

Some specialty alloys have low interstitial element content plus the addition of stabilizing elements for resistance to intergranular corrosion. These alloys include the higher-nickel Hastelloy alloy G-3 (UNS N06985), which contains 0.015% C (maximum) and niobium plus tantalum up to 0.5%. Alloy G-3 has good weldability and resistance to intergranular corrosion in the welded condition.

The intergranular corrosion behavior of high-nickel alloys was reviewed in considerable detail in Ref 61 and 62. Isothermal heat treatments produced susceptibility to intergranular corrosion in all the alloys examined in these studies. Fortunately, the problems produced by the isothermal heat treatment are not usually manifested in welding. When welded by qualified procedures, most modern high-nickel alloys are resistant to intergranular corrosion.

Commercially Pure Nickel 200

Commercially pure Nickel 200 with a maximum carbon content of 0.15% will precipitate elemental carbon or graphite in the grain boundaries when heated in the range of 315 to 760 °C (600 to 1400 °F). This results in embrittlement and susceptibility to intergranular corrosion. Where embrittlement and intergranular corrosion must be avoided, Nickel 201 (UNS N02201) with a maximum carbon content of 0.02% is specified.

Intergranular Corrosion of Aluminum Alloys

Various types of intergranular corrosion are shown in Fig. 37. The precipitated phases in high-strength aluminum alloys make them susceptible to intergranular corrosion. The effect is most pronounced for alloys such as 2014 containing precipitated $CuAl_2$ and somewhat less for those containing $FeAl_3$ (1100), Mg_2Si (2024), $MgZn_2$ (7075), and $MnAl_6$ (5*xxx*) along grain boundaries or slip lines. Solution heat treatment makes these alloys almost immune to intergranular corrosion but substantially reduces

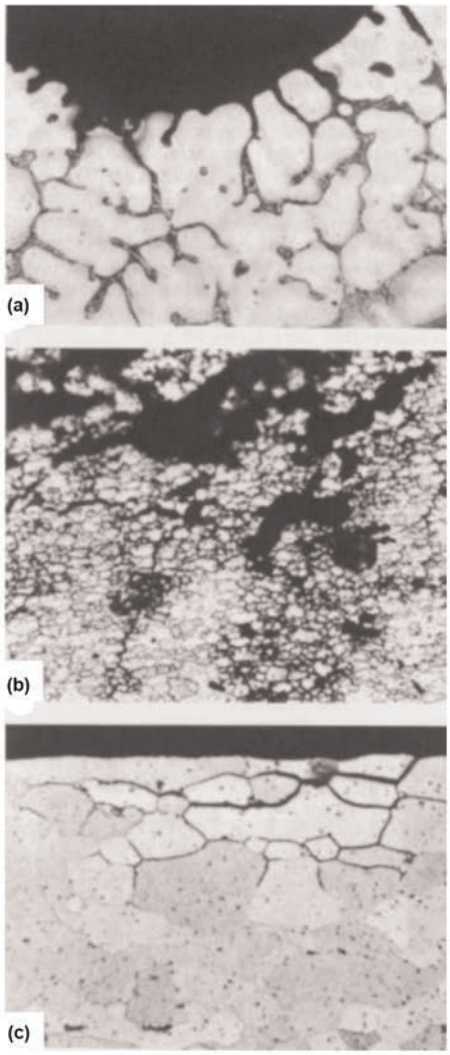

Fig. 37 Various types of intergranular corrosion. (a) Interdendritic corrosion in a cast structure. (b) Interfragmentary corrosion in a wrought, unrecrystallized structure. (c) Intergranular corrosion in a recrystallized wrought structure. All etched with Keller's reagent. Original magnification: 500×

their strength. Some magnesium alloys are similarly attacked unless solution heat treated.

Although many types of intergranular corrosion are not associated with a potential difference between the grain-boundary region and the adjacent grain bodies (as previously noted in discussions with Fig. 27), intergranular corrosion of aluminum alloys may occur from potential differences between the grain-boundary region and the adjacent grain bodies (Ref 63). The location of the anodic path varies with the different alloy systems.

In 2*xxx*-series alloys, it is a narrow band on either side of the boundary that is depleted in copper; in 5*xxx*-series alloys, it is the anodic constituent Mg_2Al_3 when that constituent forms a continuous path along a grain boundary; in copper-free 7*xxx*-series alloys, it is generally considered to be the anodic zinc- and magnesium-bearing constituents on the grain boundary; and in the copper-bearing 7*xxx*-series alloys, it appears to be the copper-depleted bands along the grain boundaries (Ref 64, 65). The 6*xxx*-series alloys generally resist this type of corrosion, although slight intergranular attack has been observed in aggressive environments. The electrochemical mechanism for intergranular corrosion proposed by E.H. Dix has been verified (Ref 66) and related to the pitting potentials of aluminum (Ref 67).

Evaluation of intergranular attack is more complex than evaluation of pitting. Visual observations are generally not reliable. For 5*xxx*-series alloys, a weight-loss test method is ASTM G 67 (Ref 33). Electrochemical techniques provide some evidence of the susceptibility of a particular alloy or microstructure to intergranular corrosion, but such techniques should be accompanied by a metallographic examination of carefully prepared sections.

Intergranular Corrosion of Copper Alloys

Intergranular corrosion is an infrequently encountered form of attack that occurs most often in applications involving high-pressure steam. This type of corrosion penetrates the metal along grain boundaries, often to a depth of several grains, which distinguishes it from surface roughening. Mechanical stress is apparently not a factor in intergranular corrosion. The alloys that appear to be the most susceptible to this form of attack are Muntz metal, admiralty metal, aluminum brasses, and silicon bronzes.

Copper Alloy C26000

Copper alloy C26000 (cartridge brass, 70% Cu) corrodes intergranularly in dilute aqueous solutions of sulfuric acid, iron sulfate, bismuth trichloride, and other electrolytes. Figure 38 shows the intergranular corrosion attack on an inhibited admiralty brass caused by hot water containing 0.1 to 0.2% H_2SO_4.

Intergranular Corrosion of Zinc

Zinc Anodes

The zinc industry has long been aware of the susceptibility of zinc alloys containing aluminum to intergranular corrosion when exposed to elevated temperatures. When zinc alloy anodes are exposed to service conditions involving elevated temperatures, the use of ASTM type II in ASTM B 41 is recommended.

Intergranular Corrosion of Galvanized Steel

It has been known since 1923 that zinc die casting alloys are susceptible to intergranular attack in an air-water environment (Ref 68). The adverse effect of intergranular corrosion of hot dip galvanized steel was first observed in 1963 and was investigated at Inland Steel Company in 1972 (Ref 69). The observed effect associated with intergranular corrosion was termed delayed adhesion failure. Delayed adhesion failure is a deterioration in coating adhesion due to selective corrosion at grain boundaries. It was found that the small amount of lead normally added to commercial galvanizing spelters was a critical factor in the susceptibility of the zinc coating to intergranular attack. By using lead-free zinc spelter (<0.01% Pb), the damaging effect of intergranular corrosion was essentially eliminated.

For the continuous hot dip galvanizing process, the main reason to add 0.07 to 0.15% Pb to zinc spelter was to produce a spangled coating and to lower the surface tension of the zinc bath in order to provide the necessary fluid properties to produce a ripple-free coating. It was found that antimony additions to the zinc spelter achieved the beneficial effects of lead additions without causing intergranular corrosion. For galvanized coatings produced by the electroplating process, no intergranular corrosion has been observed.

One study (Ref 70) describes the influence of aging at 100 °C (212 °F) on the development of intergranular cracking in a galvanized coating (from a melt containing Zn-0.2Al-0.035Pb, weight percent). Most other work indicates that high humidity is necessary for intergranular attack, but this work indicated that significant development of intergranular cracking could occur in the absence of a high-humidity environment. The researchers attributed the increased cracking to diffusion and accumulation of oxygen at the grain boundaries. This study examines the development of intergranular cracking in galvanized samples exposed to environments with different levels of humidity.

Selective Leaching

Selective leaching is defined as the removal of one element or phase from a solid alloy by a corrosion process (Ref 71). Selective leaching is also known as dealloying, and when referring to the noble metals, it is also called parting (Ref 72). The phenomenon of selective leaching was first reported by Calvert and Johnson in 1866 (Ref 73). Since that time,

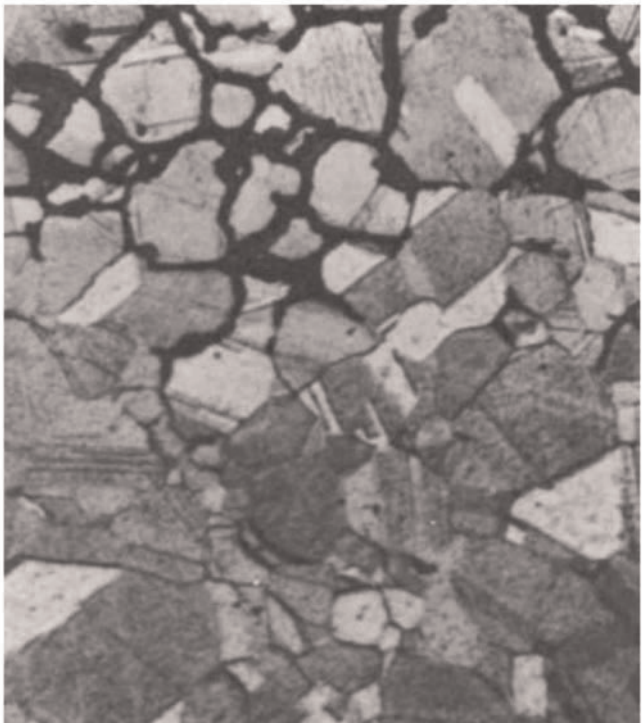

Fig. 38 Intergranular attack of admiralty brass in hot water containing a small amount of sulfuric acid. Original magnification: 150×

there has been no general consensus regarding the exact corrosion mechanism. The removal of one element results in an altered matrix usually consisting of a porous mass. There are several different alloy families that undergo selective leaching, the best known being brass alloy corrosion due to dezincification. Table 4 illustrates the various combinations of alloys and environments in which dealloying can occur (Ref 57).

Dealloying Mechanisms

There are numerous theories regarding the mechanisms of selective leaching, but two predominant mechanisms prevail. The first theory states that the two elements or phases in the alloy dissolve and then one redeposits on the surface. The second theory is that one element or phase selectively dissolves from the alloy, leaving the more noble elements or phases in a porous mass (Ref 57).

The selective leaching process has specific names based on the elements that are removed from particular alloy families.

Dezincification

The most common process of selective leaching occurs in brass alloys, and most frequently in alloys containing more than 15% Zn. This is called dezincification. Of the two dealloying mechanisms, dezincification was most commonly accepted to occur by the brass corroding, the zinc ions staying in solution, and the copper replating (Ref 72).

Figure 39 illustrates the application of each of the dezincification theories to 70Cu-30Zn alloy (UNS C26000) (Ref 73). The diagram shows that higher potentials and low pH values favor selective removal of zinc. At negative potentials and acidic conditions, copper and zinc dissolve. At zero to slightly positive potentials and acidic conditions, a region exists in which copper is expected to redeposit. Thus, the research results show that both dezincification mechanisms can occur independently or in conjunction, depending on the given environment conditions. This is the widely held current belief.

Two types of damage can be characterized; one type of dezincification is uniform, and the second is plug-type. Uniform or layer-type dezincification results in a relatively uniform zone of dezincified material, with the underlying material remaining unaffected. Brasses with high zinc content in an acidic environment are prone to uniform dezincification (Ref 72). Plug-type dezincification results in localized penetrations of dezincified areas that progress through the wall thickness of the material. Overall dimensions of the material do not change. The dezincified areas are weakened or in some cases perforated. Plug-type corrosion is most likely to occur in basic or neutral environments and at elevated temperatures.

Prevention of Dezincification

Prevention of dezincification can be achieved most readily by proper alloy selection. Alloys containing greater than 85% Cu are considered resistant to dezincification. Tin is added to act as an inhibitor. In addition, inhibited, copper-zinc alloys containing 0.020 to 0.6% arsenic, antimony, or phosphorus are also considered resistant to dezincification. This is likely due to the formation of a redeposited film of protective elements. Other possible remedies for dezincification include the use of cathodic protection, liners, or coatings.

Example 16: Dezincification of a Leaded Yellow Brass Thermowell in a Potable Hot Water System.

A brass thermowell was removed from a potable hot water system due to leaks. The shank portion of the thermowell had a 9.5 mm (0.375 in.) OD. The thermowell had only been in service for approximately six months.

Investigation

The shank portion of the thermowell exhibited through-wall cracking and white and reddish-brown deposits on its outside surface (Fig. 40a). After cross sectioning the thermowell longitudinally, the ID surface did not contain any deposits or forms of degradation (Fig. 40b). The fracture surface of the cracks was covered predominantly with a white deposit with regions of a copper color (Fig. 40c). The metallurgical examination of the tube sample showed porous material typical of layer-type dezincification initiating from the outside surface (Fig. 40d). The dezincification had progressed through the shank portion of the thermowell to a sufficient depth, and cracking propagated from these areas. The energy-dispersive spectroscopy results of the deposits removed from the OD surface of the thermowell showed the material was a leaded brass, most likely a free-machining brass, nominally 62% Cu, 35% Zn, and 3% Pb. The deposits showed varying levels of zinc, indicative of the dezincification corrosion mechanism. The copper content remained consistent.

Recommendations

The thermowell required replacement with a more dezincification-resistant material with a zinc content of 15% or less, such as a commercial bronze (90% Cu, 10% Zn) or a red brass (85% Cu, 15% Zn).

Corrosion By-Products

Copper alloys with a copper content greater than 85% are resistant to dezincification. Copper alloys such as red brass (UNS C23000), inhibited admiralty brass (UNS C44300), and arsenical aluminum brass (UNS C68700) are less susceptible to corrosion. Suitability for use in potable water systems is the prime consideration in this case, however.

This points out that not only are the degrading effects of selective leaching on the function of the component important, but also that the effects of corrosion by-products must be evaluated. Leaching of copper itself in drinking water is a matter of public health debate and regulation, beyond the scope of this article.

If the replacement must have a chromium decorative coating, ease of plating is also a factor. Here again, the high-zinc brass is susceptible to dezincification through the somewhat porous chromium plating in an aggressive exterior environment.

Graphitic Corrosion

Graphitic corrosion is a form of dealloying that occurs in cast iron material. This corrosion mechanism is usually found in gray cast irons and is associated with the presence of graphite flakes. The graphite is cathodic to the iron matrix. Exposure to an electrolyte results in

Table 4 Combinations of alloys and environments subject to selective leaching and elements removed by leaching

Alloy	Environment	Element removed
Brasses	Many waters, especially under stagnant conditions	Zinc (dezincification)
Gray iron	Soils, many waters	Iron (graphitic corrosion)
Aluminum bronzes	Hydrofluoric acid, acids containing chloride ions	Aluminum
Silicon bronzes	Not reported	Silicon
Copper-nickels	High heat flux and low water velocity (in refinery condenser tubes)	Nickel (denickelification)
Monels	Hydrofluoric and other acids	Copper in some acids, and nickel in others
Alloys of gold or platinum with nickel, copper, or silver	Nitric, chromic, and sulfuric acids	Nickel, copper, or silver (parting)
High-nickel alloys	Molten salts	Chromium, iron, molybdenum, and tungsten
Cobalt-tungsten-chromium alloys	Not reported	Cobalt
Medium-carbon and high-carbon steels	Oxidizing atmospheres, hydrogen at high temperatures	Carbon (decarburization)
Iron-chromium alloys	High-temperature oxidizing atmospheres	Chromium, which forms a protective film
Nickel-molybdenum alloys	Oxygen at high temperature	Molybdenum

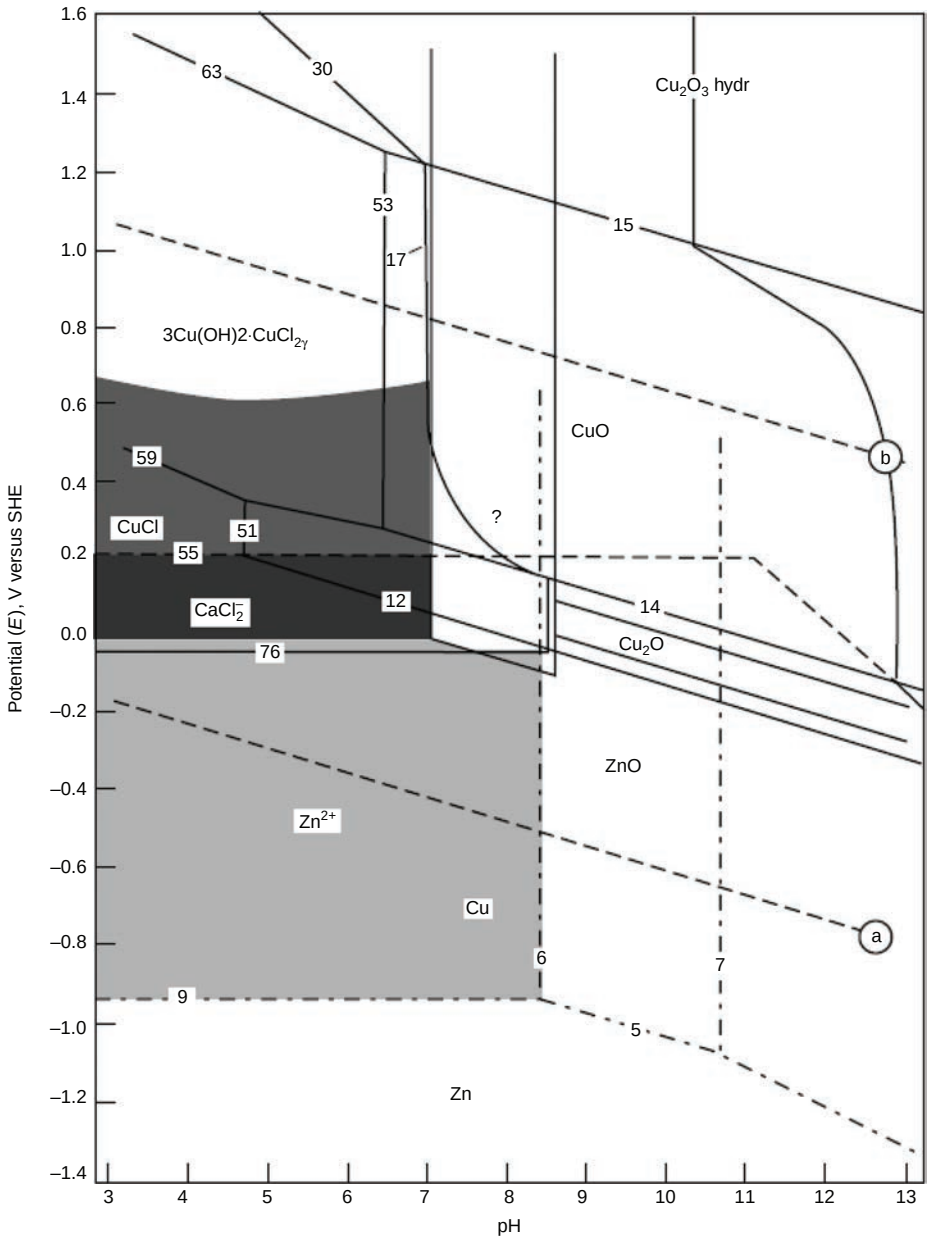

Fig. 39 Superimposed potential-pH diagram of a 70Cu-30Zn alloy in 0.1 *M* NaCl. Lightly shaded area indicates the domain in which selective removal of zinc is expected in solutions free of copper ions. Intermediate-shaded area indicates the domain in which both copper and zinc dissolve. Dark-shaded area indicates the region in which copper is expected to deposit. SHE, standard hydrogen electrode. Source: Ref 73

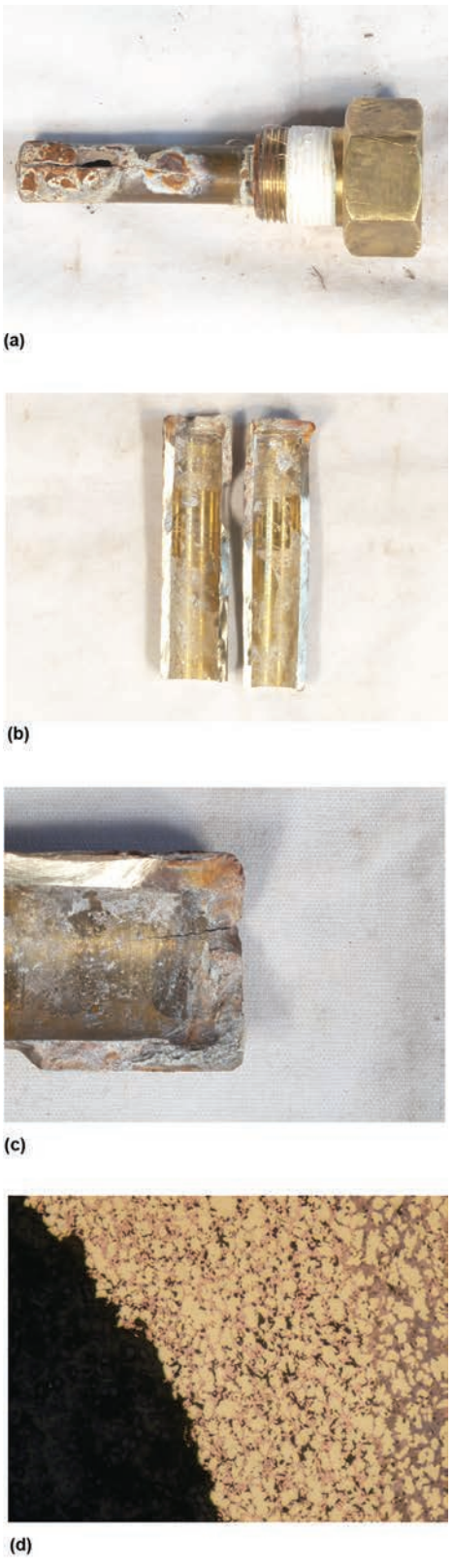

Fig. 40 Views of through-wall cracking of an alpha leaded brass (62%Cu-35%Zn-3%Pb) thermowell shank removed from a potable hot water system due to dezincification. (a) Macroview of thermowell. (b) Thermowell after sectioning longitudinally to separate mating fracture surfaces associated with cracking shown in (a). (c) Close-up view of one of mating fracture halves on thermowell shown in (b). The dezincification initiated on the outside diameter surface. (d) Micrograph of layer-type dezincification. Courtesy of M.J. Cooney, R.A. Hoffmann Engineering, P.C.

selective leaching of the iron matrix, leaving behind a porous mass of graphite flakes. Graphitic corrosion is most often a long-term mechanism, resulting from exposure of 50 years or more. Pipelines made of cast iron, especially those buried in clay-based soils and soils containing sulfates, are susceptible (Ref 74).

In cases where graphitic corrosion has caused extensive wall loss, a reduction in component strength will occur. Thus, it is not unusual for cracking to accompany graphitic corrosion. In some cases, graphitic corrosion has been observed on the fracture surfaces, indicating the long-term existence of the crack. Figure 41 shows an example of a section of gray cast iron waste pipe removed from the parking garage of a high-rise commercial building. Graphitic corrosion was apparent across approximately 75% of the total wall thickness. The pipe had been oriented horizontally during service. Figure 41(a) shows the two halves of a pipe section after having been sectioned longitudinally. The top section of the pipe fractured into several sections due to the loss of strength from the severe graphitic corrosion. Figure 41(b) is a cross section of the pipe wall thickness and illustrates the reduction in wall thickness due to graphitic corrosion.

It is generally thought that ductile and malleable irons are not affected by graphitic corrosion, so ductile cast iron is routinely used for underground water and sewer pipes. However, a case of ductile cast iron subject to graphitic corrosion and MIC was reported about a buried

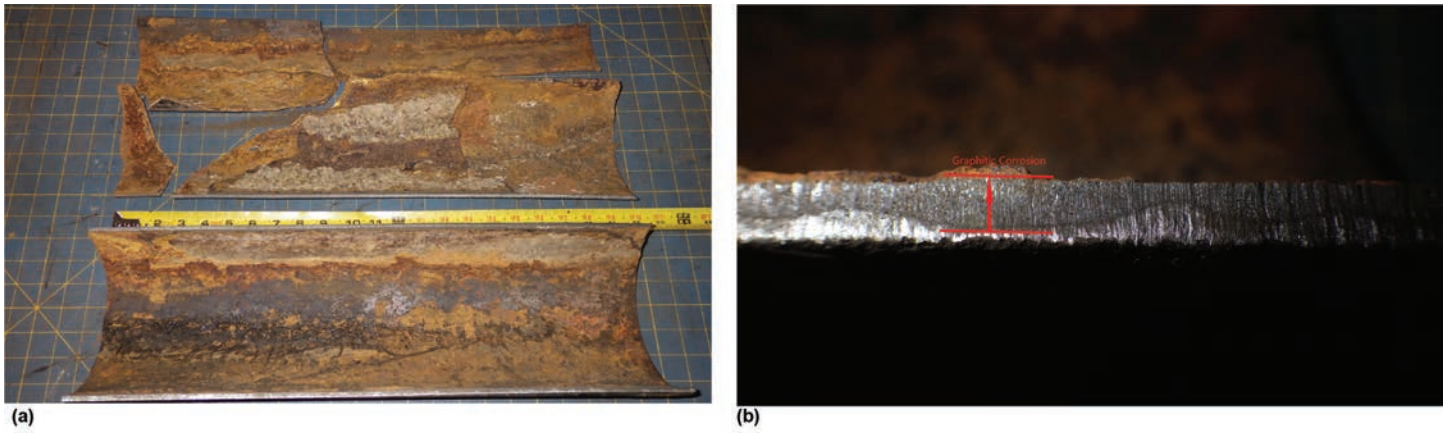

Fig. 41 Graphitic corrosion of a gray cast iron sanitary sewer pipe section removed from a high-rise commercial building. (a) Top of pipe section cracked longitudinally due to severe graphitic corrosion. (b) Graphitic corrosion on the inside diameter pipe surface is apparent for approximately 75% of the wall thickness. Courtesy of M.J. Cooney, R.A. Hoffmann Engineering, P.C.

ductile cast iron pipe (Ref 75). The porous graphite structure was accompanied by massive tubercles, indicating that the biodeposits played a significant role in the formation of a graphite mass of corrosion residue. Ductile cast iron graphitic corrosion has, otherwise, gone undocumented and is considered rare.

Graphitization

Graphitization is not related to graphitic corrosion, but the term is sometimes confused with the graphitic corrosion mechanisms. Graphitization is the microstructural change that occurs in carbon steel materials (steels with 0.5% Mo or less) after exposure to temperatures in the range of 399 to 593 °C (750 to 1100 °F) for an extended period of time. The pearlite transforms to nodular graphite and ferrite. At grain boundaries, the formation of chains of graphite can result in brittle fracture or cracking.

Example 17: Failure of a Cast Iron Water Pipe due to Graphitic Corrosion.

A 25.4 cm (10 in.) diameter gray cast iron water main pipe was buried in the soil beneath a concrete slab. The installation was believed to have been completed in the early 20th century. A leak from the pipe resulted in flooding of a warehouse. Once removed, the pipe revealed through-wall perforations and cracking along its axis. The perforations and the crack were at the 6 o'clock position.

Investigation

Visual examination of the pipe showed two large holes (Fig. 42a). The areas surrounding the holes showed delaminations and corrosion deposits. Radiography was performed to evaluate the material quality. The radiographic results showed various film densities indicating corrosion or variations in wall thickness. Secondary cracking was also observed beyond the more apparent primary crack. Three cross sections were removed: one from the

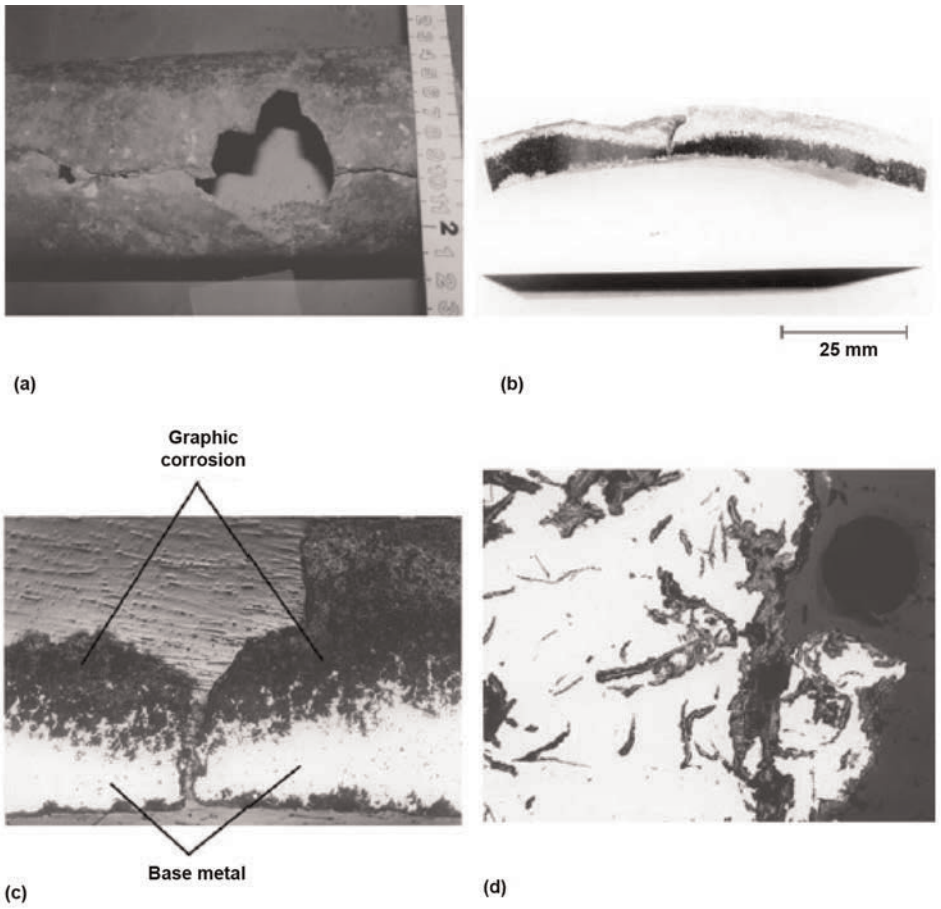

Fig. 42 A 25 cm (10 in.) diameter gray cast iron pipe that failed due to graphitic corrosion. The pipe was part of a water supply to a fire-protection system. The external surface was covered with soil and the inside surface in contact with water. The pipe experienced cracking and through-wall perforations. (a) View showing a hole and cracking in the pipe. (b) Macrograph of a cross section through the crack observed in (a) showing graphitic corrosion primarily on the outside diameter (top). (c) Micrograph of the cross section shown in (b). Significant wall loss and graphitic corrosion were observed on the outside diameter surface. Original micrograph image shows an area 16.5 mm (0.65 in.) wide. (d) Micrograph of crack surface in (c) depicting graphitic corrosion surrounding the graphite flakes. Original micrograph image shows an area 1.14 mm (0.045 in.) wide. Courtesy of S.R. Freeman, Millennium Metallurgy, Ltd.

perforated area, one from the crack area, and one from an area considered undamaged. The samples were metallurgically prepared and examined in the unetched condition. A macrograph of a cross section through the crack depicted graphitic corrosion primarily on the OD surface (Fig. 42b). A porous mass and significant wall loss were observed on the OD surface (Fig. 42c). This is indicative of graphitic corrosion. Graphitic corrosion occurs as the ferritic phase is leached from the matrix, leaving a porous mass of graphite flakes (Fig. 42d). The structure of the material was typical of gray cast iron with random orientation of the graphite flakes. Indications of graphitic corrosion were also observed to a lesser degree on the ID surface of the pipe. More than 50% of the wall thickness showed evidence of graphitic corrosion. Wall-thickness readings were fairly uniform, measuring approximately 11 mm (0.43 in.). Wall loss due to graphitic corrosion is difficult to detect because a porous mass of material remains in place.

Tensile testing was also performed. A sample was removed from the area adjacent to the crack. A second sample was removed from an area 90° from the crack. The sample near the crack showed a 40% reduction in load capacity. The pipe leak occurred as result of years of exposure to ground water in the soil, resulting in graphitic corrosion. Soils containing sulfates are particularly aggressive.

Recommendations

The extensive damage due to graphitic corrosion required pipe replacement. The wall thickness had been sufficiently reduced that the pipe could no longer support the required load. Water mains are designed for more than 100 years of life. Ductile iron or coated and lined steel pipe, generally not susceptible to graphitic corrosion, would be suitable replacement materials. Cathodic protection is also a possibility.

Dealuminification

Dealloying of aluminum bronze and nickel-aluminum bronze castings has been well known since the early 1960s. It has been determined over the years that the mechanism of dealloying or selective leaching in aluminum bronze castings occurs by corrosion of the duplex structures ($\alpha + \gamma$-2) (Ref 76). This type of dealloying is rarely detectable visually. Nickel-aluminum bronze castings containing 4% or more nickel show diminished selective leaching. When dealuminification does occur, the mechanism involves the dealloying of non-equilibrium microconstituents, such as retained β and γ-2. Figure 43 shows dealuminification of a cast aluminum bronze furnace electrode pressure ring exposed to recirculating cooling waters. A temper-anneal heat treatment has been shown to change the microstructure to all $\alpha + \kappa$, further reducing the susceptibility to selective leaching. However, large nickel-aluminum bronze castings may still be susceptible to dealloying along the $\alpha + \kappa$ eutectoid network. It appears that heat treatment is effective on smaller castings having fine and uniformly distributed microstructures, but larger castings have coarser and more segregated microstructures are less responsive.

Denickelification

Denickelification involves the removal of nickel from copper-nickel alloys. Only a few instances of this phenomenon have been reported. The conditions likely to induce this selective leaching process include low-flow conditions, temperatures above 100 °C (212 °F), and high local heat flux (Ref 77). Figure 44 shows the residual copper layer remaining from a UNS C71500 feedwater pressure tube that underwent denickelification. A recent report of selective leaching of nickel in type 304L stainless steel material occurred in lithium hydride at temperatures greater than 715 to 850 °C (1320 to 1560 °F) (Ref 78).

Destannification and Desiliconification

Specific instances of dealloying tin in cast tin bronzes have been observed in hot brine or steam. Isolated cases of desiliconification in silicon bronzes have occurred in high-temperature steam with acidic species (Ref 77).

Dealloying of Noble Metals

Dealloying may also occur in copper-gold and silver-gold alloys. A study of failure mechanisms in Cu_3Au single crystals indicated that dealloying or selective leaching of the copper occurs, leaving a gold sponge (Ref 79). Testing was performed in a ferric chloride solution and was done primarily to distinguish between true transgranular stress-corrosion cracking (T-SCC) and chemical embrittlement or selective leaching in Cu_3Au single crystals. The Cu_3Au samples 1 to 2 mm (0.04 to 0.08 in.) thick were exposed to stress-free immersion in aqueous $FeCl_3$ for 30 days. Other than a slight discoloration, the samples did not show indications of attack. There was no obvious volume change. Weight loss corresponded with total loss of copper, however. Dealloying had occurred, leaving a single-crystal gold sponge with the dimensions and crystal orientation of the original copper-gold crystal.

Evaluations in the cited work showed the gold sponge failed in a brittle manner by macrocleavage under small applied load in air. Figures 45(a) and (b) show the facet-step fracture surface. However, close examination of the fracture surface (Fig. 45c) revealed that the failure occurred by ductile overload of the small gold ligaments of the sponge.

For true T-SCC, samples failed following 1 to 20 h exposure to the corrodent, depending on the applied electrical potential. There was no evidence that cracks had occurred in the plane of localized dealloying. Crack growth was over 2 orders of magnitude greater than sponge formation.

It is believed that gold sponge formation may assist in nucleating T-SCC cracks at a free surface.

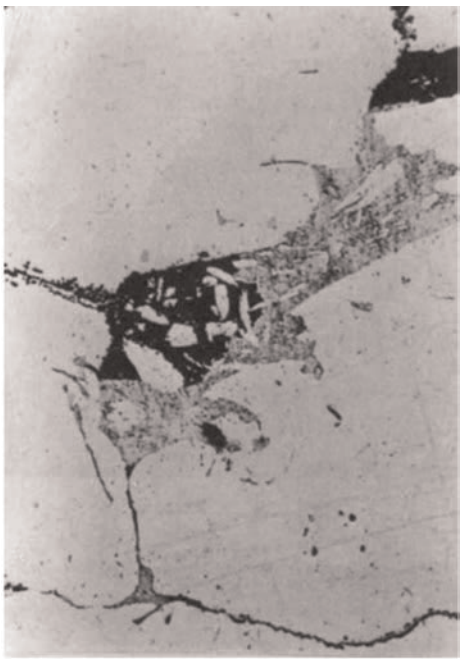

Fig. 43 Dealuminification of a cast aluminum bronze furnace electrode pressure ring exposed to recirculating cooling water (pH = 7.8 to 8.3, conductivity = 1000 to 1100 μS). The preferentially attacked γ phase left behind a residue of copper (darkened regions in eutectoid and along grain boundaries). The α particles within the eutectoid (light-gray areas) are unattacked. Etched with $FeCl_3$. Original magnification: 260×. Courtesy of R.D. Port. Permission granted by Nalco Chemical Co., 1987

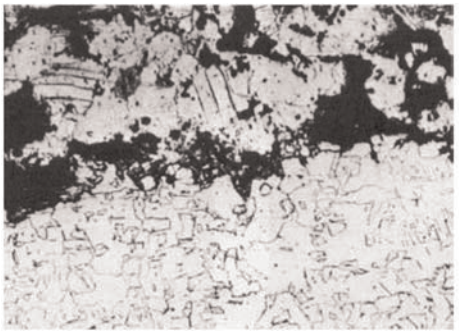

Fig. 44 Residual copper layer from a UNS C71500 feedwater pressure tube that underwent denickelification. The tube was subject to 205 °C (400 °F) steam on the external surface and 175 °C (350 °F) boiling water on the internal surface at pH 8.6 to 9.2. Courtesy of J.J. Dillion. Permission granted by Nalco Chemical Co., 1987

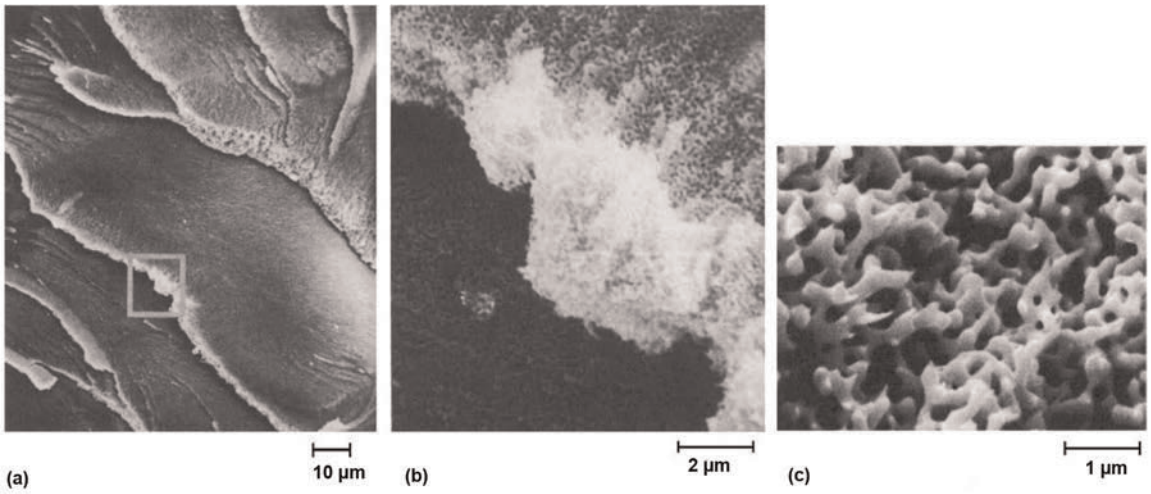

Fig. 45 Fracture surface of a Cu-25Au (at.%) single crystal upon bending in air following 30 day stress-free immersion in aqueous $FeCl_3$. (a) Scanning electron micrograph of fracture surface of gold sponge. (b) Scanning electron micrograph of the boxed area showing facet-step structure in gold sponge. (c) Scanning electron micrograph of gold sponge structure revealed on the surface of the sample shown in (b). Average interpore spacing is ~200 nm. Evidence of ductile fracture can be seen on the surface (necking of the gold ligaments).

Velocity-Affected Corrosion

The attack on metal immersed in water may vary greatly, depending on the relative velocity between the water and the metal surface. For metals that show passive behavior or form other protective films in water, as most metals do, attack will occur where the changes in water velocity are most pronounced. Water corrosivity can be dramatically increased by dissolved gases, acids, salts, strong bases, entrained abrasives, high temperature, fluctuating pressure, cavitation, or impingement.

Relative difference in velocity between the metal and the aqueous corrosive influences any of the common varieties of iron or steel, including low-carbon or high-carbon steel, low-alloy steel, wrought iron, and cast iron. These corrode in slow-moving freshwater or seawater at almost the same rate, which is approximately 0.13 mm/year (0.005 in./year). At higher temperatures with equal values of dissolved gas concentration, the rate tends to increase but remains relatively low. Therefore, steel can be used for boilers in contact with deaerated water. Commercially pure aluminum typically corrodes less in aerated or deaerated freshwater than iron and carbon steels, making it a suitable material for handling distilled water.

Low-Velocity Effects

Slow-Moving and Stagnant Waters

Slow-moving and stagnant waters can prevent, damage, or remove passive films. The low velocity allows loosely adherent solid corrosion products to form on metal surfaces and allows debris to collect, which facilitates further corrosion damage. In closed systems, if a corrosion inhibitor is used, its effectiveness is often reduced where the water is stagnant or quiet.

In designing for corrosion control, stagnant zones should be eliminated by methods such as:

- Circulation of stagnant liquids or relative movement of metallic surfaces
- Allowing free drainage of water
- Filtering suspended solids
- Providing an N_2 blanket (carbon steels) or free access to O_2 (stainless steels). Weakly passivating metals such as carbon steels are attacked by high O_2, whereas strongly passivating metals such as stainless steels are protected by uniform O_2 distributions.
- Maintaining concentration of dissolved passivating chemicals such as O_2 by infusion or injection
- Installing baffling to eliminate stagnant liquid zones
- Providing gas-vent lines
- Maintaining clean and smooth surfaces, avoiding crevices
- Using cathodic protection
- Using proper inhibitors where applicable

Example 18: Failure of Stainless Steel Piping in Stagnant Seawater.

Stagnant seawater can be quite destructive to some alloy systems. An austenitic stainless steel piping used in the fire-sprinkler system in a large saltwater passenger and car ferry failed by rapid leaking. The original author had failure analysis experience with a similar, seawater-filled fire main piping system in a high-performance hydrofoil ship two decades earlier.

Investigation

The design and parameters revealed in the failure investigation were:

- *Piping material:* Type 316/316L stainless steel, schedule 40, 64 mm (2.5 in.) diameter and larger pipe was used.
- *Pitting damage:* Observed through pipe wall directed from interior to exterior. Most pits were leaking in the HAZ at the weld joints. Some pitting was found midlength at the bottom of the pipe.
- *Environment:* Stagnant seawater at ambient temperatures. Pipe was in service for four weeks when three leaks appeared.

Figure 46 shows a pit near the end of a ballpoint pen lying in the trough of a sectioned open AISI 316L pipe. A closeup of the same pit is shown in Fig. 47. The stagnant (quiet, zero flow rate) seawater created a hole approximately 1.5 mm ($^1/_{16}$in.) diameter through the pipe wall in approximately four weeks of exposure to the stagnant and pressurized seawater inside the pipe. The location of the pit is at the bottom of the pipe in the center of a long, straight horizontal pipe run. The pipe was butt welded by electric arc processes at some joints and butt welded to flanged fittings at other joints. Some air may have been trapped in the top of this and other pipe runs.

Discussion

These conditions were ideal for three modes of highly accelerated pitting of austenitic stainless steel. The three modes can be distinguished by how and where the pit starts and how the hydrochloric acid (HCl) collects. The morphology or surface conditions, contours, waviness, and relative surface area of each mode strongly influences pit shape and depth as well as route and growth rate of corroded path.

The first mode is shown in Fig. 46 and 47, where it is characterized by pitting in the bottom of the long run of pipe. Chloride ions, which are plentiful in seawater, attack and damage the passive film and activate the

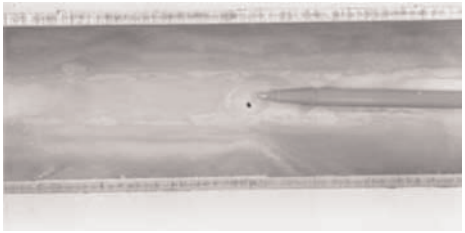

Fig. 46 Photograph of the inside of a stainless steel pipe with corrosion pits. The pipe was from a fire-sprinkler system for a car and passenger ferry boat.

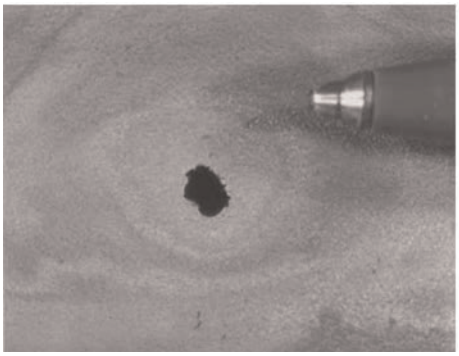

Fig. 47 Closeup of the corrosion pit in the center of Fig. 46

surface of the metal at that point. As the corrosion starts at the tiny active sites, hydrolysis and precipitates of the less-soluble Fe^{2+} hydroxides produce increased concentrations of hydrochloric acid by these reaction steps:

$$Fe \rightarrow Fe^{2+} + 2e^-$$

$$Fe^{2+} + 2e^- + 3H^+ + 2OH^- + Cl^- \rightarrow Fe(OH)_2 \downarrow + H_2 \uparrow + H^+ + Cl^-$$

or simply:

$$Fe^{2+} + 2Cl^- + 2H_2O \rightarrow Fe(OH)_2 \downarrow + 2HCl$$

The metal hydroxide precipitates, H_2 escapes, and the HCl (acid) product remains in solution, as shown by the right side of the equation. The acid is concentrated with pH lowering to near 2 by gravity in puddles or pits, which further accelerates the corrosion at the site.

In this first mode, the bottom center of the horizontal pipe run is activated when the chloride ions pick the weakest site in this massive bottom surface area and cause that location to become activated. The morphology is typical of pipe, neither very rough nor smooth. The relative surface area of the cathode to anode is large because of the expanse of the pipe involved. Corrosion by pitting starts, the dense acid puddles by gravity over a relatively wide area, and the remainder of the pipe section acts as a cathode. The pit is saucer shaped, relatively large, and uniform but grows rapidly due to decreasing pH and develops by autocatalytic corrosion (Ref 80).

Mode two pits develop in the weld or HAZ, even without the presence of sensitization, because of the inevitable surface micro-nonuniformities, roughness, and imperfections, as well as some chemical differences from welding products. The rough and irregular morphology of welds that have not been ground flat provides sites that are easily activated for pitting and hard to completely passivate. The pipe and irregular welded surface, especially if porous and if slag and spatter are present, comprise a relatively massive cathode with a small anodic pit. Pitting starts and acid collects in the tiny pores of the damaged weld, and the process of accelerated pitting results. The pits tend to be long, thin, and capillary-like, routed in a path through the weld or HAZ, just as mold grows through bread. In sensitized stainless steel, the route is clearly intergranular but still circuitous. Active pit sites can be located at any position on a weld. If an acid reservoir can be established, pits will grow in the direction preferred by gravity and will eventually penetrate the weld or pipe wall. The pitting rate can be very fast. Because only a microscopic amount of metal must be corroded to produce a leak, component failure is likewise fast.

The third mode develops by crevices. Areas around mating flanges, gaskets, O-ring seals, and machined faying surfaces all contain crevices. If O-rings are used, the flanges would be machined and polished. Other gasketed flanges are also smoother than the surrounding metal. The polished surface has the smallest overall surface area and hence is easiest to passivate, polarize, and keep clean, making it the most resistant to activation. If a crevice is present, it will produce a relatively long active site. The area under rubber or in a tight joint is easily activated by chloride ion attack. The absence of sufficient oxidizers does not allow the passive film to be replenished and maintained. The dense HCl collects by gravity in the lower regions of the crevice, and the cycle of accelerated corrosion is established.

The speed at which a leak develops depends on the direction of the crevice in relation to gravitational force. In the case of a horizontal seal edge, the corrosion damage can be very long and uniform, with a good deal of metal corrosion prior to any leaking. On the other hand, if the plane of the seal edge is vertical or just off of vertical by several degrees, the corrosion can be more like pitting than crevice corrosion. Less metal must corrode to produce a leak. Crevice corrosion and pitting are similar in the mechanisms and driving forces and identical regarding the corrosion reactions. Macroscopic geometry determines the category.

These austenitic stainless steels can be active or passive in adjacent areas on the same part or pipe. Because of the relatively large surface area of the cathode and hence the low current density of the cathode, it tends to *not* polarize. Therefore, the cathode-to-anode potential difference remains great, and thus, the high corrosion rate at the anode is maintained. However, cathodic protection (CP) can help retard or prevent the onset of pitting and reduce the rate of growth of established shallow pits. The application of CP reduces corrosion by forcing the passive and active areas to exhibit a more anodic potential, that is, protective potential. For example, the criteria for cathodically protecting steels in most waters and soils are accomplished by changing the potential of the steel by approximately 200 mV in the anodic direction.

The electromotive voltage or galvanic potential between these different metal surfaces can easily reach 500 mV open circuit. The passive area is protected and becomes passive by developing an invisible complex chromium oxide film. This passive oxide film must be maintained by the presence of a dissolved oxidizer such as O_2, $FeCl_2$, or Fe^{3+} ions.

Recommendations

Proper materials selection for piping, flanges, and weld rods can make the greatest improvement in resistance. Even low-carbon steel has better resistance to pitting in stagnant seawater piping systems. Seal design is important. The thicker the O-ring and the greater the quantity of the proper lubricant, the better for corrosion resistance. Proper filtering to prevent entrained abrasive is critical. Surface abrasion damages passivation. Corrosive agents can sometimes be countered with inhibitors. Flow rates above several feet per second (~1.5 m/s, or 5 ft/s) can reduce, but should not be expected to prevent, such pitting corrosion damage unless no locations can become active. To be effective, the flow must deliver the repairing/maintaining oxidizer and wash away any acids. Timely breakdown inspections are one way of possible early detection of damage, as shown by internal rust pits, carbuncles, and rust deposits.

High-Velocity Effects

Swift-Moving Water

Swift-moving water may carry dissolved metal ions away from corroding areas before the dissolved ions can be precipitated as protective layers. Gritty suspended solids in water scour metal surfaces and continually expose fresh metal to corrosive attack.

In freshwater, as water velocity increases, it is expected that corrosion of steel first increases, then decreases, and then increases again. The latter occurs because erosive action serves to break down the passive state.

The corrosion of steel by seawater increases as the water velocity increases. The effect of water velocity at moderate levels is shown in Fig. 48, which illustrates that the rate of corrosive attack is a direct function of the velocity until some critical velocity is reached, beyond

which there is little further increase in corrosion. At much higher velocities, corrosion rates may be substantially higher.

The effect of changes in water velocity on the corrosion resistance of stainless steels, copper alloys, and nickel alloys shows much variation from alloy to alloy at intermediate velocities. Type 316 austenitic stainless steel may pit severely in typical seawater, especially when stagnant (as indicated by the previous example) and at velocities of less than 1 or 1.5 m/s (4 or 5 ft/s), but is usually very corrosion resistant at higher velocities. Aluminum brass alloy (C68700) has satisfactory corrosion resistance if the seawater velocity is less than 2.4 m/s (8 ft/s).

Copper alloy C71500 (copper-nickel, 30% Ni) has excellent resistance to swift-moving seawater and to many types of freshwater. Because copper alloy C71500 is also subject to biofouling, velocities should be kept above 1.5 m/s (5 ft/s), because higher velocities inhibit attachment.

In seawater at high velocity, metals fall into two distinctly different groups: those that are velocity limited (carbon steels and copper alloys) and those that are not velocity limited (stainless steels and many nickel alloys).

Metals that are not velocity limited are subject to virtually no metal loss from velocity effects or turbulence short of cavitation conditions. The barrier films that form on these metals seem to perform best at high velocities with the full surface exposed and clean. It is in crevices and under deposits that form from slow-moving or stagnant seawater that local breakdown of the film and pitting begin.

Erosion-Corrosion

Erosion-corrosion is a form of corrosion, typically affecting pipelines, that involves a combination of pitting and erosion. When movement of a corrosive over a metal surface increases the rate of attack due to mechanical wear and corrosion, especially abrasive particles, the attack is called erosion-corrosion. It is encountered when particles in a liquid or gas impinge on a metal surface, causing the removal of protective surface films, such as air-formed protective oxide films or adherent corrosion products, and exposing new reactive surfaces that are anodic to noneroded neighboring areas on the surface. This results in rapid localized corrosion of the exposed areas in the form of smooth-bottomed shallow recesses. As temperature increases, the protective film may become more soluble and/or less resistant to scouring. Hence, the same flow rates, but at higher temperature, can cause an increase in corrosion rates or new forms and modes of corrosion.

Nearly all turbulent corrosive media can cause erosion-corrosion. The attack may exhibit a directional pattern related to the path taken by the corrosive as it moves over the surface of the metal.

Figure 49 shows the interior of a 50 mm (2 in.) copper river waterline that has suffered pitting and general erosion due to excessive velocity of the water. The brackish river water contained some suspended solids that caused the polishing of the copper pipe surface. The horseshoe-shaped pits (facing upstream) are typical of the damage caused by localized turbulence. The copper pipe was replaced with fiberglass-reinforced plastic piping.

Impingement Corrosion

Impingement corrosion is a severe form of erosion-corrosion. It occurs frequently in turns or elbows of tubes and pipes and on surfaces of impellers or turbines. It occurs as deep, clean, horseshoe-shaped pits with the deep, or undercut, end pointing in the direction of flow. Impingement-corrosion attack can also occur as the result of partial blockage of a tube. A stone, a piece of wood, or some other object can cause the main flow to deflect against the wall of the tube. The impinging stream can rapidly perforate tube walls. Water that carries sand, silt, or mud will have an additional severely erosive effect on tubes.

The energy transfer is the rate of change of the momentum of the flowing medium. As this energy transfer takes place over a smaller and smaller area per unit time, the energy or power density of the process becomes damaging to the substrate.

A beneficial extension of this effect at sufficiently high power densities is abrasive machining and cutting. At slower rates and lower power densities, it is called impingement corrosion. Steam erosion is another form of impingement corrosion, occurring when high-velocity wet steam impacts a metal surface. The resulting attack usually produces a roughened surface showing a large number of small cones with the points facing in the direction of flow.

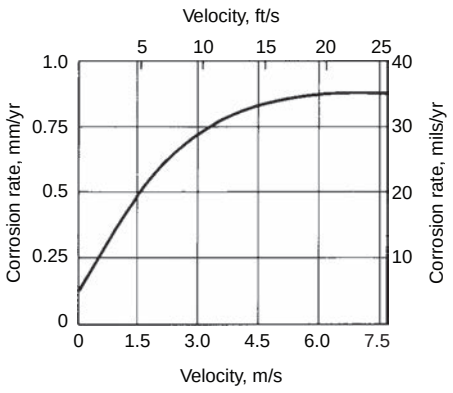

Fig. 48 Effect of velocity of seawater at atmospheric temperature on the corrosion rate of steel

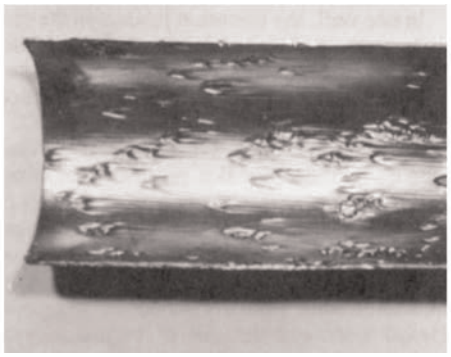

Fig. 49 Erosion pitting caused by turbulent river water flowing through copper pipe. The typical horseshoe-shaped pits point upstream. Original magnification: ~0.5× actual size

Example 19: Impingement-Corrosion Failure of a Ferritic Malleable Iron Elbow.

Leakage was detected in a malleable iron elbow after only three months in service. Life expectancy for the elbow was 12 to 24 months. The 21 mm (0.82 in.) ID 90° elbow connected segments of 19 mm (0.75 in.) pipe with a wall thickness of 2.9 mm (0.11 in.). The piping alternately supplied steam and cooling water to a tire-curing press. The supply line and elbow were subjected to 14 heating and cooling cycles per hour for at least 16 h/day, or a minimum of 224 cycles/day. Steam pressure was 1035 kPa (150 psi), and water pressure was 895 kPa (130 psi). Based on pump capacity, the water-flow rate was estimated at 1325 L/min (350 gal/min). Water-inlet temperature was 10 to 15 °C (50 to 60 °F); water-outlet temperature was 50 to 60 °C (120 to 140 °F). The water had a pH of 6.9.

The elbow was cast from ASTM A47, grade 35018, malleable iron and had a hardness of 76 to 78 HRB. ASTM A 47 (Ref 81) covers applications for normal ambient conditions up to 400 °C (750 °F). Composition of the iron was:

Element	Content, %
Carbon	1.95
Manganese	0.60
Silicon	1.00
Sulfur	0.15
Phosphorus	0.05
Copper	0.17
Chromium	0.03
Nickel	0.02
Molybdenum	0.001

Investigation

Specimens were cut from two areas on the elbow, one just below the point of leakage (region A, Fig. 50a) and another further downstream (region B, Fig. 50a). The deepest penetration in the first specimen was at the top, just below the point of leakage, where the wall thickness had been reduced to 1.6 mm (0.062 in.). Maximum wall thickness was 9.5 mm (0.37 in.).

Metallographic examination of the first specimen showed that moderate but irregular attack had occurred (Fig. 50b). A small area of ferrite remained at the top, but the surface ferritic zone (light areas, Fig. 50b)

had been eroded and corroded away on the remainder of the surface, exposing the pearlitic zone (dark areas, Fig. 50b). The interior of the specimen showed a ferritic malleable microstructure.

The second specimen, which showed no signs of attack, had a typical ferrite zone at the surface, then a subsurface pearlitic zone with approximately twice the thickness of the ferrite zone, and a ferritic malleable microstructure in the interior of the specimen (Fig. 50c).

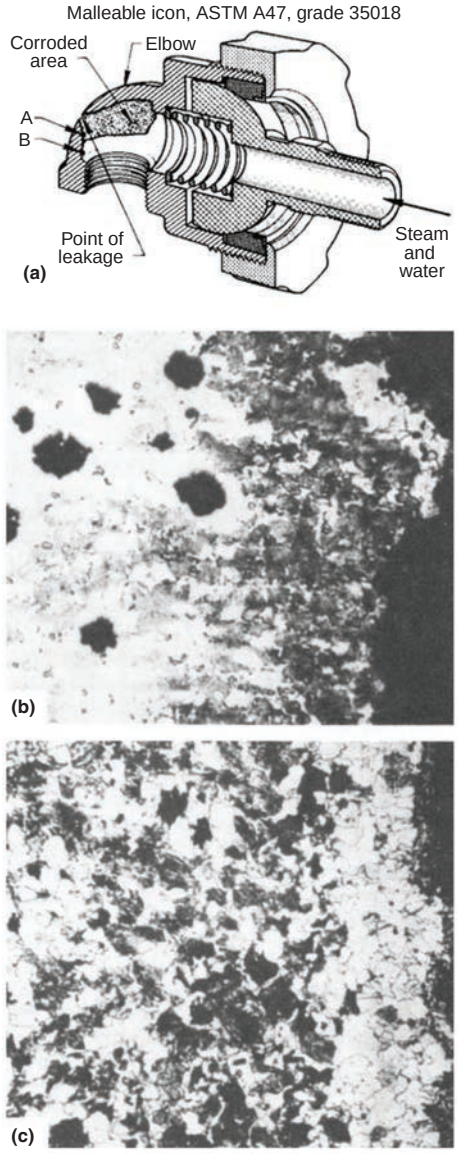

Fig. 50 Malleable iron elbow in which impingement corrosion caused leakage and failure at the bend. (a) Section through the elbow showing extent of corrosion and point of leakage. Regions A and B are locations of specimens shown in micrographs (b) and (c), respectively. (b) Micrograph of a nital-etched specimen from region A (just below the failure area) showing ferritic surface (light areas) corroded away, exposing the subsurface pearlitic zone (dark areas). Original magnification: 67×. (c) Micrograph of a nital-etched specimen from region B (an uncorroded area of the elbow) showing a typical ferrite zone at the surface, a subsurface pearlitic zone (with twice the thickness of the ferrite zone), and a ferritic malleable microstructure in the interior. Original magnification: 67×

Conclusions

Examination of the micrographs (Fig. 50b, c) indicated that the elbows had been given the usual annealing and normalizing treatment for ferritizing malleable iron. This resulted in lower resistance to erosion and corrosion than pearlitic malleable iron.

Recommendations

It was recommended that replacement elbows be heat treated to produce a pearlitic malleable microstructure, which has longer life under the given conditions of service. (Additional information on the heat treatment and properties of ferritic and pearlitic malleable irons is provided in the article "Malleable Iron" in *Properties and Selection: Irons, Steels, and High-Performance Alloys*, Volume 1 of the *ASM Handbook*, 1990.)

In piping systems, erosion-corrosion can be reduced by increasing the diameter of the pipe, thus decreasing velocity and turbulence. The streamlining of bends is useful in minimizing the effects of impingement. Inlet pipes should not be directed onto the vessel walls if this can be avoided. Flared tubing can be used to reduce problems at the inlet tubes in a tube bundle.

Cavitation Erosion

Cavitation erosion is the one of the most severe forms of erosion-corrosion. It occurs principally when relative motion between a metal surface and a liquid environment and thermodynamic conditions in the liquid causes vapor bubbles to develop and then rapidly collapse. When the bubbles collapse, they impose hammerlike blows, which produce stresses on the order of 400 MPa (60 ksi), simultaneously with the initiation of tearing action that appears to pull away portions of the surface. The tearing action can remove any protective oxide film that exists on the surface of a metal, exposing active metal to the corrosive influence of the liquid environment. It has been shown that corrosion is not essential to cavitation erosion, however, as discussed in the article "Liquid Droplet Impingement Erosion" in this Volume.

Cavitation erosion occurs on rotors, pumps, on the trailing faces of propellers and water-turbine blades, and on the water-cooled side of diesel-engine cylinders. Here, high velocities give rise to extremely low-pressure areas, vapor bubbles develop by a phase change in thermodynamically unstable liquids, and then the bubbles collapse cataclysmically as higher pressures and/or lower temperature make the vapor state thermodynamically unstable. The massive momentum change of liquid rushing in to fill the void at collapse of the vapor bubble destroys the protective film on the metal surface or disrupts and often plastically deforms the metal itself.

Damage can be reduced by operating rotary pumps at the highest possible head of pressure to avoid formation of momentarily stable vapor bubbles. For turbine blades, aeration of water serves to cushion the damage caused by the collapse of bubbles. Neoprene or similar elastomer coatings on metals are somewhat reasonably resistant to damage from this cause. To reduce cavitation damage to diesel-engine cylinder liners, the addition of 2000 ppm sodium chromate to the cooling water has proved effective, as has the use of Ni-Resist (high-nickel cast iron) liners. Table 5 rates some metals frequently used in seawater into four groups on the basis of their resistance to cavitation erosion in seawater. This corrosion mechanism represents a mechanically assisted type of material deterioration; because of this, many alloys are susceptible to this deterioration mechanism.

Flow-Accelerated Corrosion (Ref 83)

Flow-accelerated corrosion (FAC) is a corrosion mechanism that is distinct from erosion-corrosion and is primarily an electrochemical corrosion process aided by chemical dissolution and mass transfer. Flow-accelerated corrosion can result in severe wall thinning (metal thickness loss) of carbon steel piping, tubing, and vessels exposed to flowing water or wet steam. When the wall thickness of the affected component is reduced to levels lower than the critical thickness required for supporting the operating stresses over a sufficient length of the component, it results in ductile rupture overload failure of the component.

If the attack due to FAC goes undetected for an extended period of time, the deteriorated component can rupture without warning. Flow-accelerated corrosion has caused a large number of failures in piping and equipment in all types of fossil, industrial steam, and nuclear power plants. It is a predominant mode of failure of pipelines in the secondary circuit and has also affected carbon steel pipelines in the primary circuit of light water reactors.

Deoxygenated single-phase water or a water-steam mixture (dual or two phase) in the secondary circuit leads to the formation of a magnetite film on the ID surfaces of carbon steel and acts as a protective film, guarding the carbon steel components against corrosion. Such a film forms in the high-energy systems over a period of time that is dependent on temperature.

Flow-accelerated corrosion is a process where the typically protective oxide layer dissolves into the flowing stream, resulting in the oxide layer becoming thinner and less protective. The oxide layer may be thinned to an extent that exposes an apparently bare metal surface that otherwise exhibits a black color, typical of magnetite. Even with the oxide film present on the surface, the rate of dissolution of metal through the oxide film accelerates with higher velocities. The rate of this

corrosion process is enhanced by (electro) chemical dissolution and mass transfer and is not a dominant mechanical process. Flow-accelerated corrosion is thus an extension of the generalized carbon steel corrosion process in stagnant water. Without proper in-service monitoring, the thinned components typically fail due to overstress from operating pressure. Flow-accelerated corrosion occurs under both single- and two-phase flow conditions. Because water is essential in removing the oxide layer by electrochemical reactions, FAC does not occur in lines transporting dry steam.

Flow-accelerated corrosion is distinct from erosion-corrosion and is primarily a corrosion process aided by chemical dissolution and mass transfer. In practice, there may be some contribution from the mechanical factors that lead to removal of corroded scallops on the material surface to become loose and flow out with the high-velocity process fluid. This may further accelerate the overall FAC rate but is not a factor for thinning by itself (i.e., without first the electrochemical dissolution leading to FAC and the formation of loosely held scallops). The corrosion rate is first determined by the rate of transfer of ionic species between the surface and the fluid. If the corrosion reaction is rapid and the corrosion product has low solubility in bulk fluid, the corrosion rate is governed by the concentration gradient (Fig. 51).

Flow velocities associated with FAC increase this concentration gradient and thus increase the corrosion rate. No evidence of removal of the oxide film purely due to mechanical shear has been found on the FAC-damaged surfaces of feed water piping.

Table 5 Ratings of some metals for resistance to cavitation erosion in seawater

Group No. and characteristics	Alloys
Group I	
Most resistant. Subject to little or no damage. Useful under extremely severe conditions	Stellite hard-facing alloys Titanium alloys Austenitic and precipitation-hardening stainless steels Nickel-chromium alloys such as Inconel alloys 625 and 718 Nickel-molybdenum-chromium alloys such as Hastelloy C
Group II	
These metals are commonly used where a high order of resistance to cavitation damage is required. They are subject to some metal loss under the most severe conditions of cavitation.	Nickel-copper-aluminum alloy Monel K-500 Nickel-copper alloy Monel 400 Copper alloy C95500 (nickel-aluminum bronze, cast) Copper alloy C95700 (nickel-aluminum-manganese bronze, cast)
Group III	
These metals have some degree of cavitation resistance. They are generally limited to low-speed, low-performance applications.	Copper alloy C71500 (copper-nickel, 30% Ni) Copper alloys C92200 and C92300 (leaded tin bronzes M and G, cast) Manganese bronze, cast Austenitic nickel cast irons
Group IV	
These metals normally are not used in applications where cavitation damage may occur, except in cathodically inhibited solutions or when protected by elastomeric coatings.	Carbon and low-alloy steels Cast irons Aluminum and aluminum alloys

Note: Applies to normal cavitation-erosion intensities, at which corrosion resistance has a substantial influence on the resistance to damage.
Source: Ref 82

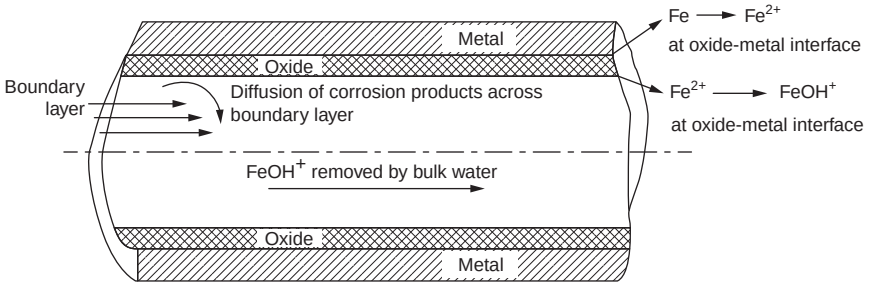

Fig. 51 Schematic of the dissolution of material through surface oxide film and removal of the dissolving species in bulk water. Adapted from Ref 84

Erosion-Corrosion

Erosion-corrosion is a form of mechanical degradation that involves corrosion as well as mechanical wear. This occurs on the surface of the material due to the action of numerous individual impacts of solid or liquid particles. Much higher flow velocities are associated with this type of degradation. Laboratory tests have also shown that the fluid velocities required for mechanical removal of the oxide are higher than those required for dissolution of an oxide layer. Definite surface patterns are formed on components undergoing FAC, which is a signature of FAC (Fig. 52), while no such signature is associated with erosion-corrosion. Due to erosion-corrosion, grooves, gullies, or rounded holes are formed. This can occur in metals and alloys that are completely resistant to a particular environment at low flow velocities, unlike FAC degradation.

Flow-accelerated corrosion is affected by many parameters, such as material composition, temperature, pH, dissolved oxygen content, pipe geometry, and flow velocity. Flow-accelerated corrosion is the most destructive corrosion mechanism for high-energy carbon steel components in light water reactors. The maximum in FAC rate appears at ~150 °C (300 °F). It has caused rupture of large-, medium-, and small-diameter pipelines carrying either single-phase (single-phase FAC) or two-phase (wet steam) flow (two-phase FAC).

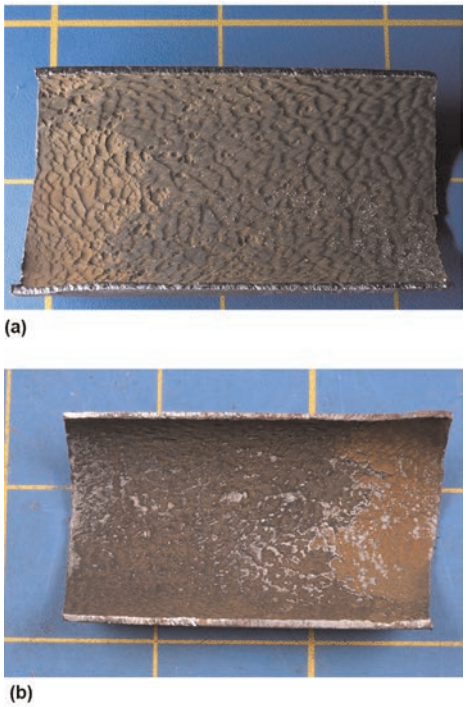

Fig. 52 Carbon steel pipe sections exhibiting surface pattern (scalloped, orange-peel) typically observed on components subject to deterioration due to flow-accelerated corrosion

ACKNOWLEDGMENTS

This article was revised from "Forms of Corrosion," *Failure Analysis and Prevention*, Volume 11, *ASM Handbook*, ASM International, 2002, p 761–795.

Sections of this article have been based in part on the corresponding sections of "Corrosion Failures" by W.G. Ashbaugh in *Failure Analysis and Prevention*, Volume 11 of *ASM Handbook*, 1986, p 172–202.

Additionally, the section "Galvanic Corrosion" is based in part on content from the following *ASM Handbook* articles:

- R. Baboian and S. Pohlman, "Galvanic Corrosion," *Corrosion*, Volume 13 of *ASM Handbook*, 1987, p 83–87
- F.P. Ford and P.L. Andresen, "Design for Corrosion Resistance," *Materials Selection and Design*, Volume 20 of *ASM Handbook*, 1997, p 545–572

The section "Uniform Corrosion" is based in part on "Evaluation of Uniform Corrosion" by C.A. Natalie, *Corrosion*, Volume 13 of *ASM Handbook*, 1987, p 229–230.

Example 15 is based on content from the ASM Committee on Corrosion of Weldments, Kenneth F. Krysiak, Chairman, in the article "Corrosion of Weldments" in *Corrosion*, Volume 13 of *ASM Handbook*, 1987, p 357–358.

REFERENCES

1. R.W. Revie, Ed., *Uhlig's Corrosion Handbook*, John Wiley & Sons, 2000, p 32
2. R.S. Treseder, Ed., *The NACE Corrosion Engineer's Reference Book*, National Association of Corrosion Engineers, 1980
3. "Standard Guide for Development and Use of a Galvanic Series for Predicting Galvanic Corrosion Performance," G 82, *Wear and Erosion; Metal Corrosion*, Vol 03.02, *Annual Book of ASTM Standards*, American Society for Testing and Materials
4. E.H. Hollingsworth and H.Y. Hunsicker, Corrosion of Aluminum and Aluminum Alloys, *Corrosion*, Vol 13, *ASM Handbook*, ASM International, 1987, p 583–609
5. "Standard Reference Test Method for Making Potentiostatic and Potentiodynamic Anodic Polarization Measurements," G 5, *Wear and Erosion; Metal Corrosion*, Vol 03.02, *Annual Book of ASTM Standards*, American Society for Testing and Materials
6. R.H. McSwain, Fatigue Fracture of a Helicopter Tail Rotor Blade due to Field-Induced Corrosion, *Handbook of Case Histories in Failure Analysis*, Vol 2, ASM International, 1993, p 30–32
7. Recommended Practice for Cathodic Protection of Aluminum Pipe Buried in Soil or Immersed in Water, *Mater. Protec.*, Vol 2 (No. 10), 1963, p 106
8. F.W. Hewes, Investigation of Maximum and Minimum Criteria for the Cathodic Protection of Aluminum in Soil, *Oil Week*, Vol 16 (No. 24–28), Aug–Sept 1965
9. R. Kent, "*Anodic Polarization Measurements of Alloyed DI*," NACE Int. Conf., National Association of Corrosion Engineers, 1987
10. R. Kent, "Potential Anodic Polarization Measurements and Mechanical Property Analysis of Ferritic Nodular Iron Alloyed with Nickel," University of Washington, 1986
11. F. Mansfeld and V. Bertocci, *Electrochemical Corrosion Testing*, STP 727, American Society for Testing and Materials, 1981
12. M. Henthorne, *Corrosion Causes and Control*, Carpenter Technology Corp., 1972, p 30
13. "Preparing, Cleaning, and Evaluating Corrosion Test Specimens," G 1, *Wear and Erosion; Metal Corrosion*, Vol 03.02, *Annual Book of ASTM Standards*, American Society for Testing and Materials
14. "Standard Practice for Conducting Atmospheric Corrosion Tests on Metals," G 50, *Wear and Erosion; Metal Corrosion*, Vol 03.02, *Annual Book of ASTM Standards*, American Society for Testing and Materials
15. G. Wranglén, *Corrosion and Protection of Metals*, Chapman & Hall, 1985, p 238
16. R.L. Martin and E.C. French, Corrosion Monitoring in Sour Systems Using Electrochemical Hydrogen Patch Probes, *J. Pet. Technol.*, Nov 1978, p 1566–1570
17. P.A. Schweitzer, *Corrosion and Corrosion Protection Handbook*, Marcel Dekker, 1983, p 483–484
18. "Standard Test Method for Conducting Potentiodynamic Polarization Resistance Measurements," G 59, *Wear and Erosion; Metal Corrosion*, Vol 03.02, *Annual Book of ASTM Standards*, American Society for Testing and Materials
19. "Standard Practice for Conventions Applicable to Electrochemical Measurement in Corrosion Testing," G 3, *Wear and Erosion; Metal Corrosion*, Vol 03.02, *Annual Book of ASTM Standards*, American Society for Testing and Materials
20. K.E. Perumal, Pitting Corrosion of Stainless Steel by Potable Municipal Water in an Organic Chemical Plant, *Handbook of Case Studies in Failure Analysis*, Vol 1, *ASM International*, 1992, p 176–177
21. A.I. Asphahani and W.L. Silence, Pitting Corrosion, *Corrosion*, Vol 13, *Metals Handbook*, 9th ed., ASM International, 1987, p 112–114
22. "Examination and Evaluation of Pitting Corrosion," G 46-94 (Reapproved 1999), *Wear and Erosion; Metal Corrosion*, Vol 03.02, *Annual Book of ASTM Standards*, American Society for Testing and Materials
23. C.R. Brooks, Fatigue Fracture of Stainless Steel Wires in an Electrostatic Precipitator at a Paper Plant, *Handbook of Case Studies in Failure Analysis*, Vol 1, ASM International, 1992, p 218–222
24. S.D. Kiser, Preventing Weld Corrosion, *Adv. Mater. Process.,* Vol 160 (No. 3), March 2002
25. J.E. Hatch, Ed., *Aluminum: Properties and Physical Metallurgy*, American Society for Metals, 1984, p 290–291
26. *Corrosion of Metals under Thermal Insulation*, STP 880, American Society for Testing and Materials, 1985
27. A.J. Sedriks, *Corrosion of Stainless Steels*, 2nd ed., Wiley-Interscience, 1996, p 217
28. "Standard Test Method for Pitting or Crevice Corrosion of Metallic Surgical Implant Materials," F 746-87 (Reapproved 1999), *Annual Book of ASTM Standards*, Vol 13.01, American Society for Testing and Materials
29. N.D. Green, Corrosion of Surgical Implant Alloys: A Few Basic Ideas, *Corrosion and Degradation of Implant Materials*, STP 859, American Society for Testing and Materials, 1985, p 7
30. H. Skinner, et al. "Corrosion, Materials Characteristics and Local Tissue Reaction Associated with Osteosynthesis Devices, Implant Retrieval: Material and Biological Analysis," *NBS Special Publication 601*, U.S. Dept. of Commerce, Jan 1981, p 425
31. D.H. Pope, "Microbial Corrosion in Fossil-Fired Power Plants, A Study of Microbiologically Influenced Corrosion and a Practical Guide for its Treatment and Prevention," Report CS-5495 prepared for EPRI, 1987
32. R.G. Kelley, *Pitting, Corrosion Tests and Standards: Application and Interpretation*, MNL 20, R. Baboian, Ed., American Society for Testing and Materials, 1995
33. "Standard Practice for Determining the Susceptibility to Intergranular Corrosion of 5*xxx* Series Aluminum Alloys by Weight Loss after Exposure to Nitric Acid (NAWLT Test)," G 67, *Wear and Erosion; Metal Corrosion*, Vol 03.02, *Annual Book of ASTM Standards*, American Society for Testing and Materials
34. M.A. Streicher, *Intergranular Corrosion of Stainless Alloys*, STP 656, R.F. Steigerwald, Ed., American Society for Testing and Materials, 1978, p 3–84
35. V. Kain, R.C. Prasad, and P.K. De, Detection of Sensitization and Intergranular Corrosion of Fe-Cr-Ni Alloys, *High Temp. Mater. Proc.*, Vol 16 (No. 3), July–Sept 1997, p 183–199
36. "Standard Practices for Detecting Susceptibility to Intergranular Attack in Austenitic Stainless Steels," A 262, *Annual Book of ASTM Standards*, Vol 01.03, American Society for Testing and Materials
37. "Test Method Standard Test Method for Electrochemical Reactivation (EPR) for

Detecting Sensitization of AISI Type 304 and 304L Stainless Steels," G 108-94, *Wear and Erosion; Metal Corrosion*, Vol 03.02, *Annual Book of ASTM Standards*, American Society for Testing and Materials, 1999
38. A.P. Majidi and M.A. Streicher, Four Non-Destructive Electrochemical Test for Detecting Sensitization in Type 304 and 304L Stainless Steels, Paper 62, *Corrosion '85,* National Association of Corrosion Engineers, 1985, p 1–17; *Nucl. Technol.*, Vol 75 (No. 3), Dec 1986, p 356–369
39. A.P. Majidi and M.A. Streicher, Potentiodynamic Reactivation Method for Detecting Sensitization in AISI 304 Stainless Steels, *Corrosion*, Vol 40 (No. 1), Jan 1984, p 21–32
40. W.L. Clarke, V.M. Romero, and J.C. Danko, "Detection of Sensitization in Stainless Steel Using Electrochemical Techniques," Paper 180 (Pamphlet), Corrosion '77, International Corrosion Forum, National Association of Corrosion Engineers, 1977
41. M. Akashi, et al. Evaluation of IGSCC Susceptibility of Austenitic Stainless Steels Using Electrochemical Reactivation Method, *Corrosion Eng.*, Vol 29, 1980, p 163
42. A.P. Majidi and M.A. Streicher, The Double Loop Reactivation Method for Detecting Sensitization in AISI 304 Stainless Steels, *Corrosion*, Vol 40 (No. 11), Nov 1984, p 584–593
43. K.J. Stoner, An Evaluation of Electrochemical Potentiokinetic Reactivation Techniques for In-Service Measurements on Type 304 Stainless Steel, *Computer-Aided Microscopy and Metallography*, ASM International, 1990, p 171–182
44. M. Verneau, J. Charles, and F. Dupoiron, Applications of Electrochemical Potentiokinetic Reactivation Test to On-Site Measurements on Stainless Steels, *Application of Accelerated Corrosion Tests to Service Life Prediction of Materials*, STP 1194, American Society for Testing and Materials, 1994, p 367–381
45. D. Van Rooyen, *Corrosion*, Vol 31, 1975, p 327–337
46. G. Kobrin, Materials Selection, *Corrosion*, Vol 13, *Metals Handbook*, 9th ed., ASM International, 1987, p 325
47. V. Kain, Intergranular Corrosion of Stainless Steels, *Conference: Workshop on Failure Analysis, Corrosion Evaluation and Metallography*, Bhabha Atomic Research Centre, Trombay, Bombay, India, 1992, p 107–128
48. V. Cihal Sr. and V. Cihal Jr., Economical Evaluation of Stainless Steels for Their Resistance to Intergranular Corrosion, *Book 556, Progress in the Understanding and Prevention of Corrosion*, Vol II, July 1993 (Barcelona, Spain), The Institute of Materials, 1993, p 1537–1541
49. G.F. Vander Voort, Embrittlement of Steels, *Properties and Selection: Irons, Steels, and High-Performance Alloys*, Vol 1, *ASM Handbook*, ASM International, 1990, p 698–736
50. T.M. Devine, Mechanism of Intergranular Corrosion and Pitting Corrosion of Austenitic and Duplex 308 Stainless Steel, *J. Electrochem. Soc.*, Vol 126 (No. 3), 1979, p 374
51. E.E. Stansbury, C.D. Lundin, and S.J. Pawel, Sensitization Behavior of Cast Stainless Steels Subjected to Simulated Weld Repair, *Proc. 38th SFSA Technical and Operating Conference*, Steel Founders' Society of America, 1983, p 223
52. C. McCaul, Evaluation of Intergranular Corrosion Susceptibility in an As-Welded High Alloy Austenitic Stainless Steel Casting, *Br. Corros. J.*, Vol 26 (No. 4), 1991, p 239–243
53. M. Henthorne, *Localized Corrosion—Cause of Metal Failure*, STP 516, American Society for Testing and Materials, 1972, p 66–119
54. R.A. Corbett and B.J. Saldanha, Evaluation of Intergranular Corrosion, *Corrosion*, Vol 13, *Metals Handbook*, 9th ed., ASM International, 1987, p 240
55. J.S. Armijo, Intergranular Corrosion of Nonsensitized Austenitic Stainless Steels, *Corrosion*, Jan 1968, p 24–30
56. W.H. Herrnstein, J.W. Cangi, and M.G. Fontana, Effect of Carbon Pickup on the Serviceability of Stainless Steel Alloy Castings, *Mater. Perform.*, Oct 1975, p 21–27
57. Corrosion Failures, *Failure Analysis and Prevention*, Vol 10, *Metals Handbook*, 8th ed., American Society for Metals, 1975, p 180
58. D.R. Johns and F.R. Beckitt, Factors Influencing the Thermal Stabilisation of Alloy 600 Tubing Against Intergranular Corrosion, *Corros. Sci.*, Vol 30 (No. 2–3), 1990, p 223–237
59. C.M. Younes, F.H. Morrissey, G.C. Allen, and P. McIntyre, Effect of Heat Treatment on the Grain Boundary Chemistry and the Resistance to Intergranular Corrosion of Alloy 600 and Alloy 690, *Second International Conference on Corrosion-Deformation Interactions, CDI '96*, Institute of Materials, 1997, p 421–434
60. P. Lin, G. Palumbo, U. Erb, and K.T. Aust, Influence of Grain Boundary Character Distribution on Sensitization and Intergranular Corrosion of Alloy 600, *Scr. Metall. Mater.*, Vol 33 (No. 9), Nov 1, 1995, p 1387–1392
61. M.H. Brown, *Corrosion*, Vol 25, 1969, p 438
62. M.H. Brown and R.W. Kirchner, *Corrosion*, Vol 29, 1973, p 470–474
63. E.H. Dix, Acceleration of the Rate of Corrosion by High Constant Stresses, *Trans. AIME*, Vol 137, 1940, p 11
64. W.L. Fink and L.A. Willey, Quenching of 75S Aluminum Alloy, *Met. Technol.*, Vol 14 (No. 8), 1947, p 5
65. M.S. Hunter, G.R. Frank, and D.L. Robinson, *Fundamental Aspects of Stress-Corrosion Cracking (Proc. Conf.)*, R.W. Staehle, Ed., National Association of Corrosion Engineers, 1969, p 497
66. H. Kaesche, Pitting Corrosion of Aluminum and Intergranular Corrosion of Aluminum Alloys, *Localized Corrosion*, B.F. Brown, J. Kruger, and R.W. Staehle, Ed., National Association of Corrosion Engineers, 1974, p 516
67. J.R. Galvele and S.M. Micheli de, Mechanism of Intergranular Corrosion of Al-Cu Alloys, *Corros. Sci.*, Vol 10, 1970, p 795
68. H.F. Brauer and W.M. Peirce, The Effect of Impurities on the Oxidation and Swelling of Zinc-Aluminum Alloys, *Trans. AIME*, Vol 60, 1923, p 796
69. H.H. Lee, Galvanized Steel with Improved Resistance to Intergranular Corrosion, *Proc. Galvanized Committee*, Vol 69, 1977, p 17
70. D.J. Willis, A. De Liseo, and B. Gleeson, Intergranular Corrosion in Continuously Galvanized Steel, *Galvatech '95, The Use and Manufacture of Zinc and Zinc Alloy Coated Sheet Steel Products into the 21st Century*, Iron and Steel Society/AIME, 1995, p 145–153
71. H. Uhlig and R.W. Revie, *Corrosion and Corrosion Control*, John Wiley & Sons, 1985, p 14, 331–334
72. M.G. Fontana and N.D. Greene, *Corrosion Engineering*, McGraw-Hill, 1978, p 67–71
73. E.D. Verink Jr. and R.H. Herdersbach Jr., Evaluation of the Tendency for Dealloying in Metal Systems, *Localized Corrosion—Causes of Metal Failure*, STP 516, American Society for Testing and Materials, 1972, p 303–322
74. S.R. Freeman, Graphitic Corrosion—Don't Forget about Buried Cast Iron Pipes, *Mater. Perform.*, Aug 1999, p 68–69
75. K. Kasahara and F. Kajtyama, "The Role of Bacteria in the Graphitic Corrosion of Buried Ductile Cast Iron Pipes," *Microbial Corrosion, Second EFC Workshop*, March 1991
76. R.J. Ferrara and T.E. Caton, Review of Dealloying of Cast Aluminum Bronze and Nickel-Aluminum Bronze Alloys in Sea Water Service, *Mater. Perform.*, Feb 1982, p 30–34
77. R. Steigerwald, Metallurgically Influenced Corrosion, *Corrosion*, Vol 13, *ASM Handbook*, ASM International, 1987, p 130–133
78. S.J. Pavel, Type 304L Stainless Steel Corrosion in Molten Lithium Hydride as a Function of Temperature, *J. Nucl. Mater.*, Vol 200 (No. 2), April 1993, p 184–199

79. T.B. Cassagne, W.F. Flanagan, and B.D. Lichter, On the Failure Mechanism of Chemically Embrittled Cu_3Au Single Crystals, *Metall. Trans.,* April 1986, p 703–710
80. M.G. Fontana, *Corrosion Engineering,* 3rd ed., *McGraw-Hill*, 1986
81. "Standard Specification for Ferritic Malleable Iron Castings," A 47, *Annual Book of ASTM Standards*, Vol 01.02, American Society for Testing and Materials
82. A.H. Tuthill and C.M. Schillmoler, "Guidelines for Selection of Marine Materials," *Ocean Science and Engineering Conference*, Marine Technology Society, Washington, June 1965
83. V. Kain, Flow Accelerated Corrosion: Forms, Mechanisms and Case Studies, *Proced. Eng*., Vol 86, 2014, p 576–588
84. V. Kain, S. Roychowdhury, P. Ahmedabai, and D.K. Barua, *Eng. Fail. Anal*., Vol 18, 2011, p 2028–2041, https://doi.org/10.1016/j.engfailanal.2011.06.007